Wireless Communication Over Time-Varying Channels With Limited Feedback

Wireless Communication Over Time-Varying Channels With Limited Feedback

Proefschrift

ter verkrijging van de graad van doctor
aan de Technische Universiteit Delft,
op gezag van de Rector Magnificus prof.ir. K.C.A.M. Luyben,
voorzitter van het College voor Promoties,
in het openbaar te verdedigen op vrijdag 4 november 2011 om 12:30 uur
door Claude SIMON
Diplom-Ingenieur, TU Kaiserslautern
geboren te Esch-sur-Alzette, Luxembourg.

Dit proefschrift is goedgekeurd door de promotor:
Prof.dr.ir. A.J. van der Veen

Copromotor:
Dr.ir. G.J.T. Leus

Samenstelling promotiecommissie:
Rector Magnificus, voorzitter
Prof.dr.ir. A.J. van der Veen, TU Delft, promotor
Dr.ir. G.J.T. Leus, TU Delft, copromotor
Prof.dr.ir. P.F.A. Van Mieghem, TU Delft
Prof.dr.ir. B. De Schutter, TU Delft
Prof.dr.ir. C.H. Slump, University of Twente
Prof.dr. F. Horlin, Université Libre de Bruxelles
Prof.dr. D. Gesbert, Eurecom

This research was supported in part by
NWO-STW under the VIDI program (DTC.6577)

ISBN 978-94-6191-065-3

Contents

Chapter 1

Introduction

In the last years wireless communication has become more and more ubiquitous. This is most visible for voice communication. We see in Fig 1.1 that the number of mobile phone subscriptions increased linearly for years. In Europe the number of mobile phone subscriptions already surpassed the number of inhabitants in 2005 [1]. At the time of writing, there are $5,3$ billion mobile cellular subscriptions worldwide [2]. The key drivers of this migration of voice communication from fixed lines, e.g., the plain old telephone service (POTS) and ISDN, to wireless networks, e.g., GSM and UMTS, are mobility and low installation hurdles.

The successful migration of voice communication raises the question whether a migration of data communication is also possible. However, the requirements for data communication are different from the requirements for voice communication. Whereas voice communication has strict delay requirements, data communication has higher data transfer rate requirements. The most popular standard for wireless data transmission today is the IEEE 802.11b standard. It was released in 1999 and has a maximum raw data rate of 11 Mbit/s. The succeeding standards, e.g., 802.11g quickly followed.

Further increasing the data rate was problematic at that time, since, as stated by Shannon's famous channel-capacity theorem, the maximal achievable data rate is ultimately limited by the available bandwidth, the available transmit energy, and the noise on the channel. Increasing the transmission power drains the

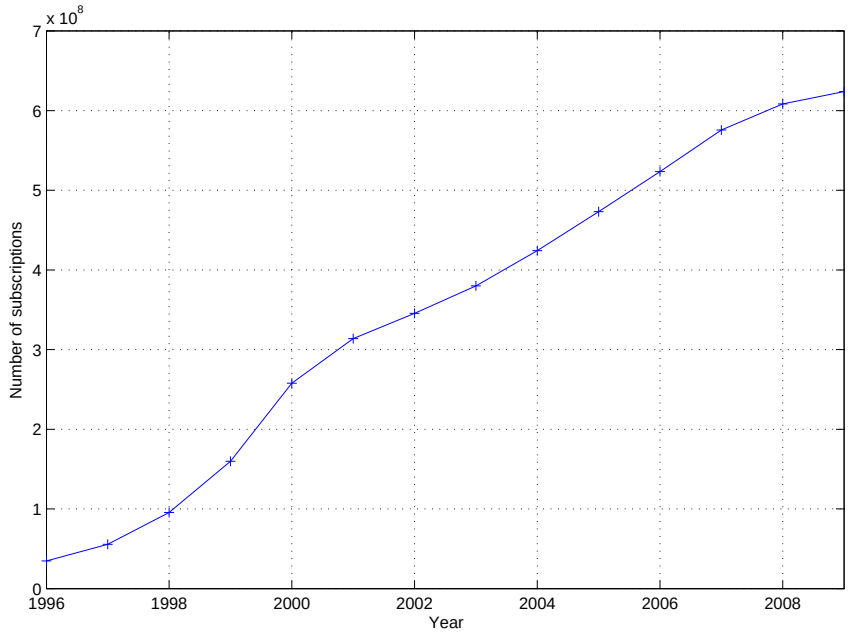

Figure 1.1: Number of mobile phone subscriptions in Europe (EU-27) [1].

batteries of the mobile devices and just provides a logarithmic growth in capacity. Thus, the only alternative is to increase the used bandwidth. The bandwidth, however, is an expensive resource as demonstrated by the UMTS auctions in 2000 and 2001.

An elegant solution to this problem is to use multiple antennas at the transmitter and the receiver side, i.e., multiple-input multiple-output (MIMO) systems [3]. It was shown in [4] that the ergodic capacity of a MIMO system increases linearly with the number of transmit and receive antennas. Recent standards already include MIMO transmission, e.g., 802.11n. Channel knowledge at the transmitter side further increases the ergodic capacity.

Channel knowledge at the base station is not just beneficial to increase the ergodic capacity of a MIMO point-to-point link but also plays an important role in scheduling the users in a broadcast system [5]. If the channels between the base station and the different users fade independently then having channel knowledge allows the base station to transmit to the user with favorable conditions. Thus, the channel state information (CSI) enables the base station to reap the multiuser diversity benefits of the system [6].

We see that modern wireless communication systems benefit from channel knowledge at the transmitter side. Channel knowledge can be easily acquired through training for time-division duplexing (TDD) where uplink and downlink share the same channel. For frequency-division duplexing (FDD), however, the downlink channel has to be estimated at the receiver and then it has to be fed back to the transmitter. Thus, acquiring perfect CSI at the transmitter side is problematic due to the generally data-rate limited feedback link. This limitation raises the question what quantized information should be fed back to the transmitter in order to enable the benefits that MIMO promises.

1.1 Problem Statements

The following section starts by presenting the general system model, as depicted in Fig 1.2, and the general assumptions used throughout the thesis. Subsequently, the more specific system models, and the related problems attacked in this thesis, are introduced.

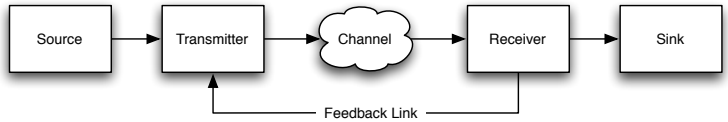

Figure 1.2: General system model for closed-loop wireless communication.

This channel model appears in many different scenarios:

- Narrowband single-carrier transmission with multiple antennas at the transmitter and the receiver
- Transmission over the different subcarriers of a single-antenna orthogonal frequency-division multiplexing (OFDM) system
- Transmission over a wire with interference from different users, e.g., DSL channels

Throughout the thesis we focus on the first scenario, i.e., the narrowband single-carrier transmission. This scenario is modeled using a simple discrete MIMO channel model.

Further, we assume that the CSI is perfectly known at the receiver. The transmission of CSI back to the transmitter is possible through a feedback link. We assume that the feedback link is instantaneous, error-free, and data-rate limited. Thus, due to the data-rate limitation on the feedback link, we must carefully choose what information we feed back to the transmitter. There are basically two major approaches: statistical CSI and instantaneous CSI. Statistical CSI feedback is beneficial if the channel changes randomly, or very fast, between the feedback instances according to given channel statistics. Feeding back instantaneous CSI would thus be suboptimal, since the instantaneous CSI would be outdated quickly. However, for slowly time-varying channels, the feedback of instantaneous CSI is beneficial. This thesis considers mainly slowly time-varying channels, and thus the focus is on the feedback of instantaneous CSI. The general problem of this thesis is the use of the data-rate limited feedback link to improve the transmission from the transmitter to the receiver. However, how the transmission can be improved depends on the detailed system model.

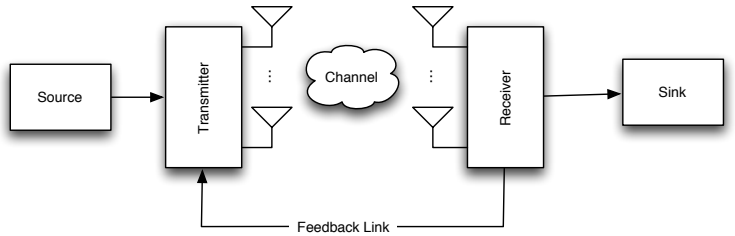

Figure 1.3: General system model for a single-user transmission over a MIMO channel.

The next sections contain more detailed system models. Further, they also contain the corresponding and more precise versions of the general problem. These problems are then subsequently attacked throughout the thesis.

1.1.1 Single-User MIMO Communication

The first part of the thesis, i.e., Part I, considers narrowband single-user MIMO systems. The transmitter has N_T antennas and the receiver has N_R antennas. The use of multiple antennas enables spatial diversity, and allows to transmit multiple symbols simultaneously. The discrete input-output relationship of this system is [7]

$$\mathbf{y}[t] = \mathbf{H}[t]\mathbf{x}[t] + \mathbf{n}[t] \tag{1.1}$$

with $\mathbf{y}[t] \in \mathbb{C}^{N_R \times 1}$ being a vector containing the received symbols, $\mathbf{H}[t] \in \mathbb{C}^{N_R \times N_T}$ the channel matrix, $\mathbf{x}[t] \in \mathbb{C}^{N_T \times 1}$ the transmitted symbol vector, and $\mathbf{n}[t] \in \mathbb{C}^{N_R \times 1}$ the noise vector. $\mathbb{C}$ denotes the field of complex numbers. We assume that the different elements in the noise vector are i.i.d. and complex white Gaussian with zero mean and variance N_0. The transmitted symbols are modeled as a random process, and thus the average transmit energy is denoted $E_T = E(\mathbf{x}^H\mathbf{x})$.

Please note that we omit the time index when the specific time instant is not important.

CSI knowledge at the transmitter side allows the application of linear pre-

coded spatial multiplexing, i.e., linear precoding. Linear precoding multiplies the transmit vector with a precoding matrix $\mathbf{F} \in \mathbb{C}^{N_T \times N_S}$ that is calculated based on the available CSI. The transmitted symbol vector is calculated as

$$\mathbf{x} = \sqrt{E_T}\mathbf{F}\mathbf{s} \tag{1.2}$$

where $\mathbf{s} \in \mathbb{C}^{N_S \times 1}$ contains the data symbols. The data symbols are i.i.d. and selected from a finite constellation. The covariance matrix of $\mathbf{s}$ is $\mathbf{R}_{ss} = E(\mathbf{s}\mathbf{s}^H) = \frac{1}{N_S}\mathbf{I}_{N_S}$. We further assume that $\|\mathbf{F}\|_F^2 = N_S$. This guarantees that $E(\|\mathbf{F}\mathbf{s}\|^2) = 1$, and makes a fair comparison with single-input single-output (SISO) systems possible.

The design of the optimal precoding matrix $\mathbf{F}_I$ depends on which optimization criteria should be optimized, but also on the constraints at the transmitter and the receiver, e.g., transmit power constraints or receiver architectures. The constraints at the transmitter can include a power constraint or the availability of limited or delayed CSI. The receiver can be constrained, in order to reduce complexity, to a linear equalizer.

Assuming a total power constraint, the optimal precoding matrix that maximizes the channel capacity of the effective channel $\mathbf{H}\mathbf{F}_I$ can be written as [4, 8]

$$\mathbf{F}_I = \mathbf{V}\mathbf{D} \tag{1.3}$$

where $\mathbf{V}$ is calculated by the singular value decomposition (SVD) decomposition of the channel $\mathbf{H} = \mathbf{U}\mathbf{\Sigma}\mathbf{V}^H$, and $\mathbf{D}$ is a diagonal power allocation matrix that can be found using the water-filling algorithm [9]. Using the left singular vectors $\mathbf{U}^H$ as an equalizer then decomposes the channel in multiple parallel SISO channels. We will denote this equalizer as the SVD transceiver.

The joint design of precoder and equalizer has a long history [10]. One of the first applications to modern MIMO channels was [11]. There, assuming a linear equalizer $\mathbf{G}^H$ and a power constraint at the transmitter, the precoding matrix $\mathbf{F}$ and $\mathbf{G}$ were jointly designed to minimize the mean square error (MSE) $E(\|\mathbf{s} - \hat{\mathbf{s}}\|^2)$ between the transmitted symbol vector $\mathbf{s}$ and the estimated symbol vector $\hat{\mathbf{s}} = \mathbf{G}^H\mathbf{y}$. The results were extended to include more general power constraints and optimization criteria based on the MSE matrix $E((\mathbf{s}-\hat{\mathbf{s}})(\mathbf{s}-\hat{\mathbf{s}})^H)$

in [12] and [11]. Interestingly, all the presented optimal precoders have the same structure as in (1.3) while only having different power allocation matrices $\mathbf{D}$.

A crucial problem of these designs is the requirement to feed back the full CSI to the transmitter, since the feedback link is generally data-rate limited. A possibility is to quantize the CSI before it is fed back, but this requires the quantization of $N_T N_R$ complex values. The structure of the optimal precoder (1.3) motivates the idea to solely feed back the first N_S columns of the unitary matrix $\mathbf{V}$ and not the power allocation matrix. The resulting precoder matrix has less degrees of freedom than the full channel matrix and can thus be easier quantized. The design of the corresponding precoder codebooks for different linear receivers was investigated in [13]. The time-correlation of the channel can also be used to reduce the required feedback, e.g., [14], [15], and [16]. However, these papers assume a slow fading channel where the precoder is limited to change to a small subset of all the available precoders at the transmitter.

Since vector quantization is a mature field [17], this leads to the first problem that is attacked in this thesis:

Problem 1. *Is it possible to use the available vector quantization techniques to improve the quantization of unitary precoding matrices for single-user MIMO transmission?*

Contribution 1. Chapter 3 presents the novel result to use entropy coding for precoder quantization. The first presented results, originally presented in [18], exploit the time-varying nature of the channel by using entropy coding to reduce the average feedback rate. The transmitter and the receiver share a common codebook that contains the precoding matrices. The receiver has full CSI knowledge, and decides which precoding matrix from the codebook is optimal. The index of this precoding matrix is compressed using entropy coding and is then fed back to the base station. The advantage of the proposed strategy is that we achieve a feedback reduction without a performance loss, compared to [15] where the feedback reduction is achieved by dropping the least-probable codebooks. Further novel results, presented in [19], do not aim to reduce the feedback rate, but instead improve the performance of the resulting linear precoded system under full exploitation of the available feedback rate. In [19] we present both

techniques in the common vector quantization framework, and compare their performances through numerical simulations. In [18, 19] we assume that the statistics of the underlying channel model do not change. We extend the use of entropy coding in [20] to compensate for changing channel statistics. There, both transmitter and receiver track the fed back precoder matrices and estimate the occurrence probabilities of the different precoder matrices after every feedback. These occurrence probabilities are then used to update the entropy code used to feed back the precoder indices. A selection of these results are published in [21]. □

In general, feedback is only possible at fixed instances, e.g., at the beginning of each transmission block. Thus, due to the time-varying nature of the channel, the available CSI becomes quickly outdated between these feedback instances. This raises the following question:

Problem 2. *Can the unitary precoding matrix be efficiently extrapolated based on the previously fed back precoding matrices for single-user MIMO communications?*

A solution is to extrapolate the current unitary precoding matrix using geodesic interpolation [22]. The advantage of geodesic interpolation is that the resulting matrix is already unitary [23].

Contribution 2. In Chapter 4, published as [24], we present an improved SVD transceiver and compare its performance to the minimum mean square error (MMSE) equalizer, assuming precoder extrapolation through geodesic interpolation. □

1.1.2 MISO Broadcast Channel

Part II and Part III of this thesis consider the multiuser multiple-input single-output (MISO) broadcast channel. All the chapters in these parts consider a single-cell scenario. The cell contains a base station with N_T antennas and N_U single-antenna users. We are using space-division multiple access (SDMA), i.e., the base station transmits data to multiple users simultaneously. We assume again a narrowband channel model, and the symbol received by a user i can be

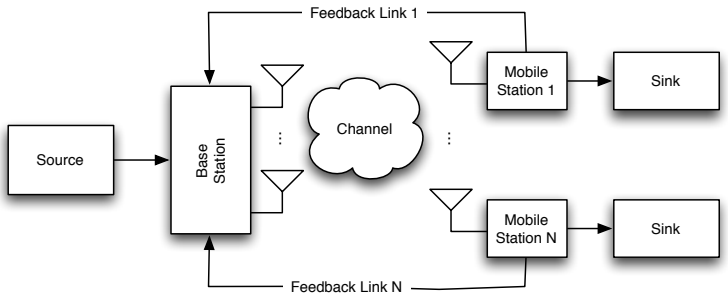

Figure 1.4: General system model for a single-cell MISO broadcast channel with N mobile stations.

written as

$$y_i = \mathbf{h}_i \mathbf{x} + n_i \tag{1.4}$$

where $y_i \in \mathbb{C}$ is the symbol received by user i, $\mathbf{h}_i \in \mathbb{C}^{1 \times N_T}$ the channel of user i, $\mathbf{x} \in \mathbb{C}^{N_T \times 1}$ the vector containing the data transmitted by the base station, and n_i the noise experienced by user i. The noise is modeled as complex white Gaussian with zero mean and variance N_0. Using SDMA the transmitted vector $\mathbf{x}$ is constructed as

$$\mathbf{x} = \sum_{j \in \mathcal{S}} \sqrt{E_j} \mathbf{w}_j s_j \tag{1.5}$$

where the set $\mathcal{S}$ contains all the users scheduled for that time instant, $\mathbf{w}_i$ is the unit-norm beamforming vector used for user i, and s_i is the data symbol transmitted to user i with $E(|s|^2) = 1$. We see that a user i receives interference by the users in $\mathcal{S} \setminus \{i\}$ if their corresponding beamforming vectors are not orthogonal to the channel $\mathbf{h}_i$ of user i. This interference leads to the signal-to-noise-plus-interference ratio (SINR). The SINR for a user i is calculated as

$$\mathrm{SINR}_i = \frac{E_i |\mathbf{h}_i \mathbf{w}_i|^2}{\sum_{j \in \mathcal{S} \setminus \{i\}} E_j |\mathbf{h}_i \mathbf{w}_j|^2 + N_0}. \tag{1.6}$$

Using the SINR's of the scheduled users, the instantaneous sum rate (R) is calculated as

$$R = \sum_{i \in \mathcal{S}} \log\left(1 + \mathrm{SINR}_i\right). \tag{1.7}$$

It was proven in [25] that the optimal sum rate, i.e., the sum rate capacity, is achieved through dirty-paper coding (DPC) [26, 27]. DPC was introduced by Costa in [26] for the SISO channels. Assuming interference on the channel known to the transmitter, DPC adapts the signal so that no penalty due to the interference occurs, i.e., the capacity of the Gaussian channel with interference known to the transmitter is identical to the capacity of the Gaussian channel without interference. An precoding technique based on DPC for the broadcast channel was presented in [27]. However, the drawback of DPC is its high computational complexity. This motivates the research of simpler linear schemes. A simple linear scheme is zero-forcing (ZF) beamforming, where $\mathbf{h}_i \mathbf{w}_j = 0$, $\forall i, j \in \mathcal{S}$, and $i \neq j$. Further, assuming opportunistic scheduling, ZF precoding achieves asymptotically the same sum rate as DPC for an increasing number of users in the cell. However, ZF beamforming requires CSI knowledge at the base station. Assuming that feedback is solely possible over a rate-limited feedback link, this requires an efficient use of the available feedback.

The first problem in this part considers the generation of quantization codebooks for spatially correlated channels.

Problem 3. *Is it possible to design codebooks that minimize the sum rate loss due to quantization for spatially correlated channels?*

Contribution 3. In Chapter 5, published as [28], we start by extending a well-known SISO channel model to the MISO case. The novel channel model allows to simulate a spatial correlation between the users. Next, codebooks are generated for this channel model that minimize the sum rate loss induced by the CSI quantization. Further, the benefit of theses adapted codebooks are depicted through simulations. □

The next problem considers temporally correlated channels.

Problem 4. *Can the current CSI be extrapolated based on the past fed back CSI for temporally correlated channels?*

Contribution 4. We exploit in Chapter 6, published as [29], the temporal correlation of the channel by introducing predictive vector quantization for CSI quantization. Both the transmitter and the receiver predict the current channel based on the previous quantized, and fed back, channel realizations. The receiver then just feeds back the quantized difference between the predicted channel and the true channel. □

It is well known that the availability of CSI at the base station allows to exploit the multiuser diversity [30]. The optimal scheduling scheme that maximizes the sum rate for a given beamforming scheme is opportunistic scheduling [6]. Opportunistic scheduling picks a set of users so that the resulting sum rate is maximized. However, it ignores any fairness issues. A scheduling scheme that realizes perfect fairness is round-robin scheduling. There, the users are scheduled in a predefined order. It achieves perfect fairness but does not achieve the available sum rate capacity. A tradeoff between both scheduling schemes is done by proportional fair scheduling [31], where scheduled users are penalized in order to give users with unfavorable channel conditions a chance.

Problem 5. *Is it possible to create an algorithm that implements round-robin scheduling but still exploits multi-user diversity?*

Contribution 5. We propose in [32] a scheduling scheme for pseudo-round-robin scheduling, i.e., every user in the cell has to be scheduled once inside a block. Further, all the users have to fulfill a strict signal-to-noise-plus-interference ratio (SINR) requirement. The system is using SDMA, i.e., the base station can transmit to multiple users at a time, and the limited feedback is then used to pair the users efficiently.

In [33] we consider real round-robin scheduling. There, the presented algorithm tries to schedule the same set of users in the same slot over multiple blocks, i.e., we assume that every block consists of the same number of slots. The feedback consists of an estimate of the minimum energy that must be assigned to every user so that he can fulfill a predefined SINR constraint. If the sum of the

required minimum energy exceeds the maximally available transmit energy, the worst user in the set is removed, and he has to be rescheduled at a different block. □

1.2 Outline

- Chapter 2: We start by introducing the quantization algorithms used throughout the thesis. We highlight their individual advantages and shortcomings.

- Chapter 3: Here, different possibilities to exploit the data-rate limited feedback link for linear precoded spatial multiplexing are investigated. The chapter was published as

  [21] C. Simon and G. Leus, "Feedback quantization for linear precoded spatial multiplexing," *EURASIP Journal Advances Signal Process.,* vol. 2008 (2008), Article ID 683030, 13 pages, doi:10.1155/2008/683030.

  and the individual results were initially published as:

  [18] C. Simon and G. Leus, "Feedback reduction for spatial multiplexing with linear precoding," in *Proc. IEEE Int. Conf. Acoust., Speech, and Signal Process. (ICASSP),* Honolulu, HI, USA, Apr. 2007.

  [20] C. Simon and G. Leus, "Adaptive feedback reduction for precoded spatial multiplexing MIMO systems," in *Proc. Int. ITG/IEEE Workshop Smart Antennas (WSA),* Vienna, Austria, Feb. 2007.

  [19] G. Leus and C. Simon, "Quantized feedback and feedback reduction for precoded spatial multiplexing MIMO systems," in *Proc. Int. Symp. Signal Process. and Applicat. (ISSPA),* Sharjah, United Arab Emirates, Feb. 2007.

- Chapter 4: This chapter investigates precoder and decoder extrapolation for a linear transceiver assuming a temporally correlated channel. The results have been published in

  [24] G. Leus, C. Simon, and N. Khaled, "Spatial multiplexing with linear precoding in time-varying channels with limited feedback," in *Proc. European Signal Process. Conf. (EUSIPCO),* Florence, Italy, Sept. 2006.

- Chapter 5: An existing channel model is extended to create a spatially correlated broadcast channel model. We create CSI quantization codebooks

for this channel model in order to feed back the CSI from the single-antenna users to a multi-antenna base station. The results have been published in:

[28] R. de Francisco, C. Simon, D. T. Slock, and G. Leus, "Beamforming for correlated broadcast channels with quantized channel state information," in *Proc. IEEE Workshop Signal Process. Advances Wireless Commun. (SPAWC),* Recife, Brazil, July 2008.

- Chapter 6: Predictive vector quantization is used to feed back the CSI from single-antenna users to a multi-antenna base station. The CSI is used for zero-forcing beamforming. The results have been published in:

  [29] C. Simon, R. de Francisco, D. T. Slock, and G. Leus, "Feedback compression for correlated broadcast channels," in *Proc. IEEE Symp. Commun. Vehicular Techn. Benelux (SCVT),* Delft, The Netherlands, Nov. 2007.

- Chapter 7: The next chapter considers scheduling for the broadcast channel. We adapt the BestFit algorithm to work with Grassmannian beamforming. The performance of the two resulting variants are compared by simulations. The results have been published in:

  [32] C. Simon and G. Leus, "Low-delay scheduling for Grassmannian beamforming with a SINR constraint," in *Proc. IEEE Int. Conf. Acoust., Speech, and Signal Process. (ICASSP),* Taipei, Taiwan, Apr. 2009.

- Chapter 8: This chapter considers a novel scheduling algorithm that allows round-robin scheduling for SDMA. All the scheduled users fulfill a strict SINR constraint and the fed back CSI is limited to a scalar. The results have been submitted to:

  [33] C. Simon and G. Leus, "Round-robin scheduling for orthogonal beamforming with limited feedback," *IEEE Trans. Wireless Commun.,* accepted in May 2011 for publication.

- Chapter 9: The final chapter concludes the thesis with a short review and by proposing future work.

Chapter 2

Quantization

This chapter gives a short overview of basic scalar quantization, vector quantization, and the algorithms used to design the quantization codebooks. We limit our presentation of codebook design algorithms to the three most popular algorithms, i.e., the Lloyd algorithm [34], the Generalized Lloyd algorithm (GLA) [35], and Monte-Carlo Codebook Design (MC).

The design of quantization systems has a long history. One of the first papers [36] to discuss the advantages of using nonuniform codebooks over uniform codebooks was published in 1951. The presented asymptotic results were generalized to codebooks with limited size by Lloyd in [34]. He also presented necessary conditions to minimize the average distortion, and proposed two algorithms based on these conditions to find good quantization codebooks for scalar inputs. The first algorithm, i.e., denoted Method 1, will be called the Lloyd algorithm throughout the thesis. The GLA [35] extends the Lloyd algorithm to vector quantization and is the most popular vector quantization algorithm. The notation in this chapter is selected to be close to [17] where an in-depth treatment of quantization can be found.

2.1 Introduction

Quantization is a mapping Q that maps every element from a set $\mathcal{X}$ to a corresponding element from a set $\mathcal{C}$

$$Q : \mathcal{X} \to \mathcal{C} \qquad \text{with } |\mathcal{C}| \leq |\mathcal{X}|. \tag{2.1}$$

The set $\mathcal{C}$ is called the quantization codebook. The size of the quantization codebook is generally limited to fulfill a data-rate constraint. Quantization divides the input space $\mathcal{X}$ into $|\mathcal{C}|$ disjoint regions $\mathcal{R}_i$, $i = 1, \ldots, |\mathcal{C}|$, i.e.,

$$\mathcal{X} = \bigcup_{i=1}^{|\mathcal{C}|} \mathcal{R}_i \qquad \text{and} \qquad \mathcal{R}_i \cap \mathcal{R}_j = \emptyset \qquad \forall i, j. \tag{2.2}$$

Every input element x that lies in the same region $\mathcal{R}_i$ is mapped to the same codebook element c_i

$$Q(x) = \{c_i \in \mathcal{C} \mid x \in \mathcal{R}_i\}. \tag{2.3}$$

Thus, a quantizer is entirely defined by the codebook $\mathcal{C}$ and the quantization regions $\mathcal{R}_i$ with $i = 1, \ldots, |\mathcal{C}|$.

2.2 Distortion Function

The distortion function $d : \mathcal{X} \times \mathcal{C} \to \mathbb{R}$ is a measure for the quality of the quantization process. However, the quality of the quantization often depends on a subjective assessment and thus the selected distortion function has to be chosen according to the application.

The average distortion of the quantization system is the most popular performance metric of a quantization system and is defined as

$$D = E\{d(x, Q(x))\} \tag{2.4}$$

where the expectation is taken over the possible input elements

$$D = \int_{-\infty}^{+\infty} d(x, Q(x)) f_X(x) dx. \tag{2.5}$$

We assume that the input x of the quantizer is a realization of the random variable X and its pdf is denoted $f_X(x)$.

The most common overall distortion used to design a quantization system is the mean-squared error (MSE) between the unquantized element $x \in \mathcal{X}$ and the quantized element $Q(x) \in \mathcal{C}$

$$D = E\{|x - Q(x)|^2\}. \tag{2.6}$$

One of the major advantages of the MSE is that its simple form often leads to simple mathematical expressions. Further it has a physical meaning, i.e., it corresponds to the energy of the error signal. A detailed treatment of the advantages and disadvantages of the MSE as a distortion function can be found in [37].

2.3 Optimality Conditions

The quantization codebook $\mathcal{C}$ should be designed so that the overall distortion D of the quantization system is minimized, i.e.,

$$\mathcal{C}_{\text{opt}} = \arg\min_{\mathcal{C}} D. \tag{2.7}$$

However, solving (2.7) in closed-form is cumbersome since it requires to jointly find the optimal quantization regions and the optimal codebook elements. However, solving the problems separately is straightforward and leads to two necessary conditions that the optimal quantizer must fulfill [34]. The first condition, the so-called *nearest neighbor condition*, defines the optimal quantization regions for a fixed codebook. The second condition, the so-called *centroid condition*, defines the optimal quantization codebook if the quantization regions are fixed. These two necessary conditions yield the topic of this section.

2.3.1 Nearest Neighbor Condition

The nearest neighbor condition states that the optimal quantizer maps an unquantized element x to an element from the codebook $\mathcal{C}$ so that the resulting distortion $d(x, Q(x))$ is minimized

$$Q(x) = \arg\min_{c_i \in \mathcal{C}} d(x, c_i). \tag{2.8}$$

Thus, the quantization regions $\mathcal{R}_i$ for $i = 1, \ldots, |\mathcal{C}|$ can be determined as

$$\mathcal{R}_i = \{x \in \mathcal{X} \mid d(x, c_i) \leq d(x, c_j), \forall j \in \{1, \ldots, |\mathcal{C}|\} \setminus \{i\}\}. \tag{2.9}$$

Note that it is possible that a given input x has the same distortion between two elements in the codebook, i.e., $d(x, c_i) = d(x, c_j)$ with $i \neq j$. In this case, the input symbol x can simply be mapped to one of the two regions, i.e., $\mathcal{R}_i$ or $\mathcal{R}_j$. The simplest solution is to randomly assign this boundary point to one of the regions that minimize the distortion, e.g., to the quantization region with the smallest index. Which one of this regions is selected is irrelevant since they all lead to the same overall distortion.

2.3.2 Centroid Condition

The centroid condition states that all the input symbols from the same region $\mathcal{R}_i$ have to be mapped to the element c_i that minimizes the resulting distortion. The corresponding element, the so-called centroid, c_i is found as

$$c_i = \arg\min_{y} \int_{\mathcal{R}_i} d(x, y) f_X(x) dx. \tag{2.10}$$

For the simple case where the squared error is used as distortion function, $d(x, y) = (x - y)^2$, the centroid is given by

$$c_i = \frac{\int_{\mathcal{R}_i} x f_X(x) dx}{\int_{\mathcal{R}_i} f_X(x) dx}. \tag{2.11}$$

2.4 The Lloyd Algorithm

Besides introducing the optimality conditions [34], Lloyd also proposed two algorithms for scalar quantization. Both algorithms, called Method 1 and Method 2, are described in this section. Method 2 was also independently proposed by Max [38]. Sufficient conditions for the optimality of the Lloyd algorithms were presented in [39].

Please note that we just consider scalar quantization in this section. The extension to vector quantization will be described in the next section.

2.4.1 Method 1

Lloyd's Method 1, depicted in Algorithm 1, starts by choosing a random codebook $\mathcal{C}_0$. The algorithm then calculates the corresponding optimal quantization regions that are given by the nearest neighbor condition. However, the initial codebook is probably not optimal for the given quantization regions, i.e., it does not fulfill the centroid condition. Thus, a new codebook $\mathcal{C}_1$ is calculated that fulfills the centroid condition. Now, the quantization regions are no longer optimal for the new codebook and have to be recalculated. The algorithm continues to iteratively apply the optimality conditions by recalculating the quantization regions and the quantization codebook. The algorithm stops when the overall distortion of the new codebook just provides a minor improvement to the last codebook, i.e., $\frac{D_{j-1}-D_j}{D_{j-1}} \leq \epsilon$ where ϵ is a threshold that is fixed beforehand. However, as Lloyd noted [34], this stationary point is not necessarily the global optimum codebook. Since the resulting codebook is determined by the initial codebook $\mathcal{C}_0$ the algorithm can be run multiple times with different initial codebooks, and finally the codebook with the best overall distortion is selected.

2.4.2 Method 2

In order to simplify the exposition of Method 2, we will assume that the squared error is used as the distortion function. We further assume that the elements in the codebook $\mathcal{C} = \{c_1, \ldots, c_{|\mathcal{C}|}\}$ are ordered, i.e., $c_i < c_j, \forall i < j$.

The algorithm starts by randomly picking a value for c_1. This also fixes

Algorithm 1 Designing a codebook based on the Lloyd algorithm.

1: $j := 0$
2: Generate a random initial codebook $\mathcal{C}_j$
3: Calculate the distortion D_j for the current codebook $\mathcal{C}_j$.
4: **repeat**
5: $j := j + 1$
6: Calculate the optimal quantization region $\mathcal{R}_i$ for every element $c_i \in \mathcal{C}_{j-1}$ for $i = 1, \ldots N$.
7: Calculate the new codebook $\mathcal{C}_j$ by determining the centroid c_i of $\mathcal{R}_i$ for $i = 1, \ldots N$.
8: Calculate the overall distortion D_j for the codebook $\mathcal{C}_j$.
9: **until** $\frac{D_{j-1}-D_j}{D_{j-1}} \leq \epsilon$
10: The final codebook is $\mathcal{C}_j$.

the upper bound of the quantization region $\mathcal{R}_1 = (-\infty, r_1]$ due to the centroid condition (2.10). The upper bound r_1 is found by finding the r_1 that satisfies

$$c_1 = \frac{\int_{-\infty}^{r_1} x f_X(x) dx}{\int_{-\infty}^{r_1} f_X(x) dx}. \tag{2.12}$$

If a closed form solution to r_1 cannot be found, then it can be determined by numerical means. Using the nearest neighbor condition, we find the next codebook element c_2 by choosing the element that fulfills $d(r_1, c_1) = d(r_1, c_2)$. For the simple case of using the squared error as the distortion function, this is

$$c_2 = 2r_1 - c_1. \tag{2.13}$$

The algorithm can now find the upper bound r_2 of region $\mathcal{R}_2 = [r_1, r_2]$ by using the centroid condition (2.10) again. The algorithm continues until all the codebook elements are determined.

We see that the initial random selection of c_1 uniquely determines the resulting codebook. However, the optimal codebook must also fulfill the centroid condition

for the last region, i.e.,

$$c_{|\mathcal{C}|} - \frac{\int_{r_{|\mathcal{C}|-1}}^{+\infty} x f_X(x) dx}{\int_{r_{|\mathcal{C}|-1}}^{+\infty} f_X(x) dx} = 0. \tag{2.14}$$

If the difference in (2.14) is positive (resp. negative), then the initial value c_1 was chosen to be too large (resp. too small), and the algorithm has to restart with a smaller (resp. larger) value of c_1. The difference varies as a continuous function of c_1, and the initial value of c_1 is adapted until the difference becomes lower than some given threshold.

2.4.3 Comparison

The advantage of Method 2 over Method 1 is that the algorithm does not require $f_X(x)$ to be continuous. This makes it a popular algorithm for scalar quantization. However, Method 1 can be extended to vector quantization but not Method 2.

2.5 The Generalized Lloyd Algorithm

The most popular algorithm to design codebooks for vector quantization is the Generalized Lloyd algorithm (GLA) [35]. It extends the Lloyd algorithm to vector quantization, and additionally does not need to know the pdf of the quantizer input. The GLA requires solely a large training set that contains samples of the quantizer input. If the input to the quantizer is ergodic and stationary then the resulting quantizer also performs well for future inputs. The larger the training set, the better the performance of the resulting quantizer. Theoretical results about the convergence of the GLA are published in [40]. There, the convergence has been proven for several distortion functions.

Note, that we use boldface letters to denote the fact that the variables can be vectors.

2.5.1 Algorithm

The input of the GLA is a large training set $\mathcal{T}$ that contains $|\mathcal{T}|$ samples of the quantizer input.

The GLA is identical to the Lloyd algorithm, presented in the previous section, with the exception that it calculates the quantization regions and the centroids without a proper knowledge of the pdf f_X.

Quantization Regions

The precise quantization regions cannot be determined without proper knowledge of the underlying pdf f_X. Alternatively, the training set is partitioned into $|\mathcal{C}|$ disjoint regions

$$\mathcal{T} = \bigcup_{i=1}^{|\mathcal{C}|} \mathcal{P}_i \qquad \text{and} \qquad \mathcal{P}_i \cap \mathcal{P}_j = \emptyset \qquad \forall i, j. \tag{2.15}$$

This is done by uniquely assigning every element in the training set $\mathcal{T}$ to a set $\mathcal{P}_i$ as

$$\mathcal{P}_i = \{\mathbf{x} \in \mathcal{T} \mid d(\mathbf{x}, \mathbf{c}_i) \leq d(\mathbf{x}, \mathbf{c}_j)\} \qquad i \neq j. \tag{2.16}$$

Note that if $d(\mathbf{x}, \mathbf{c}_i) = d(\mathbf{x}, \mathbf{c}_j)$ then $\mathbf{x}$ can be randomly assigned to either $\mathcal{P}_i$ or $\mathcal{P}_j$ The resulting partitions $\mathcal{P}_i$ approximate the optimal quantization regions $\mathcal{R}_i$ for $i = 1, \ldots, |\mathcal{C}|$ if the training set is large enough.

Centroids

For a give partition $\mathcal{P}_i = \{\mathbf{p}_1, \ldots, \mathbf{p}_{|\mathcal{P}_i|}\}$ the centroid is calculated as

$$\mathbf{c}_i = \arg\min_{\mathbf{c}} \sum_{i=1}^{|\mathcal{P}_i|} d(\mathbf{p}_i, \mathbf{c}) \tag{2.17}$$

For the simple case where the squared error is used as distortion function, the centroid is calculated as

$$\mathbf{c}_i = \frac{1}{|\mathcal{P}_i|} \sum_{i=1}^{|\mathcal{P}_i|} \mathbf{p}_i. \tag{2.18}$$

2.5.2 Initial Codebook

The basic GLA starts with a random codebook and then gradually refines it. An additional approach was proposed in [35]. This variant starts by designing a codebook $\mathcal{C}_1$ with $|\mathcal{C}_1| = 1$ entry using the GLA. The element $\mathbf{c}_{1,1}$ in the resulting codebook $\mathcal{C}_1$ is then split into two elements using $\mathbf{c}_{2,1} = \mathbf{c}_{1,1} - \boldsymbol{\epsilon}$ and $\mathbf{c}_{2,2} = \mathbf{c}_{1,1} + \boldsymbol{\epsilon}$, where $\boldsymbol{\epsilon}$ is a fixed perturbation vector. The new codebook $\mathcal{C}_2 = \{\mathbf{c}_{2,1}, \mathbf{c}_{2,2}\}$ is now optimized using the GLA. Once a codebook is found the number of entries is doubled by splitting and the resulting codebook is optimized using the GLA. The algorithm stops when we have found a codebook with the desired number of entries.

2.6 Monte-Carlo Codebook Design

An alternative simple and robust codebook design algorithm is Monte-Carlo codebook design. It randomly generates an initial codebook, and then calculates its performance, e.g., the average distortion, for the given training set. Then, it generates a new codebook, and again calculates the performance for the training set. The performance for both codebooks is compared, and the best codebook is kept. This process is repeated until a predefined stopping condition is fulfilled. The stopping condition can be that a predefined number of random codebooks has been tested, or that the best codebook did not change for a predefined number of iterations.

The big advantage of this approach is its simplicity and the robustness. The algorithm has a small probability to get caught in a local minimum and it is easy to parallelize which is beneficial for a software implementation.

Part I

Linear Precoding for Single-User MIMO Channels

Chapter 3

Feedback Reduction and Optimization*

This chapter addresses Problem 1 of the thesis, i.e., the application of existing vector quantization techniques to quantize unitary precoding matrices. The chapter starts by giving an overview and a comparison of recent feedback quantization schemes for linear precoded spatial multiplexing systems. In addition, feedback compression methods are presented that exploit the time correlation of the channel. These methods can be roughly divided into two classes. The first class tries to minimize the data rate on the feedback link while keeping the performance constant. This class is novel and relies on entropy coding. The second class tries to optimize the performance while using the maximal data rate on the feedback link. This class is presented within the well-developed framework of finite-state vector quantization. Within this class, existing as well as novel methods are presented and compared.

*The results in this chapter have been published in [18–21].

3.1 Introduction

An attractive scheme to make spatial multiplexing more robust against rank deficient channels, and to reduce the receiver complexity, is linear precoding. The linear precoding matrix is a function of the channel state information (CSI), which is, in general, only available at the receiver. Thus, the required information to calculate the precoding matrix must be fed back to the transmitter over a feedback link, which is assumed to be data-rate limited. An important approach to improve the performance of linear precoded spatial multiplexing is optimizing the exploitation of the limited data-rate on the feedback link.

The notion of linear precoding was introduced in [12], there the optimal linear precoder that minimizes the symbol mean square error for linear receivers under different constraints was derived. The bit-error-rate (BER) optimal precoder was introduced in [41], and the capacity optimal precoder in [4]. The first use of partial CSI at the transmitter was presented in [42], where the Lloyd algorithm is used to quantize the CSI. Other approaches focused on feeding back the mean of the channel [43], or the covariance matrix of the channel [44]. An overview of the achievable channel capacity with limited channel knowledge can be found in [45]. Schemes that directly select a quantized precoder from a codebook at the receiver, and feed back the precoder index to the transmitter have been independently proposed in [46] and [47]. There the authors proposed to design the precoder codebooks to maximize a subspace distance between two codebook entries, a problem which is known as the Grassmannian line packing problem. The advantage of directly quantizing the precoder is that the unitary precoder matrix [12] has less degrees of freedom than the full CSI matrix, and is thus more efficient to quantize. Several subspace distances to design the codebooks were proposed in [48], whereas the selected subspace distance depends on the function used to quantize the precoding matrix. In [49] a precoder quantization design criterion was presented that maximizes the capacity of the system and also the corresponding codebook design. A quantization function that directly minimizes the uncoded BER was proposed in [50].

This chapter presents existing and novel schemes for linear precoding in the well-known vector quantization framework. We present the most popular selec-

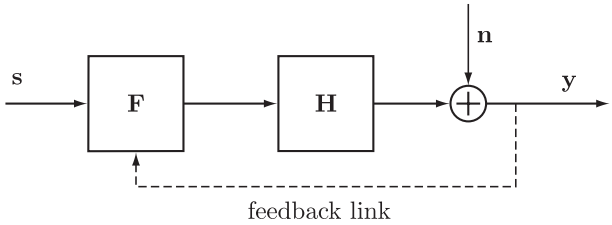

Figure 3.1: System model of the linear precoded spatial multiplexing MIMO system with limited feedback.

tion and distortion criteria used for linear precoding, but also novel techniques like entropy coding, and finite state vector quantization. Further, we show how these schemes can be adapted to changing channel statistics, i.e., to non-stationary sources.

Notation: We use capital boldface letters to denote matrices, e.g., $\mathbf{A}$, and small boldface letters to denote vectors, e.g., $\mathbf{a}$. The Frobenius norm and the 2-norm of a matrix $\mathbf{A}$ is denoted as $\|\mathbf{A}\|_F$, and $\|\mathbf{A}\|_2$, respectively. $E(\cdot)$ denotes expectation and $P(\cdot)$ probability. $[\mathbf{A}]_{m,n}$ is the element in the mth row and nth column of $\mathbf{A}$. The $n \times n$ identity matrix is denoted $\mathbf{I}_n$, and $\mathcal{U}_{m\times n}$ is the set of unitary $m \times n$ matrices. $\mathrm{tr}(\mathbf{A})$ is the trace of $\mathbf{A}$, and $\det(\mathbf{A})$ the determinant of $\mathbf{A}$. $\Re(\mathbf{A})$ is the real part of the complex matrix $\mathbf{A}$.

3.2 System Model

Throughout the chapter, we assume a narrowband spatial multiplexing MIMO system with N_T transmit and N_R receive antennas. The system transmits $N_S \leq \min(N_T, N_R)$ symbol streams, as depicted in Fig. 3.1.

The system equation at time instant t is

$$\mathbf{y}[t] = \mathbf{H}[t]\sqrt{E_T}\mathbf{F}[t]\mathbf{s}[t] + \mathbf{n}[t], \tag{3.1}$$

where $\mathbf{y}[t] \in \mathbb{C}^{N_R\times 1}$ is the received vector, $\mathbf{n}[t] \in \mathbb{C}^{N_R\times 1}$ is the additive noise vector, $\mathbf{s}[t] \in \mathbb{C}^{N_S\times 1}$ is the data symbol vector, $\mathbf{H}[t] \in \mathbb{C}^{N_R\times N_T}$ is the channel matrix, E_T is the transmit energy, and $\mathbf{F}[t] \in \mathbb{C}^{N_T\times N_S}$ is the linear precoding

matrix. We assume the data symbol vector $\mathbf{s}[t]$ is zero mean spatially and temporally white distributed over a complex finite alphabet, e.g., the entries belong to a QAM alphabet $\mathcal{A}$, and the noise vector $\mathbf{n}[t]$ is zero mean spatially and temporally white complex Gaussian distributed. The channel matrix $\mathbf{H}[t]$ is zero mean possibly spatially and temporally correlated complex Gaussian distributed. We assume without loss of generality that the symbols and the noise have unit variance.

The singular value decomposition (SVD) of $\mathbf{H}[t]$ is defined as

$$\mathbf{H}[t] = \bar{\mathbf{U}}[t]\bar{\mathbf{\Sigma}}[t]\bar{\mathbf{V}}^H[t] \tag{3.2}$$

where $\bar{\mathbf{U}}[t] \in \mathcal{U}_{N_R \times N_R}$, $\bar{\mathbf{V}}[t] \in \mathcal{U}_{N_T \times N_T}$, and $\bar{\mathbf{\Sigma}}[t]$ is a real non-negative diagonal $N_R \times N_T$ matrix (the diagonal starts in the top left corner) with non-increasing diagonal entries. The columns of $\bar{\mathbf{U}}[t]$ and $\bar{\mathbf{V}}[t]$ are called the left and right singular vectors, respectively, whereas the diagonal entries of $\bar{\mathbf{\Sigma}}[t]$ are the corresponding singular values. Only focusing on the N_S strongest modes of the channel (the ones with the largest singular values), let us define $\mathbf{U}[t] = [\bar{\mathbf{U}}[t]]_{:,1:N_S} \in \mathcal{U}_{N_R \times N_S}$, $\mathbf{V}[t] = [\bar{\mathbf{V}}[t]]_{:,1:N_S} \in \mathcal{U}_{N_T \times N_S}$, and $\mathbf{\Sigma}[t] = [\bar{\mathbf{\Sigma}}[t]]_{1:N_S,1:N_S}$, where $[\mathbf{A}]_{a:b,c:d}$ selects the submatrix of $\mathbf{A}$ on the rows a to b and the columns c to d, and the range indices are omitted when all rows or columns should be selected.

Many studies have been carried out to derive the optimal precoding matrix for a certain performance measure, see [4, 12, 41, 51]. In general, the optimal precoding matrix looks like

$$\mathbf{F}_{\text{opt}}[t] = \mathbf{V}[t]\mathbf{\Theta}[t]\mathbf{M}[t], \tag{3.3}$$

where $\mathbf{\Theta}[t] \in \mathbb{C}^{N_S \times N_S}$ is a diagonal unitary power loading matrix, and $\mathbf{M}[t] \in \mathcal{U}_{N_S \times N_S}$ is a unitary mixing matrix. For some performance measures, the mixing matrix is arbitrary, whereas for other performance measures its value matters. In any case, it has been shown that for low-rate feedback channels, it is better not to feed back the power loading matrix and to stick to feeding back a unitary precoder [52]. That is why we will limit the precoding matrix $\mathbf{F}$ to be unitary, i.e., $\mathbf{F} \in \mathcal{U}_{N_T \times N_S}$.

The maximum data rate on the feedback link is assumed to be R bits per

channel use, and the feedback is assumed to be instantaneous and error-free. We consider two different types of feedback channels: a dedicated feedback channel and a non-dedicated feedback channel. A dedicated feedback channel is only used to transmit the precoder index to the transmitter, whereas a non-dedicated feedback channel is also used for data transmission. The transmission is organized in a block-wise fashion, i.e., feedback is only possible at the beginning of each new block, and every block has a duration of T_f. We assume the channel is perfectly known at the beginning of every block.

3.3 Vector Quantization (VQ)

The data-rate limited feedback link requires quantization of the channel matrix, resulting in a unitary precoder. The simplest approach is to use a memoryless vector quantizer (VQ), which quantizes every channel matrix $\mathbf{H}[t]$ separately. Hence, we can drop the time index t everywhere in this section. In memoryless VQ, we select a unitary $N_T \times N_S$ matrix $\mathbf{F}_i$ from a codebook $\mathcal{C} = \{\mathbf{F}_1, \ldots, \mathbf{F}_K\}$ that minimizes or maximizes a given selection function S. The size of the codebook $\mathcal{C}$ is denoted $K = |\mathcal{C}|$. We will denote $Q(\mathbf{H})$ as the quantized version of the channel matrix, but note that it actually represents the unitary precoder. More specifically, for a given selection function S and a given codebook $\mathcal{C}$, $Q(\mathbf{H})$ can be defined as

$$Q(\mathbf{H}) = \arg \min_{\mathbf{F} \in \mathcal{C}} / \max S(\mathbf{H}, \mathbf{F}), \tag{3.4}$$

where we take the minimum or the maximum depending on the selection function S. The quantization process can be further separated into an encoding step and a decoding step. The encoder α maps the channel into one of K precoder indices, which for simplicity reasons can be represented by the set $\mathcal{I} = \{1, 2, \ldots, K\}$:

$$\alpha(\mathbf{H}) = \arg \min_{i \in \mathcal{I}} / \max S(\mathbf{H}, \mathbf{F}_i). \tag{3.5}$$

precoders	bitwords non-dedicated	bitwords dedicated
$\mathbf{F}_1$	$w_1 = 00$	$w_1 = /$
$\mathbf{F}_2$	$w_2 = 01$	$w_2 = 0$
$\mathbf{F}_3$	$w_3 = 10$	$w_3 = 1$
$\mathbf{F}_4$	$w_4 = 11$	$w_4 = 00$

Table 3.1: Example of a 4-entry ($K = 4$) codebook for a non-dedicated and dedicated feedback link.

The decoder β simply maps the precoder index into one of the K precoders:

$$\beta(i) = \mathbf{F}_i. \tag{3.6}$$

So we actually have

$$Q(\mathbf{H}) = \beta(\alpha(\mathbf{H})).$$

Note that the index $i \in \mathcal{I}$ is transmitted over the feedback channel as a bitword w_i. What type of bitwords we have to feed back strongly depends on the type of feedback link: dedicated or non-dedicated. In case of a non-dedicated feedback channel, the transmitter has to be able to differentiate between a bitword and the data. This means the bitwords should be instantaneously decodable and thus prefix-free (PF), i.e., a bitword can not contain any other bitword as a prefix. This is not the case in a dedicated feedback channel, where we can use non-prefix-free (NPF) bitwords. If the quantizer is well-designed, all precoders $\mathbf{F}_i$ have more or less the same probability. Under that assumption, we can think of two ways to design our bitwords w_i. For a non-dedicated feedback link, we can take K equal-length PF bitwords, leading to a feedback rate of $\lceil \log_2 K \rceil$ bits per channel use. For a dedicated feedback link, however, we can take any K bitwords with the smallest average length, leading to an average feedback rate of $1/K \sum_{i=1}^{K} \lfloor \log_2 i \rfloor$. An example is given in Table 3.1, where we assume a codebook with $K = 4$ entries. Next we focus on a number of selection functions for linear precoding, and we discuss the design of precoder codebooks.

3.3.1 Precoder Selection

In this section, we will give an overview of some common selection functions S that have been proposed in recent literature. Whether we have to minimize or to maximize the selection function will be clear from the context. In [48], selection criteria are derived based on different performance measures. Optimizing the performance of the maximum likelihood (ML) receiver is related to maximizing the minimum Euclidean distance between any two possible noiseless received vectors:

$$S_{\mathrm{ML}}(\mathbf{H},\mathbf{F}) = \min_{\mathbf{s}_1,\mathbf{s}_2 \in \mathcal{A}^{N_S \times 1}, \mathbf{s}_1 \neq \mathbf{s}_2} \left\| \mathbf{HF}(\mathbf{s}_1 - \mathbf{s}_2) \right\|_2 . \tag{3.7}$$

For linear receivers, two performance measures are considered in [48]: the minimum SNR on the substreams and the trace or determinant of the MSE matrix. Maximizing the first measure for the zero forcing (ZF) receiver is related to maximizing the minimum singular value (MSV) of the effective channel $\mathbf{HF}$:

$$S_{\mathrm{MSV}}(\mathbf{H},\mathbf{F}) = \lambda_{\min}\left\{\mathbf{HF}\right\}, \tag{3.8}$$

where $\lambda_{\min}\left\{\mathbf{A}\right\}$ denotes the MSV of the matrix $\mathbf{A}$. Minimizing the second measure for the minimum mean square error (MMSE) receiver, leads to minimizing the following selection function:

$$S_{\mathrm{MSE}}(\mathbf{H},\mathbf{F}) = m(\mathbf{I}_{N_S} + \mathbf{F}^H\mathbf{H}^H\mathbf{HF})^{-1}, \tag{3.9}$$

where $m = \mathrm{tr}$ or $m = \det$. Finally, [48] also proposes to maximize the mutual information (MI) between the transmitted symbol vector $\mathbf{s}$ and the received symbol vector $\mathbf{y}$ over the effective channel $\mathbf{HF}$:

$$S_{\mathrm{MI}}(\mathbf{H},\mathbf{F}) = \log_2 \det(\mathbf{I}_{N_S} + \mathbf{F}^H\mathbf{H}^H\mathbf{HF}). \tag{3.10}$$

It has been shown in [48] that the above performance measures can be associated to a subspace distance between the right singular vectors of $\mathbf{H}$, collected in $\mathbf{V}$, and $\mathbf{F}$. As such this subspace distance could also be used as the selection function to be minimized. The performance of the ML receiver, the minimum

SNR on the substreams for the ZF receiver, and the trace of the MSE matrix for the MMSE receiver are all related to the projection 2-norm distance:

$$S_{\mathrm{P2}}(\mathbf{H},\mathbf{F}) = d_{\mathrm{P2}}(\mathbf{V},\mathbf{F}) = \|\mathbf{V}\mathbf{V}^H - \mathbf{F}\mathbf{F}^H\|_2, \tag{3.11}$$

whereas the determinant of the MSE matrix for the MMSE receiver and the MI criterion can be connected to the Fubini-Study distance:

$$S_{\mathrm{FS}}(\mathbf{H},\mathbf{F}) = d_{\mathrm{FS}}(\mathbf{V},\mathbf{F}) = \arccos|\det(\mathbf{V}^H\mathbf{F})|. \tag{3.12}$$

Next to minimizing those subspace distances, minimizing the chordal distance is also used as selection criterion:

$$\begin{aligned} S_C(\mathbf{H},\mathbf{F}) = d_C(\mathbf{V},\mathbf{F}) &= 1/\sqrt{2}\|\mathbf{V}\mathbf{V}^H - \mathbf{F}\mathbf{F}^H\|_F \\ &= \sqrt{\mathrm{tr}(\mathbf{I}_{N_S} - \mathbf{V}^H\mathbf{F}\mathbf{F}^H\mathbf{V})}. \end{aligned} \tag{3.13}$$

This function is related to the performance of an orthogonal space-time block code (OSTBC) that is used on top of the precoder [53].

For all the above selection criteria the optimal unitary precoder is given by $\mathbf{V}\mathbf{M}$, where $\mathbf{M}$ is an arbitrary $N_S \times N_S$ unitary matrix, i.e., $\mathbf{M} \in \mathcal{U}_{N_S \times N_S}$. This unitary ambiguity can be a problem when we are interested in other performance measures, such as uncoded bit-error-rate (BER) for instance. We know that in that case, the actual structure of the ambiguity matrix becomes important [50]. One solution could of course be to simply minimize the BER:

$$S_{\mathrm{BER}}(\mathbf{H},\mathbf{F}) = \mathrm{BER}(\mathbf{H},\mathbf{F}). \tag{3.14}$$

However, this is often difficult to compute. A simpler solution might be to encode $\mathbf{V}$ using VQ and to adopt the optimal (or a suboptimal) unitary mixing matrix $\mathbf{M}$ according to [50]. Hence, in that case, we do not use $\mathbf{F}_i$ but $\mathbf{F}_i\mathbf{M}$ as a precoder at the transmitter. We could encode $\mathbf{V}$ for instance by minimizing the Frobenius

norm between $\mathbf{V}$ and $\mathbf{F}$ [53]:

$$\begin{aligned} S_F(\mathbf{H},\mathbf{F}) &= d_F(\mathbf{V},\mathbf{F}) = \|\mathbf{V}-\mathbf{F}\|_F \\ &= \sqrt{2\,\mathrm{tr}(\mathbf{I}_{N_S} - \Re(\mathbf{V}^H\mathbf{F}))}. \end{aligned} \tag{3.15}$$

This selection function is however not invariant to a phase shift of the singular vectors collected in $\mathbf{V}$. That is why the Frobenius norm has been extended to the so-called modified Frobenius norm [24]:

$$\begin{aligned} S_{\mathrm{MF}}(\mathbf{H},\mathbf{F}) &= d_{\mathrm{MF}}(\mathbf{V},\mathbf{F}) = \underset{\boldsymbol{\Theta}\in\mathcal{D}_{N_S}}{\arg\min}\,\|\mathbf{V}\boldsymbol{\Theta}-\mathbf{F}\|_F \\ &= \|\mathbf{V}\,\mathrm{diag}(\mathbf{V}^H\mathbf{F})\,\mathrm{diag}(|\mathbf{V}^H\mathbf{F}|)^{-1} - \mathbf{F}\|_F \\ &= \sqrt{2\,\mathrm{tr}(\mathbf{I}_{N_S} - |\mathbf{V}^H\mathbf{F}|)}, \end{aligned} \tag{3.16}$$

where $\mathcal{D}_n \subset \mathcal{U}_{n\times n}$ is the set of all complex, diagonal, and unitary $n\times n$ matrices. Notice how through the use of the real or absolute value of $\mathbf{V}^H\mathbf{F}$, instead of the product $\mathbf{V}^H\mathbf{F}\mathbf{F}^H\mathbf{V}$ in (3.13), we truly encode $\mathbf{V}$ instead of its subspace. Let us now discuss the codebook design.

3.3.2 Codebook Design

In general, a codebook design aims at finding a set of precoders $\mathcal{C}$ that minimizes some average distortion:

$$D_{\mathrm{av}} = \int_{\mathbb{C}^{N_R\times N_T}} D(\mathbf{H},Q(\mathbf{H}))p(\mathbf{H})d\mathbf{H}, \tag{3.17}$$

where $D(\mathbf{H},Q(\mathbf{H}))$ is the distortion between $\mathbf{H}$ and $Q(\mathbf{H})$, and $p(\mathbf{H})$ is the probability density function (PDF) of the channel matrix $\mathbf{H}$. The distortion function D can take many different forms depending on the performance measure we are interested in (as was the case for the selection function). In [48], it has been shown that if we are interested in the performance of the ML receiver, the minimum SNR on the substreams for the ZF receiver, or the trace of the MSE matrix for the MMSE receiver, we can take as distortion function, the squared projection 2-norm distance between $\mathbf{V}$ and $Q(\mathbf{H})$: $D_{\mathrm{P2}}(\mathbf{H},Q(\mathbf{H})) = d^2_{\mathrm{P2}}(\mathbf{V},Q(\mathbf{H}))$. On the

other hand, if we care about the determinant of the MSE matrix for the MMSE receiver or the MI, we should take the squared Fubini-Study distance between $\mathbf{V}$ and $Q(\mathbf{H})$ as distortion function: $D_{\mathrm{FS}}(\mathbf{H}, Q(\mathbf{H})) = d^2_{\mathrm{FS}}(\mathbf{V}, Q(\mathbf{H}))$. Finally, the distortion function related to the performance of an STBC that is used on top of the precoder is presented in [53] as $D_C(\mathbf{H}, Q(\mathbf{H})) = d^2_C(\mathbf{V}, Q(\mathbf{H})) = \mathrm{tr}(\mathbf{I}_{N_S} - \mathbf{V}^H Q(\mathbf{H}) Q(\mathbf{H})^H \mathbf{V})$. The reason why squared subspace distances are used as distortion functions (and not the performance measures themselves) is because they lead to simpler design procedures as detailed later on.

In [49], an alternative and more exact distortion measure for the MI is proposed, namely the capacity loss introduced by quantization:

$$D_{\mathrm{CL}}(\mathbf{H}, Q(\mathbf{H})) = \mathrm{tr}(\mathbf{\Lambda} - \mathbf{\Lambda}\mathbf{V}^H Q(\mathbf{H}) Q(\mathbf{H})^H \mathbf{V}), \tag{3.18}$$

where $\mathbf{\Lambda} = (\mathbf{I}_{N_S} + \mathbf{\Sigma}^2)^{-1}\mathbf{\Sigma}^2$. Note that this distortion function converges to the squared chordal distance D_C when the diagonal elements of $\mathbf{\Sigma}^2$ go to infinity.

All the above distortion functions are invariant to a left multiplication of the precoder with a unitary matrix. As already indicated in the previous section, this could create a problem when performance measures like the uncoded BER are considered. Taking the distortion function equal to the BER, i.e., $D_{\mathrm{BER}}(\mathbf{H}, Q(\mathbf{H})) = \mathrm{BER}(\mathbf{H}, Q(\mathbf{H}))$ leads to a difficult codebook design. But as before, we could take the squared Frobenius norm or squared modified Frobenius norm between $\mathbf{V}$ and $Q(\mathbf{H})$ as a distortion function to solve this complexity problem: $D_F(\mathbf{H}, Q(\mathbf{H})) = 2\,\mathrm{tr}(\mathbf{I}_{N_S} - \Re(\mathbf{V}^H Q(\mathbf{H})))$, $D_{\mathrm{MF}}(\mathbf{H}, Q(\mathbf{H})) = 2\,\mathrm{tr}(\mathbf{I}_{N_S} - |\mathbf{V}^H Q(\mathbf{H})|)$. In this case our goal is again to feedback $\mathbf{V}$, and we will not use the precoder $Q(\mathbf{H})$ but $Q(\mathbf{H})\mathbf{M}$ at the transmitter, where $\mathbf{M}$ is the optimal (or a suboptimal) unitary mixing matrix [50].

Now the question is how we can solve (3.17) for a certain distortion function. We can basically distinguish between three different approaches: Grassmannian subspace packing, the generalized Lloyd (GL) algorithm, and the Monte-Carlo (MC) algorithm.

Grassmannian Subspace Packing

In case the distortion function is a subspace distance and the channel is spatially white, we can simplify (3.17) by means of a Grassmannian subspace packing problem. In such a problem, the objective is to find a set of unitary precoders that maximizes the minimal subspace distance between them [48, 53]:

$$\max_{\mathcal{C}} \min_{\substack{\mathbf{F}_i, \mathbf{F}_j \in \mathcal{C} \\ \mathbf{F}_i \neq \mathbf{F}_j}} d(\mathbf{F}_i, \mathbf{F}_j), \tag{3.19}$$

where d is any of the subspace distances we discussed above. Of course, such a codebook can also be used when the channel is not spatially white, but the performance will decrease with an increased spatial correlation of the channel.

Unfortunately, there still does not exist a closed form solution to design such codedooks. However, good codebooks, i.e., codebooks that are sufficient for practical applications, can be designed using numerical algorithms [50, 54].

Generalized Lloyd Algorithm

The generalized Lloyd (GL) algorithm tries to solve (3.17) by iteratively optimizing the encoder and the decoder [17, 35]. For a given decoder β, the encoder is optimized by taking the precoder index leading to the smallest distortion (the so-called nearest neighbor condition):

$$\alpha(\mathbf{H}) = \arg\min_{i \in \mathcal{I}} D(\mathbf{H}, \beta(i)), \tag{3.20}$$

thereby splitting the space of channel matrices into K channel regions $\mathcal{R}_i$, $i \in \mathcal{I}$:

$$\mathcal{R}_i = \{\mathbf{H} : D(\mathbf{H}, \mathbf{F}_i) \leq D(\mathbf{H}, \mathbf{F}_j), \mathbf{F}_i, \mathbf{F}_j \in \mathcal{C}, \mathbf{F}_i \neq \mathbf{F}_j\}. \tag{3.21}$$

On the other hand, for a given encoder α, the decoder β is optimized by taking the centroid of the related channel region (the so-called centroid condition):

$$\beta(i) = \arg\min_{\mathbf{F} \in \mathcal{U}_{N_T, N_S}} \int_{\mathcal{R}_i} D(\mathbf{H}, \mathbf{F}) p(\mathbf{H}) d\mathbf{H}. \tag{3.22}$$

The GL algorithm converges to a local minimum, which might not necessarily be the global minimum. To avoid working with the continuous channel distribution, the GL algorithm makes use of a set of training channels $\mathcal{T} = \{\mathbf{H}^{(r)}\}$, where r is the realization index. This set can be interpreted as the discrete channel distribution that approximates the continuous one. The more training vectors in the set, the better the approximation. Computing the exact centroid based on $\mathcal{T}$ is not always easy [40]. For the squared subspace distances as well as the capacity loss distortion function in (3.18), closed form expressions for the centroid exist. However, for the BER and even the squared Frobenius norm or squared modified Frobenius norm, a closed form expression does not exist. For those distortion functions, we simply apply a brute-force (approximate) centroid computation by exhaustively searching the best possible candidate among the set of matrices $\mathbf{V}^{(r)}$ for which $\mathbf{H}^{(r)}$ belongs to the related region.

Monte-Carlo Algorithm

Another interesting approach is the pure Monte-Carlo based design. Instead of trying to optimize an existing codebook, this design randomly generates codebooks, checks the average distortion (3.17) of these codebooks, and keeps the best one. As for the GL algorithm, we will make use of the set of training channels $\mathcal{T}$ to approximate the continuous channel distribution. Although this algorithm becomes computationally expensive for large dimensions, for small dimensions we have observed that the MC algorithm is a very good alternative to Grassmannian subspace packing or the GL algorithm.

3.4 Feedback Compression Through Entropy Coding

This section explores methods to compress the feedback requirements on the feedback link, without sacrificing performance. It uses variable-rate codes to encode highly probable precoder matrices with small bitwords and less probable precoder matrices with longer bitwords. This is called entropy coding [17]. However, as we already indicated in Section 3.3, if the memoryless VQ is well-designed all

precoders $\mathbf{F}_i$ have more or less the same probability. We therefore try to exploit the time correlation of the channel and make use of the transition probabilities between precoders instead of the occurrence probabilities. Hence, instead of assigning a bitword w_i to a precoder $\mathbf{F}_i$, we assign a bitword $w_{i,j}$ to a precoder $\mathbf{F}_i$ if the previous precoder was the precoder $\mathbf{F}_j$. Our goal then is to minimize the average length

$$\sum_{i=1}^{K} l(w_{i,j}) P(Q(\mathbf{H}[t]) = \mathbf{F}_i \,|\, Q(\mathbf{H}[t-1]) = \mathbf{F}_j), \tag{3.23}$$

where $l(w_{i,j})$ is the length of the bitword $w_{i,j}$ and $P_{i,j} = P(Q(\mathbf{H}[t]) = \mathbf{F}_i \,|\, Q(\mathbf{H}[t-1]) = \mathbf{F}_j)$ is the transition probability from $\mathbf{F}_j$ to $\mathbf{F}_i$. Depending on the type of feedback channel, we obtain different solutions for (3.23). For a non-dedicated feedback link, or in other words for PF bitwords, the solution of (3.23) is given by the Huffman code [9]. For a dedicated feedback link, or in other words for NPF bitwords, the solution of (3.23) is simply given by selecting any K bitwords with the smallest possible average length, and assigning the longest (smallest) bitwords to the lowest (highest) transition probabilities.

An example of a codebook for a dedicated feedback link and a non-dedicated feedback link is depicted in Table 3.2. The transition probabilities are estimated through Monte-Carlo simulations. This example assumes that the previous quantized precoder is $Q(\mathbf{H}[t-1]) = \mathbf{F}_8$. Due to the time correlation of the channel, the most probable precoder in this example at time instant t is then again $\mathbf{F}_8$. Thus, the most probable precoder matrix $\mathbf{F}_8$ gets a short bitword assigned, whereas the precoders with lower probabilities get longer bitwords assigned.

Please note that for OFDM, where several precoder matrices for different tones are transmitted at the same time instant, the individual precoding matrices do not need to be instantaneously decodable. They can be jointly encoded, e.g., through the use of arithmetic coding.

The scheme can be extended to incorporate error correcting codes to make it robust against errors on the feedback channel.

The above techniques rely on the exact knowledge of or the knowledge of the ordering of the transition probabilities between the past precoder $Q(\mathbf{H}[t-1])$ and the actual precoder $Q(\mathbf{H}[t])$. Unfortunately, a closed form expression of

Codebook	$P_{i,8}$	Huffman Code	NPF Code
$\mathbf{F}_8$	0.25	01	/
$\mathbf{F}_2$	0.20	11	0
$\mathbf{F}_7$	0.18	000	1
$\mathbf{F}_4$	0.16	001	00
$\mathbf{F}_3$	0.10	101	01
$\mathbf{F}_6$	0.08	1000	10
$\mathbf{F}_5$	0.02	10010	11
$\mathbf{F}_1$	0.01	10011	000

Table 3.2: Example of feedback compression through entropy coding. ($P_{i,8} = P(Q(\mathbf{H}[t]) = \mathbf{F}_i \,|\, Q(\mathbf{H}[t-1]) = \mathbf{F}_8)$)

the transition probabilities is not known, and difficult to derive due to the non-linearity of the quantization. For the special case of known channel statistics, they can be estimated offline through a Monte-Carlo approach [55]. However, in practice the underlying channel statistics are unknown, or are changing at runtime. The next section provides a solution to this problem.

It is possible to adaptively estimate the transition probabilities at runtime. This allows to adapt the used entropy code to changing channel statistics. The algorithm starts by assuming that all the different transitions are equiprobable. After each feedback, the transition probabilities are updated depending on the feedback. If the feedback at time instant $t-1$ signifies a switch from precoder $\mathbf{F}_j$ to precoder $\mathbf{F}_i$, then the transition probability $P_{i,j}$ for time instant t is updated as [17]

$$P_{i,j}[t] = \frac{(N-1)P_{i,j}[t-1]+1}{N}. \tag{3.24}$$

The remaining transition probabilities are updated as

$$P_{k,j}[t] = \frac{(N-1)P_{k,j}[t-1]}{N} \qquad \text{for} \quad k \neq i. \tag{3.25}$$

The factor N controls how fast or how accurate the probabilities are estimated. Larger values of N lead to a smaller increase or decrease after each iteration, and thus, to a slower, but more accurate estimation. Since both the transmitter and receiver know the feedback, they can both keep track of the changed transition

probabilities. The changed transition probabilities are then used, both at the transmitted and at the receiver, to update the used entropy code on the feedback link. Note that this approach relies on the errorless transmission of the feedback. Feedback errors would lead to different codebooks at the transmitter and the receiver.

Instead of updating the transition probabilities, one can also directly update the Huffman code, in the case of a non-dedicated feedback link [56–58]. However, the effect is very similar to the two step approach of first updating the transition probabilities and then computing the new Huffman code.

3.5 Finite-State Vector Quantization (FSVQ)

In this section, we will look at a number of methods to improve the performance exploiting the maximal data rate of R bits per channel use on the feedback channel. We will present the different methods in the well-developed framework of finite-state vector quantization (FSVQ), and we closely follow [17].

3.5.1 Introduction

Before introducing FSVQ, let us consider a so-called switched VQ, consisting of a finite number of memoryless VQs and a classifier that periodically decides which memoryless VQ is best and feeds back the index of this VQ to the decoder. The decision of the classifier is generally based on an estimate of the statistics of the channel. An example of this approach is given in [59], where the different memoryless VQ codebooks are constructed by rotating and scaling a specific root codebook. The drawback of this approach is of course the additional feedback overhead due to the fact that the classifier periodically feeds back the index of the best memoryless VQ.

FSVQ solves this problem since it does not require any additional side information. An FSVQ has some built in mechanism to determine which of the memoryless VQs should be used to transform the current channel into a quantization index. It is the current state that determines which memoryless VQ to employ, and that is why the related codebook is called the state codebook. The

current state together with the obtained quantization index then determines the next state through the so-called next-state function. This is explained in more detail next.

Suppose we have a set $\mathcal{S}$ of $N_{\mathcal{S}}$ states, which without loss of generality can be denoted as $\mathcal{S} = \{1, 2, \ldots, N_{\mathcal{S}}\}$. Every state $s \in \mathcal{S}$ is related to a state codebook $\mathcal{C}_s = \{\mathbf{F}_{1,s}, \mathbf{F}_{2,s}, \ldots, \mathbf{F}_{K,s}\}$. The encoder α maps the current channel and state into one of K quantization indices, which for simplicity reasons can be represented by the set $\mathcal{I} = \{1, 2, \ldots, K\}$. Assume for instance that at time instant t the channel and state are given by $\mathbf{H}[t]$ and $s[t]$, respectively, then we can describe our encoder as

$$\alpha(\mathbf{H}[t], s[t]) = \arg\min_{i \in \mathcal{I}} S(\mathbf{H}[t], \mathbf{F}_{i,s[t]}), \tag{3.26}$$

where S is one of the selection functions described in Section 3.3.1. The decoder β simply maps the current quantization index and state into one of the K precoders of the related state codebook. Assume for instance that at time instant t the quantization index and state are given by $i[t]$ and $s[t]$, respectively, then our decoder can be expressed as

$$\beta(i[t], s[t]) = \mathbf{F}_{i[t],s[t]}. \tag{3.27}$$

So the overall quantization procedure can be written as

$$Q(\mathbf{H}[t], s[t]) = \beta(\alpha(\mathbf{H}[t], s[t]), s[t]). \tag{3.28}$$

Finally, we need a mechanism that tells us how to go from one state to the next. This is obtained by the next-state function. Keeping in mind that both the encoder and decoder should be able to track the state, the next-state function f_{NS} can only be guided by the quantization index. Assume that at time instant t the current quantization index and state are given by $i[t]$ and $s[t]$, respectively, then the next-state function can be expressed as:

$$s[t+1] = f_{\text{NS}}(i[t], s[t]). \tag{3.29}$$

An FSVQ is now completely determined by the state space $\mathcal{S}$, the state code-

books $\mathcal{C}_s = \{\mathbf{F}_{1,s}, \mathbf{F}_{2,s}, \ldots, \mathbf{F}_{K,s}\}$ for all $s \in \mathcal{S}$, the next state function f_{NS}, and the initial state $s[0]$. Note that the union of all state codebooks is called the super codebook $\mathcal{C} = \bigcup_{s\in\mathcal{S}} \mathcal{C}_s$, which contains no more than $KN_{\mathcal{S}}$ precoders.

As in memoryless VQ, we can consider two ways to assign bitwords w_i to the indices $i \in \mathcal{I}$. We can use K equal-length PF bitwords (for a non-dedicated feedback link), with a feedback rate of $\lceil \log_2 K \rceil$ bits per channel use, or K increasing-length NPF bitwords (for a dedicated feedback link), with an average feedback rate of $1/K \sum_{i=1}^{K} \lfloor \log_2 i \rfloor$. This assignment is again based on the assumption that for a certain state s, the precoders $\mathbf{F}_{i,s}$ have more or less the same probability.

As will be illustrated later on, the design of an FSVQ is often based on an initial classifier that classifies channels into states. Such a classifier could for instance be a simple memoryless VQ with a codebook $\mathcal{C}_{\text{class}} = \{\mathbf{F}_1, \mathbf{F}_2, \ldots, \mathbf{F}_{N_{\mathcal{S}}}\}$ that assigns a state $s \in \mathcal{S}$ to a channel $\mathbf{H}[t]$ using the function f_{class}:

$$f_{\text{class}}(\mathbf{H}[t]) = \arg\min_{s\in\mathcal{S}} S_{\text{class}}(\mathbf{H}[t], \mathbf{F}_s), \tag{3.30}$$

where the selection function S_{class} is one of the functions introduced in Section 3.3.1, and could possibly be different from the selection function S chosen in the encoder (3.26). We will come back to this issue in Section 3.5.3.

In the next few subsections, we will describe a few methodologies to design the state codebooks and the next state function based on the initial classifier. In the first subsection, we will discuss some FSVQ designs. These are basically existing designs, although they have not always been introduced in the framework of FSVQ or in the context of time-correlated channels. In the second subsection, we describe the so-called omniscient design, which is a FSVQ design approach which has not yet been used for feedback compression. Note that due to the dependence of the codebooks on the next-state function it is still possible to iteratively improve the obtained state codebooks as illustrated in [17, p.536]. However, this generally only shows marginal performance gains over the initial designs, and thus we will not consider it in this work.

s'	$P(f_{\text{class}}(\mathbf{H}[t]) = s' \mid f_{\text{class}}(\mathbf{H}[t-1]) = 8)$	$d(\mathbf{F}_{s'}, \mathbf{F}_8\ )$
1	0.0380	$1,6292$
2	0.0200	$1,4550$
3	0.0132	$1,3461$
4	0.0365	$1,2801$
5	0.0250	$1,1548$
6	0.0397	$1,3112$
7	0.0232	$1,4487$
8	0.8045	0

Table 3.3: Example of transition probabilities and precoder distances assuming the previous state was $s = 8$.

3.5.2 FSVQ Designs

We first discuss a few FSVQ feedback designs, where the super codebook $\mathcal{C}$ corresponds to the classifier codebook $\mathcal{C}_{\text{class}}$, and the state codebooks $\mathcal{C}_s$ are subsets of the classifier codebook $\mathcal{C}_{\text{class}}$.

Conditional Histogram Design

For the conditional histogram design, the next states of a current state s are the K states s' that have the highest probability to be reached from state s in terms of the initial classifier. Hence, the state codebook $\mathcal{C}_s$ is the set of K precoders $\mathbf{F}_{s'}$ corresponding to the K states s' that have the highest transition probability $P(f_{\text{class}}(\mathbf{H}[t]) = s' | f_{\text{class}}(\mathbf{H}[t-1]) = s)$. If we define, without loss of generality, $\mathbf{F}_{i,s}$ as the precoder $\mathbf{F}_{s'}$ of the state s' with the i-th highest transition probability $P(f_{\text{class}}(\mathbf{H}[t]) = s' | f_{\text{class}}(\mathbf{H}[t-1]) = s)$, then the next-state function $f_{\text{NS}}(i, s)$ is simply given by this state s'. Note that the transition probabilities can be computed as in Section 3.4, but the adaptive approach cannot be used here because the decoder does not have knowledge about the current channel. An example is given in Table 3.3, where we assume that the current state is $s = 8$. Assuming the state codebooks have size $K = 4$, the state codebook $\mathcal{C}_8$ is given by $\mathcal{C}_8 = \{\mathbf{F}_8, \mathbf{F}_6, \mathbf{F}_1, \mathbf{F}_4\}$. Although presented in a different framework, a similar approach has been proposed in [55].

Nearest Neighbor Design

For the nearest neighbor design, the next states of a current state s are not the K states s' that have the highest transition probability, but the K states s' that have the closest precoder to the precoder of state s in terms of some distance d, which could be a subspace distance, the Frobenius norm d_F, or the modified Frobenius norm d_{MF}, although the latter are not strictly speaking distances. Hence, the state codebook $\mathcal{C}_s$ is the set of K precoders $\mathbf{F}_{s'}$ that have the smallest distance $d(\mathbf{F}'_s, \mathbf{F}_s)$. If we define, without loss of generality, $\mathbf{F}_{i,s}$ as the precoder $\mathbf{F}_{s'}$ of the state s' with the i-th smallest distance $d(\mathbf{F}_{s'}, \mathbf{F}_s)$, then the next-state function $f_{\mathrm{NS}}(i, s)$ is simply given by this state s'. Again looking at the example in Table 3.3, we now see that the state codebook $\mathcal{C}_8$ is given by $\mathcal{C}_8 = \{\mathbf{F}_8, \mathbf{F}_5, \mathbf{F}_4, \mathbf{F}_6\}$.

In the context of orthogonal frequency division multiplexing (OFDM), this approach has already been proposed in [60] to compress the feedback of the precoders on the different subcarriers. The advantage of the Nearest Neighbor Design over the Conditional Histogram Design is that it does not require the transition probabilities between the different states.

Discussion

The problem of both the conditional histogram design and the nearest neighbor design is that if the time between feedback is large and the time correlation of the channel is small, the optimal transition might be not one of the K most likely ones or not one of the K transitions with the smallest distance between precoders. This could lead to a so-called *derailment problem*. As suggested in [17, p.540], the derailment problem could also be solved by periodic re-initialization.

3.5.3 Omniscient Design

In this section, we present a novel feedback compression method, based on what in the field of vector quantization is known as the *omniscient* design [17]. In general, the omniscient design provides the best performance of all the FSVQ design approaches [17].

To explain the omniscient design, let us assume that the next-state function is not determined by the current quantization index and state, but simply by the current channel, for instance by means of the classifier function f_{class}:

$$s[t+1] = f_{\text{class}}(\mathbf{H}[t]). \tag{3.31}$$

The state codebook $\mathcal{C}_s$ for a state s can then be designed by minimizing some average distortion

$$D_{\text{av},s} = \int_{\mathbb{C}^{N_R \times N_T}} D(\mathbf{H}, Q(\mathbf{H}, s))\ p(\mathbf{H}[t] \mid f_{\text{class}}(\mathbf{H}[t-1]) = s)\ d\mathbf{H}, \tag{3.32}$$

where $D(\mathbf{H}, Q(\mathbf{H}, s))$ is the distortion between $\mathbf{H}$ and $Q(\mathbf{H}, s)$, and $p(\mathbf{H}[t] \mid f_{\text{class}}(\mathbf{H}[t-1]) = s)$ is the conditional probability density function of $\mathbf{H}[t]$ given $f_{\text{class}}(\mathbf{H}[t-1]) = s$, or equivalently, given the current state $s[t] = s$. Any of the distortion functions presented in Section 3.3.2 can be considered. We can now solve (3.32) by the GL algorithm or the MC algorithm, as was done in Sections 3.3.2 and 3.3.2. This requires a set of training channels $\mathcal{T}_s$. To construct $\mathcal{T}_s$, we first generate a large set of pairs of consecutive channels based on the channel statistics, $\mathcal{P} = \{(\mathbf{H}^{(r)}[t-1], \mathbf{H}^{(r)}[t])\}$, where r is the realization index. From this set $\mathcal{P}$ we construct $\mathcal{T}_s$ as the set of channels $\mathbf{H}^{(r)}[t]$ for which $f_{\text{class}}(\mathbf{H}^{(r)}[t-1]) = s$, i.e., $\mathcal{T}_s = \{\mathbf{H}^{(r)}[t] | (\mathbf{H}^{(r)}[t-1], \mathbf{H}^{(r)}[t]) \in \mathcal{P}$ and $f_{\text{class}}(\mathbf{H}^{(r)}[t-1]) = s\}$. The problem of this approach is that the decoder can not track the state, because it does not have access to the current channel. Hence, it is assumed here that the decoder is *omniscient*, i.e., that is knows the unquantized channel. Hence, we should replace $\mathbf{H}[t]$ in the next-state function by its estimate $\hat{\mathbf{H}}[t]$ that is computed based on the quantized precoder $Q(\mathbf{H}[t], s[t])$ known to the decoder. As an estimate, we could for instance consider

$$\hat{\mathbf{H}}[t] = \begin{bmatrix} Q(\mathbf{H}[t], s[t]) & \mathbf{0}_{N_T \times (N_R - N_S)} \end{bmatrix}. \tag{3.33}$$

This is of course not a good channel estimate for equalization, but it is good in terms of the N_S largest right singular vectors collected in $\mathbf{V}[t]$. Hence, if the classifier f_{class} is designed based on a selection function $\mathcal{S}_{\text{class}}$ that only depends on $\mathbf{V}[t]$, then $f_{\text{class}}(\hat{\mathbf{H}}[t])$ is a good approximation of $f_{\text{class}}(\mathbf{H}[t])$. That is why

we often choose S_{class} based on a subspace distance (S_{P2}, S_{FS}, or S_C), the Frobenius norm (S_F), or the modified Frobenius norm (S_{MF}), irrespective of what is chosen as selection function S in the encoder (3.26). So, we keep the idealized state codebooks $\mathcal{C}_s$ but we change the next-state function into

$$s[t+1] = f_{\text{class}}(\hat{\mathbf{H}}[t]) = f_{\text{NS}}(i[t], s[t]). \tag{3.34}$$

This way we obtain an FSVQ.

3.5.4 Adaptive FSVQ

Unfortunately, it is not trivial to extend the FSVQ to adapt to changing channel characteristics. The adaptation of the state codebooks $\mathcal{C}_s$ has to rely on information that is available both at the encoder and the decoder. This shared information can for instance consist of the last l states $s[t], s[t-1], \ldots, s[t-l+1]$ and the last l quantized precoders $Q(\mathbf{H}[t], s[t]), Q(\mathbf{H}[t-1], s[t-1]), \ldots, Q(\mathbf{H}[t-l+1], s[t-l+1])$. We restrict our approach to such a window of l samples due to memory restrictions, and we forget past samples for which the channel might have different characteristics. Whenever the precoder is $Q(\mathbf{H}[t], s[t]) = \mathbf{F}_{i,s[t]}$, we know that the channel matrix $\mathbf{H}[t]$ lies in some region $\mathcal{R}_{i,s[t]}$. Assuming a realistic channel distribution, we can then define one or more random channel matrices that also lie in the region $\mathcal{R}_{i,s[t]}$. Finally, the FSVQ design algorithms mentioned previously can be used with the new training sequence to design the new state codebooks. Note that the state codebooks, and thus the quantizer regions, are recalculated from scratch after each feedback. Instead, we could also consider updating the codebook as done in competitive learning [61]. However, such techniques still have to be adapted to take the unitary constraint of the precoding matrix into account, and they are considered future work.

3.6 Simulations

In this section we are providing numerical results for the different schemes and design approaches presented so far. We assume that $N_S = 2$ data streams are transmitted over $N_T = 4$ antennas. The receiver is equipped with $N_R = 2$ receive

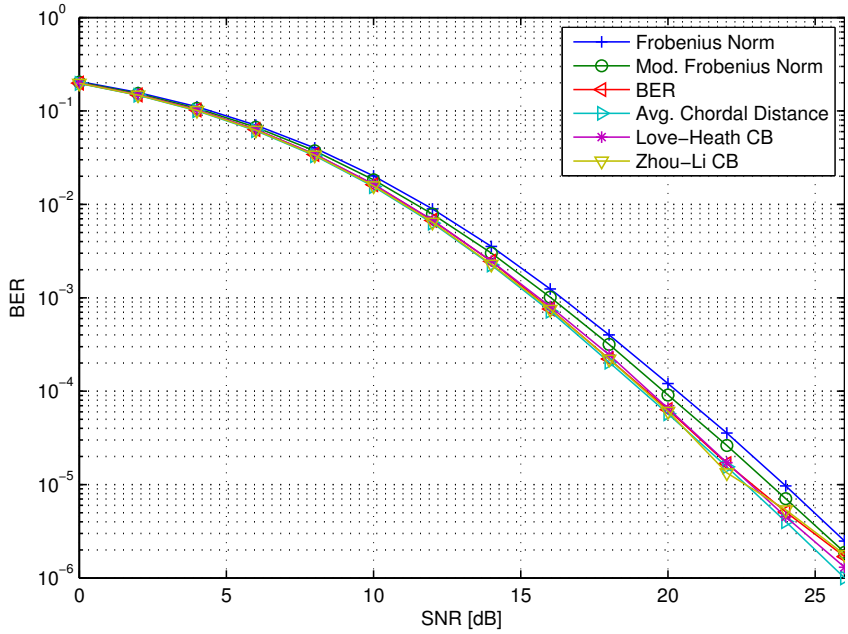

Figure 3.2: Comparison between different codebooks using the BER selection criterion. ($N_S = 2$, $N_T = 4$, $N_R = 2$, $|\mathcal{C}| = 16$, ZF receiver).

antennas, and quadrature phase-shift keying (QPSK) modulation is used.

We start in Subsection 3.6.1 by comparing the BER performance for different codebooks using the BER criterion as selection function. Subsection 3.6.2 then shows the performance of Monte-Carlo and subspace packing codebooks for spatially correlated channels. In subsection 3.6.3 the possible feedback compression gains of entropy coding over memoryless VQ are shown for time-correlated channels. Subsection 3.6.4 shows how fast the adaptive entropy coding schemes adapt to changing channel statistics. The following subsection then compares FSVQ to memoryless VQ, and it also compares the different FSVQ design approaches. Finally, Subsection 3.6.6 shows the duality between FSVQ and entropy coding.

3.6.1 Memoryless VQ

Fig. 3.2 compares the performance of different codebook designs presented in Subsection 3.3.2. The BER is used as selection function (3.14). The Frobenius norm, the modified Frobenius norm, and the chordal distance codebook are using the Monte-Carlo algorithm to solve (3.17), using the respective squared distances as distortion function. The BER codebook is also designed using the Monte-Carlo algorithm. The Love-Heath codebook [48] and the Zhou-Li codebook [50] are designed to optimize (3.19) with the chordal distance as subspace distance. Love and Heath were using techniques from [62], and Zhou and Li were using the generalized Lloyd algorithm. The simulation shows that the performance of the different codebooks is similar, and even using the BER as a distortion function in the codebook design does not yield a noticeable performance gain.

3.6.2 Codebook Design for Spatially Correlated Channels

Fig. 3.3 compares the performance of two codebooks for a spatially correlated channel. One codebook is designed using the Grassmannian subspace packing approach with the chordal distance, and the other codebook is designed using the Monte-Carlo algorithm with the squared modified Frobenius norm as distortion function. The channel is modeled using the measurements in [63], and the BER selection function (3.14) is used to choose the best codebook entry. We see that the Monte-Carlo codebook, which takes the channel correlation into account, outperforms the Grassmannian subspace packing codebook, which aims at spatially white channels.

3.6.3 Entropy Coding

Fig. 3.4 depicts the compression gains possible through entropy coding. The channel is modeled through Jakes' model with the Doppler spread fixed. The mean feedback rate is depicted as a function of the frame duration T_f. A small frame duration implies a highly correlated channel, whereas a longer frame duration implies a less correlated channel. The Huffman code is used as prefix-free code, and the simple binary numbering from Table 3.2 is used as the non-prefix-free code. The modified Frobenius norm (3.16) is used as selection function and the

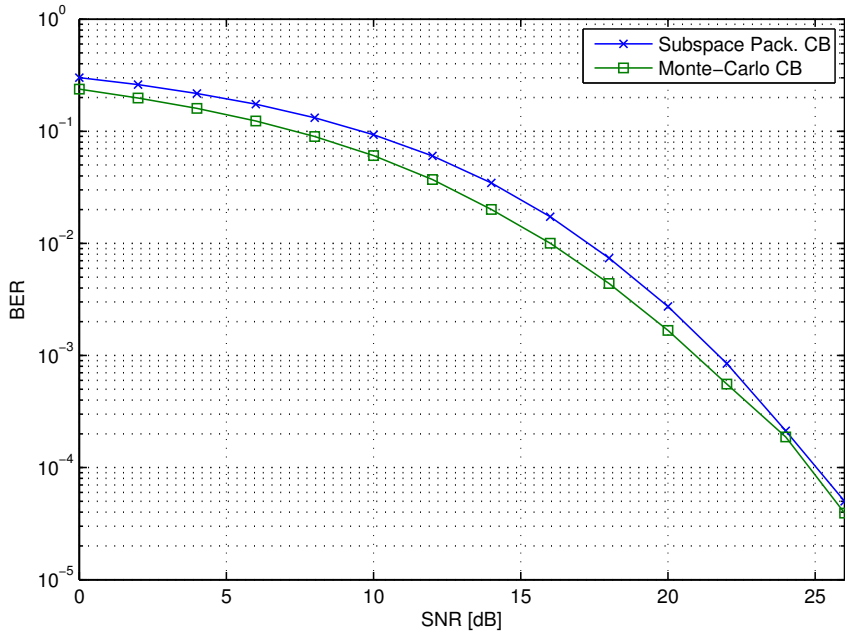

Figure 3.3: Comparison of different codebooks for memoryless VQ for a spatially correlated channel. ($N_S = 2$, $N_T = 4$, $N_R = 4$, $|\mathcal{C}| = 4$, ZR receiver).

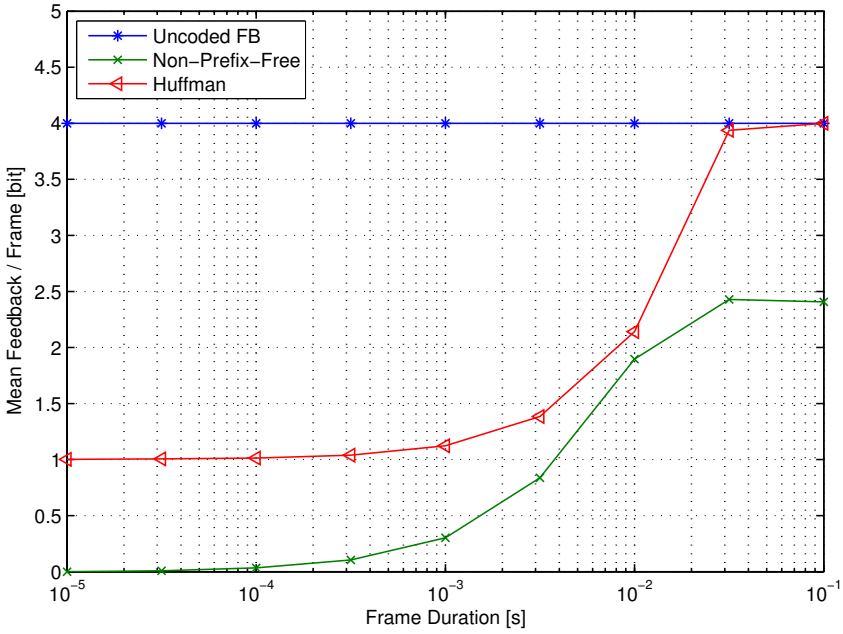

Figure 3.4: Feedback compression with entropy coding for different frame lengths ($N_S = 2$, $N_T = 2$, $f_D = 30$ Hz, $|\mathcal{C}| = 16$).

squared modified Frobenius norm as distortion function to design the codebook using the Monte-Carlo algorithm. The transition probabilities used to design the entropy codes are estimated through Monte-Carlo simulations.

We see that the prefix-free code achieves a mean feedback rate of 1 bit for highly correlated channels, whereas the non-prefix-free code can even achieve 0 bits, i.e., no feedback is necessary. For longer frame durations, i.e., uncorrelated channels, the mean feedback rate for the Huffman encoded bitwords converges to 4 bits, since the transitions between the different codewords become equiprobable, and then the Huffman code assigns equal-length bitwords to all the precoders. The non-prefix-free code converges to $2,375$ bits for uncorrelated channels since the transitions between the different codewords become equiprobable as well, and thus it assigns the binary numbering bitwords randomly.

3.6.4 Adaptive Entropy Coding

The tradeoff between adaptation speed and accuracy for adaptive entropy coding is depicted in Fig. 3.5 and Fig. 3.6. To depict the adaptation of the adaptive entropy coding to changing channel statistics, we changed the frame duration from 10^{-3} s to 10^{-2} s after 3000 frames, and back after another 3000 frames. The remaining simulation parameters are identically as in the previous subsection.

Fig. 3.5 assumes a non-dedicated feedback channel. We see how the selection of the weighting factor N controls the tradeoff between performance and speed of the adaptive encoding process. For small N, the transition probabilities are estimated faster but less accurate, and for higher N, the estimation is slower but more accurate.

Fig. 3.6 shows a similar scenario, but for a dedicated feedback channel, where the bitwords are designed using the non-prefix-free code from Table 3.2. We see that the system quickly adapts to the changing frame lengths for both values of N, since the encoding of the bitwords does no longer depend on the exact transition probabilities but only on their order.

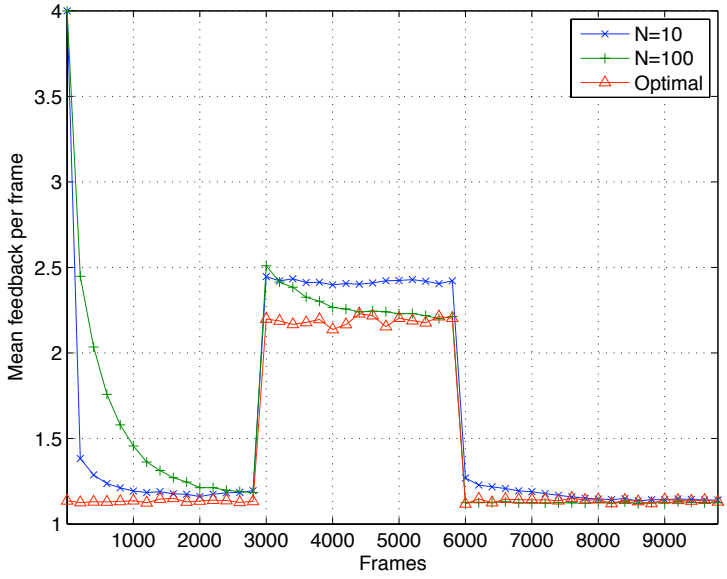

Figure 3.5: Tradeoff between adaptation speed and accuracy using a Huffman code ($f_D = 30$ Hz, $N_S = N_T = 2$, $|\mathcal{C}| = 16$).

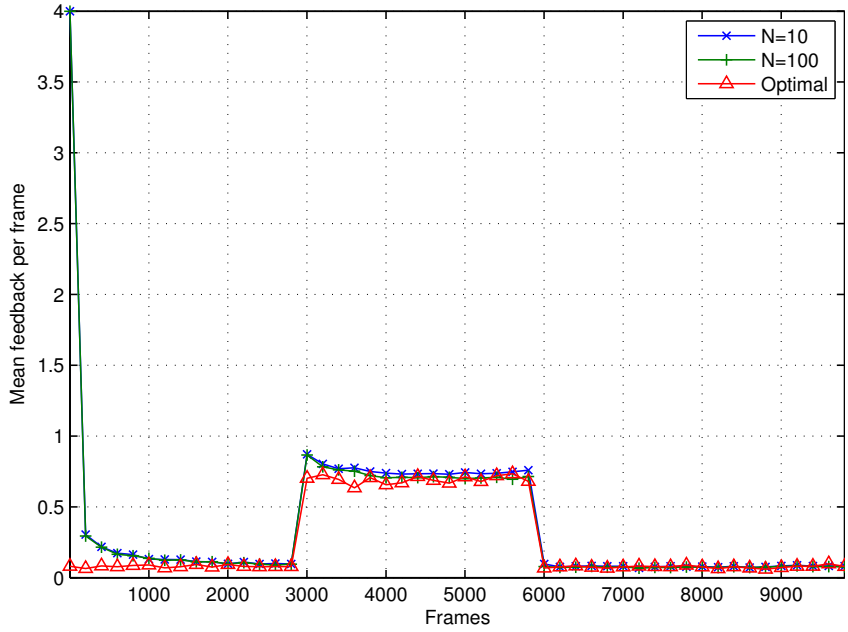

Figure 3.6: Tradeoff between adaptation speed and accuracy using a non-prefix-free code ($f_D = 30$ Hz, $N_S = N_T = 2$, $|\mathcal{C}| = 16$).

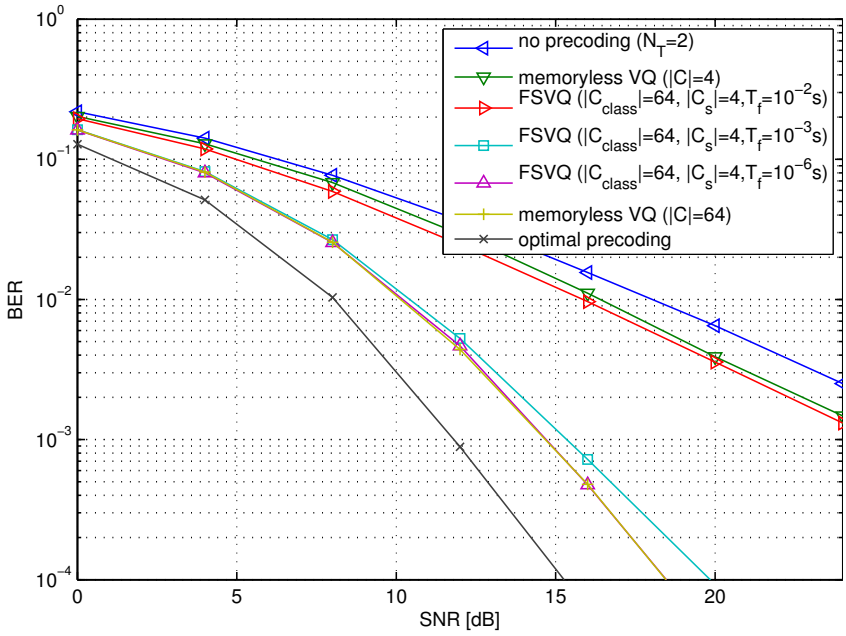

Figure 3.7: Comparison of several codebook design approaches ($N_S = 2$, $N_T = 4$, $N_R = 2$, $f_D = 30$ Hz, MMSE receiver).

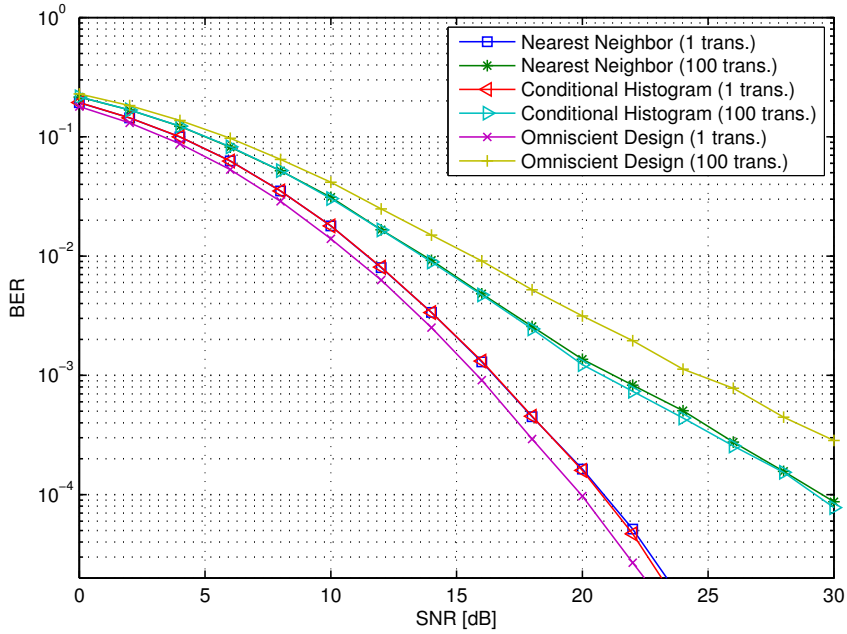

Figure 3.8: Comparison between the different FSVQ design approaches ($N_S = 2$, $N_T = 4$, $N_R = 2$, $|\mathcal{C}_{\text{class}}| = 16$, $|\mathcal{C}_s| = 4$, $T_f = 10^{-3}$ s, $f_D = 30$ Hz, SNR = 10 dB, ZF receiver).

3.6.5 FSVQ

The performance of different state codebook designs is depicted in Fig. 3.7. The FSVQs are created using the omniscient design. The different codebooks are designed with the squared modified Frobenius norm as distortion function, and the mod. Frobenius norm (3.16) is used as selection function for the classifier (3.31) as well as for the quantization (3.28).

We see that the performance of the FSVQ highly depends on the time correlation of the channel. If the time correlation between the channels is high, the 2 bit feedback of a FSVQ has the same BER performance as the 4 bit memoryless VQ. However, for less correlated channels the performance drops to the same performance as the 2 bit memoryless VQ.

Different design approaches for FSVQ codebooks are shown in Fig. 3.8. We

simulate for the different design approaches the performance after 1 transmission and after 100 transmissions. We use the same distortion and selection functions as in the previous simulations.

We see that the omniscient design performs best after 1 transmission, but it also suffers the most from the derailment problem, i.e., its performance after 100 transmissions is worse than the nearest neighbor and the conditional histogram design. This effect can be counteracted through periodic reinitialization.

3.6.6 Comparison Entropy Coding and FSVQ

We compare the omniscient design with the entropy coding approach for a MIMO system with a non-dedicated feedback link. Fig. 3.9 shows the average feedback rate and the BER of the linear MMSE receiver as a function of the frame length T_f. The modified Frobenius norm is used as selection function, and the squared modified Frobenius norm is used as distortion function to design the codebooks. We consider codebooks for the entropy coding approach with $|\mathcal{C}| = 2$, 4, 8, and 16, whereas for the omniscient design we take $|\mathcal{C}_{\text{class}}| = 64$ and $|\mathcal{C}_s| = 2$, 4, 8, and 16. For the entropy coding approach, the BER is constant and the average feedback rate increases with an increasing Doppler spread. On the other hand, for the omniscient design, the average feedback rate is constant and the BER increases with an increasing Doppler spread. Hence, the question basically is how their average feedback rates (BERs) compare for the same BER (average feedback rate). To answer this question, let us take a look at a few examples. We see that the entropy coding approach with $|\mathcal{C}| = 8$ has the same average feedback rate as the omniscient design with $|\mathcal{C}_{\text{class}}| = 64$ and $|\mathcal{C}_s| = 4$ at $T_f \approx 0.01$ s. However, at this frame length, the first has a worse BER as the latter. Similarly, we see that the entropy coding approach with $|\mathcal{C}| = 8$ has the same BER as the omniscient design with $|\mathcal{C}_{\text{class}}| = 64$ and $|\mathcal{C}_s| = 4$ at $T_f \approx 0.02$ s. But at this frame length, the first has a higher average feedback rate as the latter. Other examples show the same behavior. Hence, we can conclude that for this particular set-up, the entropy coding approach is worse than the omniscient design. The main reason for this behavior is that the super codebook of the omniscient design is much larger than the codebooks used for entropy coding.

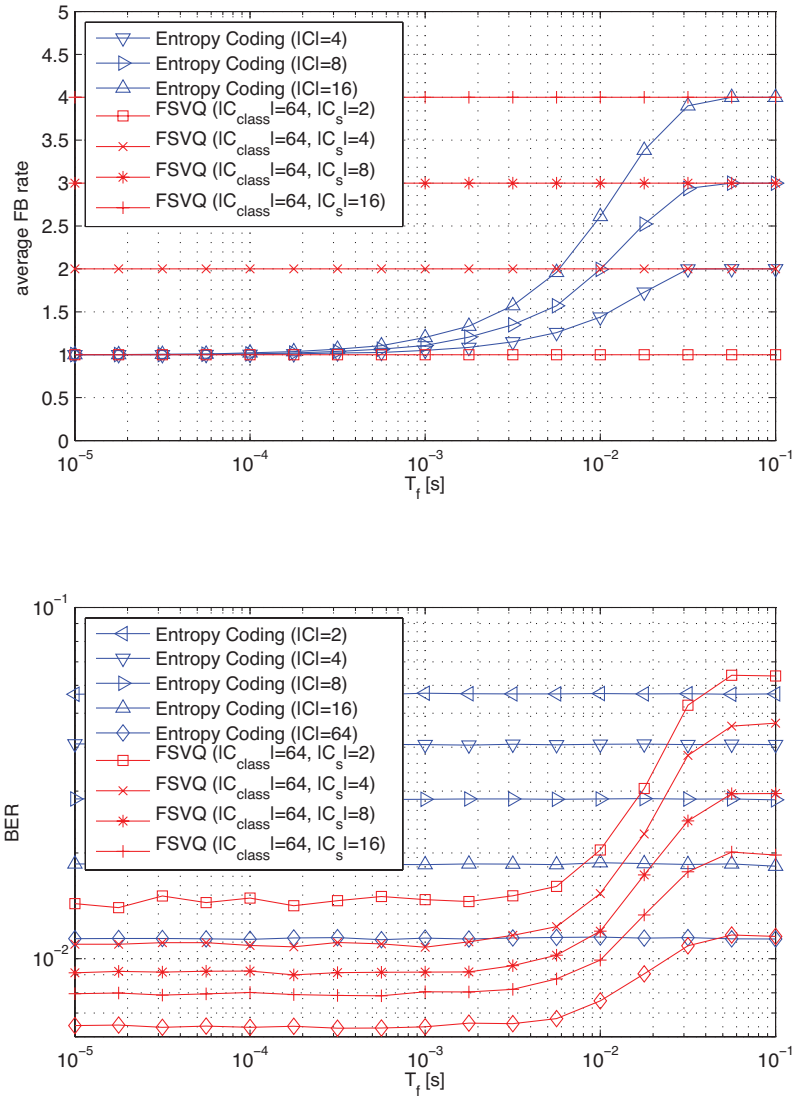

Figure 3.9: Comparison of adaptive entropy coding and FSVQ ($N_S = 2$, $N_T = 4$, $N_R = 2$, $f_D = 30$ Hz, SNR = 10 dB, MMSE receiver).

3.7 Conclusions

In this chapter, we presented existing and novel schemes exploiting limited feedback for linear precoded spatial multiplexing in the framework of vector quantization. We depicted the different selection and distortion functions to generate the codebooks, and to quantize the input. Further, we considered the problem of reducing the data rate on the feedback link, and the problem of optimizing the overall performance of the system. The simulations show the benefit of using FSVQ and entropy coding to better exploit the limited feedback channel for for temporally correlated channels. As an extension we show that entropy coding can also be easily adapted to changing channel characteristics.

In conclusion, we see that existing techniques from the field of vector quantization can be easily and beneficially used for better exploiting the limited feedback link.

Chapter 4

Precoder and Equalizer Extrapolation*

The following chapter attacks Problem 2 of the thesis. As in the previous chapter we also focus on quantizing and feeding back the unitary precoding matrix. Additionally, we are trying to extrapolate the unitary precoding matrix throughout the block using the past feedback. Further, we investigate both the linear minimum mean square error (LMMSE) detector, which minimizes the mean square error (MSE) between the transmitted and estimated symbols, and the singular value decomposition (SVD) detector, which is a detector that aims at diagonalizing the channel matrix. Simulation results illustrate the efficiency of the proposed extrapolation methods.

4.1 Introduction

Spatial multiplexing has emerged in the last years as an efficient technique to reach high data rates. To make it more resistant against rank deficient channels, it is advantageous to use linear precoding [12] on top of spatial multiplexing. As mentioned in the previous chapter, the optimal precoding matrix is the product

*Parts of this chapter are taken from [24].

of a diagonal power loading matrix and a unitary matrix. In order to reduce the feedback requirements, we discard the diagonal power loading matrix, and just use the unitary matrix as precoding matrix. Note that without the diagonal power loading matrix it is no longer possible to apply the water-filing algorithm to balance the power levels of the different spatial streams. The unitary matrix is quantized and fed back to the transmitter. The quantization of the precoding matrices requires a suitable codebook design and code selection procedure. This could for instance be based on average mean square error (MSE) [64]. However, this does not necessarily lead to a decoupling of the different spatial streams, which generally results in a better performance if only a few of the spatial streams are used. This is due to the fact that when the spatial streams are stronger decoupled, the average performance of the stronger modes is better. Hence, we will focus on a precoder that consists of a few right singular vectors of the channel matrix, and we will adopt the codebook design and code selection procedure that was proposed in [65]. But since this approach still has a phase ambiguity for every singular vector, we modify the codebook design and code selection accordingly, leading to a better performance.

To limit the amount of feedback, we will only feed back the right singular vectors at regular time instants. At other time instants, we can extrapolate the precoder by exploiting the coherence of the channel in the time domain. The extrapolation scheme we will adopt here is similar to the one proposed in [22]. Since the precoder is only fed back at regular time instants, it is only necessary to estimate the channel at those time instants, which means we can also reduce the amount of training overhead. At other time instants, we can then extrapolate the channel, again exploiting its coherence in the time domain. We will investigate two receiver methods: the linear minimum mean square error (LMMSE) detector, which minimizes the mean square error (MSE) between the transmitted and estimated symbols, and the singular value decomposition (SVD) detector, which is a detector that aims at diagonalizing the channel matrix. We select these two receivers as a comparison since both are popular linear receivers.

Notation: We designate vectors with lowercase boldface letters, and matrices with capital boldface letters. The notation $[\mathbf{A}]_{i,j}$ denotes the (i,j)th entry of the matrix $\mathbf{A}$, and $[\mathbf{A}]_{:,1:n}$ is the submatrix of $\mathbf{A}$ consisting of the columns 1 to n. $\mathbf{I}_n$

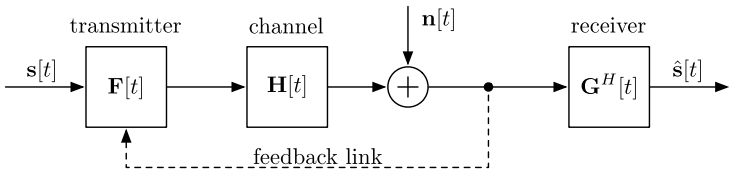

Figure 4.1: Spatial multiplexing MIMO system with linear precoding and a feedback link.

is the $n \times n$ identity matrix. Further, $\mathbf{A}^H$ denotes the conjugate transpose of the matrix $\mathbf{A}$, $\mathbf{A}^{-1}$ the inverse, and $\text{expm}(\mathbf{A})$ the matrix exponential. Finally, $E(\cdot)$ represents expectation and $p(\cdot)$ probability.

4.2 System Model

We assume a narrowband spatial multiplexing MIMO system with N_T transmit antennas and N_R receive antennas. The system input-output relation at time instant t is given by

$$\mathbf{y}[t] = \mathbf{H}[t]\sqrt{E_T}\mathbf{F}[t]\mathbf{s}[t] + \mathbf{n}[t], \tag{4.1}$$

as specified in Section 1.1.1, where $\mathbf{y}[t] \in \mathbb{C}^{N_R \times 1}$ is the received vector, $\mathbf{s}[t] \in \mathbb{C}^{N_S \times 1}$ is the vector that contains the N_S transmitted data symbols, $\mathbf{H}[t] \in \mathbb{C}^{N_R \times N_T}$ is the channel matrix, $E_T \in \mathbb{R}$ is the transmit energy, $\mathbf{F}[t] \in \mathbb{C}^{N_T \times N_S}$ is the linear precoder, and $\mathbf{n}[t] \in \mathbb{C}^{N_R \times 1}$ is the additive noise vector.

We assume that the elements of $\mathbf{s}[t]$ are i.i.d. and uniformly distributed over a finite alphabet with zero mean and variance $\frac{1}{N_S}$. We further assume that the elements of $\mathbf{n}[t]$ are i.i.d. and complex Gaussian distributed with zero mean and variance N_0. We finally assume that the elements of $\mathbf{H}[t]$ are i.i.d. and distributed according to Jakes' model [66] with zero mean and variance 1:

$$[\mathbf{H}[t]]_{n_R,n_T} = \frac{1}{\sqrt{S}} \sum_{s=1}^{S} A_{s,n_R,n_T} \exp(j2\pi f_d t T \cos(\phi_{s,n_R,n_T})), \tag{4.2}$$

where S is the number of scatterers, A_{s,n_R,n_T} is complex Gaussian distributed

with zero mean and variance 1, ϕ_{s,n_R,n_T} is uniformly distributed in $[0, 2\pi]$, T is the symbol period, and f_d is the Doppler frequency. The index of A and ϕ indicates that they are different for every scatterer and for every receiver-transmitter pair. The SVD of $\mathbf{H}[t]$ will be denoted as $\mathbf{H}[t] = \mathbf{U}[t]\mathbf{\Sigma}[t]\mathbf{V}^H[t]$, where $\mathbf{U}[t]$ and $\mathbf{V}[t]$ belong to $\mathcal{U}_{N_R}$ and $\mathcal{U}_{N_T}$, respectively, with $\mathcal{U}_n$ denoting the set of unitary $n \times n$ matrices, and $\mathbf{\Sigma}[t]$ is a diagonal $N_R \times N_T$ matrix with the diagonal starting in the top left corner.

Generally, the precoding matrix is restricted to have orthonormal columns, i.e., $\mathbf{F}^H[t]\mathbf{F}[t] = \mathbf{I}_{N_S}$. Within that class, it can for instance be shown that $\mathbf{F}[t] = [\mathbf{V}[t]]_{:,1:N_S}\mathbf{Q}$ is optimal with respect to the average MSE [65], where $\mathbf{Q}$ is an arbitrary matrix belonging to $\mathcal{U}_{N_S}$.

Note that this $\mathbf{Q}$ matrix does not change the average MSE but can be used to enforce a certain MSE profile across the different spatial streams. For instance, selecting a $\mathbf{Q}$ matrix with constant modulus entries enforces an even MSE profile across the different spatial streams, thereby minimizing the uncoded BER [67,68]. However, selecting $\mathbf{Q} = \mathbf{I}_{N_S}$ links a specific spatial stream to a specific spatial mode of the channel, leading to a better seperation of the spatial streams. Hence, we consider $\mathbf{F}[t] = [\mathbf{V}[t]]_{:,1:N_S}$ to be the optimal precoder in this work. Note that if $N_S \neq N_T$, then the precoding matrix is not a unitary matrix. However, in order to keep our notation consistent with the literature, we still also call the non-square precoding matrix, the unitary precoder.

To estimate the symbols, we make use of a linear detector $\mathbf{G}[t]$, i.e., $\hat{\mathbf{s}}[t] = \mathbf{G}^H[t]\mathbf{y}[t]$. We will consider two types of linear detectors in this work. The first detector is the LMMSE detector, which is given by

$$\mathbf{G}_{\text{LMMSE}}[t] = \mathbf{H}[t]\mathbf{F}[t](\mathbf{F}^H[t]\mathbf{H}^H[t]\mathbf{H}[t]\mathbf{F}[t] + N_0\mathbf{I}_{N_S})^{-1}. \tag{4.3}$$

The second detector, referred to as the SVD detector, relies on the left singular vectors $\mathbf{U}[t]$ of the channel matrix $\mathbf{H}[t]$, and is given by

$$\mathbf{G}_{\text{SVD}}[t] = [\mathbf{U}[t]]_{:,1:N_S}. \tag{4.4}$$

For the SVD detector, the relationship between the estimated symbols $\hat{\mathbf{s}}$ and the

transmitted symbols $\mathbf{s}$ then becomes

$$\hat{\mathbf{s}}[t] = [\mathbf{\Sigma}]_{1:N_S,1:N_S}\mathbf{s}[t] + ([\mathbf{U}[t]]_{:,1:N_S})^H\mathbf{n}. \tag{4.5}$$

We see that this corresponds to the transmission over N_S SISO channels. Note that the receiver does not know $\mathbf{\Sigma}$, and thus, the scaling of the data symbols. Hence, the SVD detector only works for phase-shift keying (PSK) modulation whereas the LMMSE detector works for any type of modulation.

4.3 Precoder Quantization

It is clear that the use of the optimal precoder requires feedback from the receiver to the transmitter. However, since the feedback link only has a limited rate, we have to quantize the information. We can either feed back the channel or the precoder. But since the precoder has less degrees of freedom than the channel, it is better to send the quantized precoder than the quantized channel to the transmitter, as illustrated in the simulations section.

Hence, we have to select the precoder $\mathbf{F}[t]$ from a finite codebook $\mathcal{F} = \{\mathbf{F}_i\}$. The code selection and codebook design criteria can for instance be based on average MSE [64]. However, as we discussed before, this does not necessarily lead to a one-to-one link between the spatial streams and the spatial modes. Hence, in this work, we will quantize the right singular vectors $\mathbf{V}[t]$ and we will pick the quantized right singular vectors $\mathbf{V}_Q[t]$ from a finite codebook $\mathcal{V} = \{\mathbf{V}_i\}$. The precoder is then selected as $\mathbf{F}[t] = [\mathbf{V}_Q[t]]_{:,1:N_S}$. Note that if we follow this approach, the codebook design and code selection are independent of the number of spatial streams N_S that are selected. This allows for the use of code extrapolation when different spatial streams are selected at different time instants, a procedure known as multi-mode precoding. Code extrapolation will be discussed later on.

4.3.1 Codebook Design and Code Selection

The first codebook design we consider here is the same as in [65]. We review this design here shortly. First of all, assuming that the elements of $\mathbf{H}[t]$ are i.i.d.

and complex Gaussian distributed, $\mathbf{V}[t]$ is isotropically distributed in $\mathcal{U}_{N_T}$ [69,70]. Within that space we have to look for an optimal set of regions $\{\mathcal{R}_i\}$ and centroids $\mathcal{V} = \{\mathbf{V}_i\}$, such that $\mathbf{V}_Q[t] = \mathbf{V}_i$ if $\mathbf{V}[t] \in \mathcal{R}_i$. We can find such an optimal set of regions and matrices in $\mathcal{U}_{N_T}$, by minimizing the average quantization distortion, measured by the mean square error between $\mathbf{V}[t]$ and its quantized version. In other words, we try to solve

$$\{\mathcal{R}_i, \mathbf{V}_i\} = \underset{\{\mathcal{R}_i, \mathbf{V}_i\} \mid \mathcal{R}_i \subset \mathcal{U}_{N_T}, \mathbf{V}_i \in \mathcal{U}_{N_T}}{\arg\min} \sum_i E(\|\mathbf{V}[t] - \mathbf{V}_i\|_F^2 \mid \mathbf{V}[t] \in \mathcal{R}_i) p(\mathbf{V}[t] \in \mathcal{R}_i). \quad (4.6)$$

The solution is not known in closed form, but can be identified iteratively by the generalized Lloyd algorithm. Based on this codebook design, the optimal $\mathbf{V}_Q[t]$ is then found as

$$\mathbf{V}_Q[t] = \underset{\mathbf{V}_i \in \mathcal{V}}{\arg\min} \|\mathbf{V}[t] - \mathbf{V}_i\|_F^2. \quad (4.7)$$

4.3.2 Modified Codebook Design and Code Selection

Note that the right singular vectors $\mathbf{V}[t]$ are actually only known up to a phase shift of their columns. We refer to this ambiguity of $\mathbf{V}[t]$ as the orientation ambiguity of $\mathbf{V}[t]$, and it is characterized by a right multiplication of $\mathbf{V}[t]$ with an orientation matrix $\mathbf{\Theta}[t] \in \mathcal{DU}_{N_T}$, where $\mathcal{DU}_{N_T}$ is the set of diagonal unitary $N_T \times N_T$ matrices. The previous codebook design and code selection, however, do not take this orientation ambiguity of $\mathbf{V}[t]$ into account. We can therefore improve the previous approach by not simply using the mean square error between $\mathbf{V}[t]$ and its quantized version, but between the optimally oriented $\mathbf{V}[t]$ and its quantized version. Hence, we have to solve a problem of the form

$$\min_{\mathbf{\Theta}[t] \in \mathcal{DU}_{N_T}} \|\mathbf{V}[t]\mathbf{\Theta}[t] - \mathbf{V}_i\|_F^2. \quad (4.8)$$

The solution can easily be computed in closed form and is given by [71, pp. 431-432]

$$[\mathbf{\Theta}_{\text{opt},i}[t]]_{p,q} = \begin{cases} \dfrac{[\mathbf{V}^H[t]\mathbf{V}_i]_{p,p}}{|[\mathbf{V}^H[t]\mathbf{V}_i]_{p,p}|}, & \text{if } p = q, \\ 0, & \text{otherwise.} \end{cases} . \tag{4.9}$$

As a result, we modify the codebook design into

$$\{\mathcal{R}_i, \mathbf{V}_i\} = \underset{\{\mathcal{R}_i, \mathbf{V}_i\} | \mathcal{R}_i \subset \mathcal{U}_{N_T}, \mathbf{V}_i \in \mathcal{U}_{N_T}}{\arg\min} \sum_i E(\|\mathbf{V}[t]\mathbf{\Theta}_{\text{opt},i}[t] - \mathbf{V}_i\|_F^2 \,|\, \mathbf{V}[t] \in \mathcal{R}_i) p(\mathbf{V}[t] \in \mathcal{R}_i). \tag{4.10}$$

Again, the solution is not known in closed form, but can be identified iteratively by the generalized Lloyd algorithm. Based on this codebook design, the optimal $\mathbf{V}_Q[t]$ is then found as

$$\mathbf{V}_Q[t] = \underset{\mathbf{V}_i \in \mathcal{V}}{\arg\min} \|\mathbf{V}[t]\mathbf{\Theta}_{\text{opt}}[t] - \mathbf{V}_i\|_F^2. \tag{4.11}$$

4.4 Precoder Extrapolation

By exploiting the coherence of the channel in the time domain, we can avoid feeding back the quantized right singular vectors $\mathbf{V}_Q[t]$ at every time instant t. More specifically, we will feed back the quantized right singular vectors every N time instants, i.e., $\mathbf{V}_Q[kN]$ is fed back for all k. We can then extrapolate the quantized right singular vectors at some time instant $kN+t$, for $t = 1, 2, \ldots, N-1$, using the last K known quantized right singular vectors $\{\mathbf{V}_Q[(k+l)N]\}_{l=-K+1}^{0}$. The method we use is the same as proposed in [22]. To estimate $\mathbf{V}_Q[kN+t]$, for $t = 1, 2, \ldots, N-1$, we first transform the set $\{\mathbf{V}_Q[(k+l)N]\}_{l=-K+1}^{0}$ to a new set $\{\mathbf{V}_{k,l}\}_{l=-K+1}^{0}$, correcting the orientation of all matrices such that they are as close as possible to $\mathbf{V}_Q[kN]$ in Frobenius norm, and rotating all matrices such that $\mathbf{V}_Q[kN]$ becomes the identity matrix. Note, that the identity matrix

is arbitrary chosen as the reference.

$$\begin{aligned}
\mathbf{V}_Q[kN] &\rightarrow \mathbf{V}_{k,0} = \mathbf{I} \\
\mathbf{V}_Q[(k-1)N] &\rightarrow \mathbf{V}_{k,-1} = \mathbf{V}_Q^H[kN]\mathbf{V}_Q[(k-1)N]\boldsymbol{\Theta}_{k,-1} \\
&\vdots \\
\mathbf{V}_Q[(k-K+1)N] &\rightarrow \mathbf{V}_{k,-K+1} = \mathbf{V}_Q^H[kN]\mathbf{V}_Q[(k-K+1)N]\boldsymbol{\Theta}_{k,-K+1},
\end{aligned}$$

where $\boldsymbol{\Theta}_{k,l}$ is the orientation matrix that minimizes the Frobenius norm between $\mathbf{V}_Q[(k+l)N]\boldsymbol{\Theta}_{k,l}$ and $\mathbf{V}_Q[kN]$. The solution is similar to (4.9) and is given by

$$[\boldsymbol{\Theta}_{k,l}]_{p,q} = \begin{cases} \dfrac{[\mathbf{V}_Q^H[(k+l)N]\mathbf{V}_Q[kN]]_{p,p}}{\left|[\mathbf{V}_Q^H[(k+l)N]\mathbf{V}_Q[kN]]_{p,p}\right|}, & \text{if } p = q, \\ 0, & \text{otherwise} \end{cases}. \tag{4.12}$$

In a next step we transform the set of unitary matrices $\{\mathbf{V}_{k,l}\}_{l=-K+1}^{0}$ to a set of related skew-Hermitian matrices[†] $\{\mathbf{S}_{k,l}\}_{l=-K+1}^{0}$, such that $\mathbf{V}_{k,l} = \text{expm}(\mathbf{S}_{k,l})$.

Then we try to fit a Pth order polynomial through $\{\mathbf{S}_{k,l}\}_{l=-K+1}^{0}$, i.e., we solve

$$\min_{\{\mathbf{C}_{k,p}\}} \sum_{l=-K+1}^{0} \|\mathbf{S}_{k,l} - \sum_{p=0}^{P} \mathbf{C}_{k,p}((k+l)N)^p\|_F^2. \tag{4.13}$$

Hence, extrapolating $\{\mathbf{S}_{k,l}\}_{l=-K+1}^{0}$ to time instant $kN+t$, for $t = 1, 2, \ldots, N-1$, we get $\sum_{p=0}^{P} \mathbf{C}_{k,p}(kN+t)^p$, and thus extrapolating $\{\mathbf{V}_{k,l}\}_{l=-K+1}^{0}$ to time instant $kN+t$, for $t = 1, 2, \ldots, N-1$, we get $\text{expm}(\sum_{p=0}^{P} \mathbf{C}_{k,p}(kN+t)^p)$. Note that this extrapolated $\mathbf{S}_{k,l}$ is still skew-Hermitian, and thus the extrapolated $\mathbf{V}_{k,l}$ is still unitary. Finally, correcting for the fact that all matrices $\{\mathbf{V}_Q[(k+l)N]\}_{l=-K+1}^{0}$ were rotated such that $\mathbf{V}_Q[kN]$ becomes the identity matrix, an estimate for $\mathbf{V}_Q[kN+t]$ is obtained as

$$\hat{\mathbf{V}}_Q[kN+t] = \mathbf{V}_Q[kN]\text{expm}\left(\sum_{p=0}^{P} \mathbf{C}_{k,p}(kN+t)^p\right). \tag{4.14}$$

[†] A square matrix $\mathbf{A}$ is called skew-hermitian if $\mathbf{A}^H = -\mathbf{A}$ [71, p. 100].

4.5 Receiver Design

Note that the above precoder extrapolation was intended to reduce the amount of feedback that would be required. However, it generally coincides with a reduction of the training overhead, since we can also exploit the coherence of the channel in the time domain to reduce the amount of training required to estimate the channel. We could for instance send some pilot symbols and estimate the channel at regular time instants, after which we can extrapolate the channel for future time instants. For simplicity, we assume that the feedback and training frequencies are the same. Hence, we may assume that the channel is known at the receiver every N time instants, i.e., $\mathbf{H}[kN]$ is known for all k. We can then extrapolate the channel at some time instant $kN+t$, for $t = 1, 2, \ldots, N-1$, using the last K known channels $\{\mathbf{H}[(k+l)N]\}_{l=-K+1}^{0}$. In order to estimate $\mathbf{H}[kN+t]$, for $t = 1, 2, \ldots, N-1$, we try to fit a Pth order polynomial through $\{\mathbf{H}[(k+l)N]\}_{l=-K+1}^{0}$, i.e., we solve

$$\min_{\{\mathbf{D}_{k,p}\}} \sum_{l=-K+1}^{0} \|\mathbf{H}[(k+l)N] - \sum_{p=0}^{P} \mathbf{D}_{k,p}((k+l)N)^p\|_F^2. \tag{4.15}$$

The channel $\mathbf{H}[kN+t]$, for $t = 1, 2, \ldots, N-1$, is then estimated as

$$\hat{\mathbf{H}}[kN+t] = \sum_{p=0}^{P} \mathbf{D}_{k,p}(kN+t)^p. \tag{4.16}$$

4.5.1 LMMSE Detector

If we want to adopt the LMMSE detector (4.3), we carry out the above channel extrapolation approach and mimic the precoder extrapolation at the receiver, in order to find an estimate of the LMMSE receiver at every time instant.

4.5.2 SVD Detector

If we want to adopt the SVD detector [72], we can actually choose between two approaches. In the first approach, we carry out the above channel extrapolation approach and compute the left singular vectors $\hat{\mathbf{U}}[t]$ for every channel estimate

$\hat{\mathbf{H}}[t]$ (note that for $t = kN$ these estimates are assumed to be exact). We then use $[\hat{\mathbf{U}}[t]]_{:,1:N_S}$ or $[\hat{\mathbf{U}}[t]\mathbf{\Theta}_{\text{opt}}[\lfloor t/N \rfloor N]]_{:,1:N_S}$ as detector, for the conventional or modified feedback approach, respectively. In the second approach, we compute $\mathbf{U}[kN]$ for all k at the receiver, and we carry out an extrapolation approach that is similar to the one for the precoder. We extrapolate between the $\mathbf{U}[kN]$s or the $\mathbf{U}[kN]\mathbf{\Theta}_{\text{opt}}[kN]$s, for the conventional or modified feedback approach, respectively, and use the first N_S columns of those matrices as detectors. Note that the latter approach is less complex than the first approach, because the amount of SVDs that has to be computed is reduced by a factor of N.

4.6 Simulation Results

In this section, we study the performance of the proposed methods on a 2×2 MIMO system ($N_R = N_T = 2$). The system is modeled as in Section 4.2 with a Doppler frequency of $f_d = 30$ Hz. For simplicity, we assume the number of spatial streams is fixed and equal to the number of spatial modes, i.e., $N_S = \min\{N_T, N_R\} = 2$, and we assume that QPSK modulation is used on every spatial stream. To illustrate the decoupling between the two spatial streams, we will plot the symbol error rate (SER) of the two spatial streams separately. The larger the distance between the two SER curves, the larger the decoupling. All performances are computed based on 10^4 channel realizations.

First, we consider no extrapolation, and a feedback link that is instantaneous, error-free, and limited to 8 bits per symbol period. Figs. 4.2 and 4.3 show the performance of the LMMSE and SVD detector, respectively, assuming perfect channel knowledge at the receiver. In both figures, we compare the conventional precoder quantization approach of Section 4.3.1 with the modified precoder quantization approach of Section 4.3.2. Also shown is the performance of channel quantization, where the sign of the real and imaginary part of every channel tap is fed back (optimal for the considered channel model). Clearly, precoder quantization realizes a larger decoupling between the spatial streams. In addition, the modified precoder quantization approach outperforms the conventional one.

Next, we include extrapolation in our simulations. We assume a feedback and training frequency of once every $NT = 10^{-3}$ s. Hence, the channel is assumed

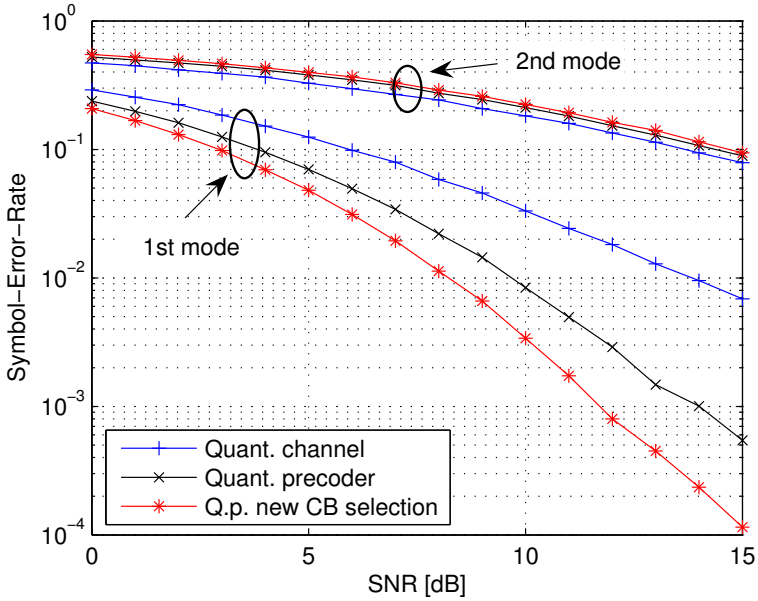

Figure 4.2: LMMSE detector, 8 bit feedback every time instant, $f_d = 30$ Hz.

perfectly known once every $NT = 10^{-3}$ s, at which point 8 bits of information are fed back to the transmitter. Note that we do not give specific values for N and T, since the performance is only determined by their product NT and its relationship to the Doppler frequency f_d. We only consider the modified precoder quantization approach of Section 4.3.2 and compare the extrapolated LMMSE detector with the two extrapolation schemes for the SVD detector (see Section 4.5 for more details). In all extrapolation schemes, we consider a memory depth of $K = 3$ and a polynomial degree of $P = 2$. We see that the LMMSE detector performs the best. In addition, the SVD detector based on channel extrapolation performs worse than the SVD detector based on left singular vector extrapolation. A possible explanation for this phenomena is that the polynomial channel extrapolation is better suited to keep track of the simulated channel, i.e., the channel generated by Jakes' Model, than geodesic extrapolation.

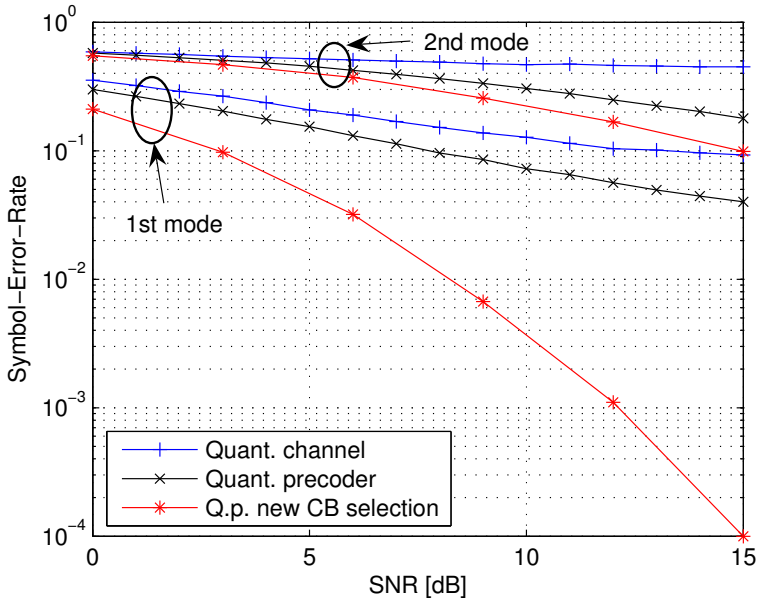

Figure 4.3: $M_T = 2$, $M_R = 2$, SVD detector, 8 bit feedback every time instant, $f_d = 30$ Hz.

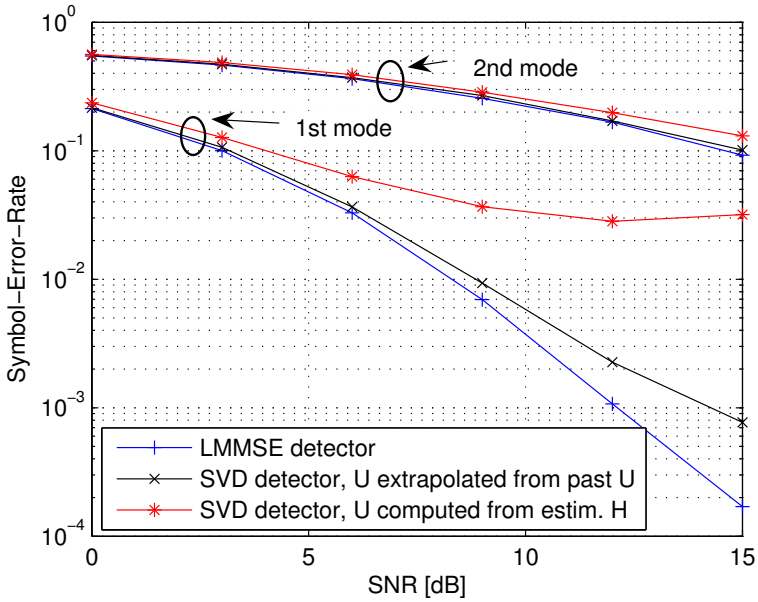

Figure 4.4: Results for extrapolation, 8 bit feedback every $NT = 10^{-3}$ s, $f_d = 30$ Hz, $K = 3$, and $P = 2$

4.7 Conclusions

As the previous chapter, this chapter evaluates the performance of spatial multiplexing with linear precoding, exploiting a low-rate feedback link. However, in this chapter we considered as a performance metric the ability of the system to link the different spatial streams as tight as possible to the different spatial modes, leading to an increased gap between the SER curves of the different spatial streams, and as a result, to an increased average performance if only a few of the spatial streams are used. We have observed that quantizing and feeding back the precoder outperforms quantized channel feedback. Furthermore, we have proposed a modified precoder quantization approach that outperforms the conventional one. Both the LMMSE and SVD detector are investigated, assuming perfect channel knowledge at every time instant. The LMMSE detector is shown to perform slightly better than the SVD detector. We have also discussed precoder extrapolation, when the precoder is only fed back at a limited number of time instants, as well as a related detector extrapolation scheme for the LMMSE and SVD detector, when the channel is only known at some specific time instants. Simulation results using these extrapolation ideas have revealed that the LMMSE detector works better or slightly better than the SVD detector, depending on the extrapolation method that has been chosen for the SVD detector.

These results would suggest to drop the SVD detector for the sake of the LMMSE detector. Even though these results hold for the used system parameters, a general conclusion is not possible using these results.

Part II

Correlated Multi-User MISO Channels

Chapter 5

CSI Codebook Design

In this and the next part of the thesis we consider the multi-user broadcast channel. Two channels are considered, the spatially correlated channel and the temporally correlated channel.

In this specific chapter we address the design of codebooks to quantize the CSI of spatially correlated broadcast channels. A design criterion that effectively exploits the cell statistics is proposed, based on minimizing the average sum-rate distortion in a system with joint linear beamforming and multiuser scheduling. The proposed average distortion function is optimized by generating a set of quantization codebooks through random trials, keeping the codebook that yields the lowest distortion. Comparisons with limited feedback approaches relying on random codebooks are provided, highlighting the importance of matching the codebook design to the cell statistics. Numerical results show a performance gain in scenarios with non-uniform user distributions. Further, we propose a scheme that exploits the limited channel knowledge at the base station to reduce the computational complexity of determining the beamforming vectors and of finding the optimal user set.

The results in this chapter have been published in [28]. The contribution of the author of this thesis was the codebook design for quantizing the channels generated by the model proposed by the first author.

5.1 Introduction

Multiple-input multiple-output (MIMO) systems can significantly increase the spectral efficiency by exploiting the spatial degrees of freedom created by multiple antennas [3]. In the MIMO broadcast channel, it has recently been proven [73] that the sum capacity is achieved by dirty paper coding (DPC) [26]. However, the applicability of DPC is limited due to its computational complexity and the need for full channel state information (CSI) at the transmitter. As a low complexity alternative, downlink techniques based on Space-Division Multiple Access (SDMA) have been proposed that achieve the same asymptotic sum rate as that of DPC, e.g., zero-forcing beamforming [74]. On the other hand, while having full CSI at the receiver can be assumed, this assumption is not reasonable at the transmitter side. Several limited feedback approaches have been considered in point-to-point systems [42, 47], where each user sends to the transmitter the index of a quantized version of its channel vector from a codebook. An extension for MIMO broadcast channels is made in [75], in which each mobile feeds back a finite number of bits regarding its channel realization at the beginning of each block based on a codebook.

Codebook designs for MIMO broadcast channels with limited feedback follow in general simple design criteria, with the purpose of simplifying codebook generation and system analysis. Opportunistic SDMA (OSDMA) has been proposed in [76] as an SDMA extension of opportunistic beamforming [31], in which feedback from the users to the base station is conveyed in the form of a beamforming vector index and an individual signal-to-interference-plus-noise ratio (SINR). An extension of OSDMA is proposed in [77], coined as OSDMA with limited feedback (OSDMA-LF), in which the transmitter counts on a codebook containing an arbitrary number of unitary bases. In this approach, the users quantize the channel direction (channel shape) to the closest codeword in the codebook, feeding back the quantization index and the expected SINR. Multiuser scheduling is performed based on the available feedback, using as beamforming matrix the unitary basis in the codebook that maximizes the system sum rate. Other schemes for MIMO broadcast channels propose to use simple Random Vector Quantization (RVQ) [78] for quantizing the user vector channels, such as the approach de-

scribed in [75]. A simple geometrical framework for codebook design is proposed in [47], which divides the unit sphere in quantization cells with equal surface area. This framework is used for channel direction quantization in [79], where feedback to the base station consists of a quantization index along with a channel quality indicator for user selection. These codebook designs do not take into account either spatial correlations or user distributions present in the system, which could yield better quantization codebooks and in turn better sum-rate performance.

The gains of adaptive cell sectorization have been studied in [80] in the context of code division multiple access (CDMA) networks and single antenna communications, with the aim of minimizing the total transmit power in the uplink of a system with non-uniform user distribution over the cell. This situation is analogous to a system with multiple transmit antennas in which beamforming is performed, adapting its beams to uneven user distributions. In a scenario with limited feedback available, adaptation of quantization codebooks can be performed instead in order to improve the system performance. In [81], an approach for exploiting long term channel state information in the downlink of multiuser MIMO systems is proposed. A flat-fading multipath channel model is assumed, with no line of sight (NLOS) between the base station and user terminals. Each user can be reached through a finite number of multipath components with a certain mean angle of departure (AoD) from the antenna broadside and angle spread. The mean angles of departure are fixed and thus no user mobility is considered.

In this chapter, we highlight the importance of cell statistics for codebook design in MIMO broadcast channels with limited feedback. The average sum rate distortion in a system with joint linear beamforming and multiuser scheduling is minimized, exploiting the information on the macroscopic nature of the underlying channel. A non-geometrical stochastic channel model is considered, in which each user can be reached in different spatial directions and with different angle spread. Based on this model, comparisons with limited feedback approaches relying on random codebooks are provided in order to illustrate the importance of matching the codebook design to the cell statistics. As shown through numerical simulations, the proposed approach provides considerable performance gains in scenarios with non-uniform user distributions.

5.2 System Description

We consider a broadcast channel consisting of N_T antennas at the base station and N_U single-antenna users in a single cell scenario. Let $\mathcal{S}$ denote an arbitrary set of users with cardinality $|\mathcal{S}| = N_T$. Given the user set $\mathcal{S}$ scheduled for transmission, the signal received at the k-th user terminal is given by

$$y_k = \mathbf{h}_k \sqrt{E}_k \mathbf{w}_k s_k + \sum_{i \in \mathcal{S}, i \neq k} \mathbf{h}_k \sqrt{E}_i \mathbf{w}_i s_i + n_k \tag{5.1}$$

where $\mathbf{h}_k \in \mathbb{C}^{1 \times N_T}$, $\mathbf{w}_k \in \mathbb{C}^{N_T \times 1}$, s_k and n_k are the channel vector, the beamforming vector, the transmitted signal, and the additive white Gaussian noise at receiver k, respectively. E_k is the energy associated to user k. The first term in the above equation is the useful signal, while the second term corresponds to the interference by the other users. We assume that the variance of the transmitted signal s_k is normalized to one and n_k is independent and identically distributed (i.i.d.) circularly symmetric complex Gaussian with zero mean and variance N_0.

The channel is assumed to be perfectly known at the user side. The CSI is transmitted to the base station over a feedback link that is limited to B bits per transmission. Hence, the CSI has to be quantized before it is fed back using a codebook $\mathcal{C}$ with N entries. We assume throughout the chapter that $N = 2^B$. Thus, it is possible to feed back every element of the codebook, and the data rate on the feedback link is fully exploited. Strategies that exploit the time correlation of the channel to use larger codebooks with $N > 2^B$ are presented in [19, 55].

The user channels are mapped to the closest codeword in $\mathcal{C}$, as described by

$$\hat{\mathbf{h}}_k = \arg\min_{\mathbf{c} \in \mathcal{C}} \|\mathbf{h}_k - \mathbf{c}\|^2 . \tag{5.2}$$

Note, that this function also takes the norm of the channel into account unlike the quantization functions used for pure channel direction quantization.

5.2.1 Linear Beamforming

At the base station the beamforming vectors are computed on the basis of the matrix $\hat{\mathbf{H}}$, whose rows are the quantized user channels $\hat{\mathbf{h}}_k$, $k \in \mathcal{S}$. Different linear

beamforming techniques may be considered. Commonly applied low-complexity linear beamforming techniques are transmit matched filtering (TxMF) and zero-forcing (ZF) beamforming [74]. Transmit matched filtering uses the normalized columns of $\hat{\mathbf{H}}$ as beamforming vectors. Zero-forcing beamforming uses the normalized columns of the pseudo-inverse of $\hat{\mathbf{H}}$.

5.2.2 User Selection

We consider optimal scheduling throughout the chapter, i.e., we do not consider fairness issues between the users. Let $\mathcal{Q}$ be the set of all possible user subsets of cardinality N_T with disjoint indices in $\{1, \ldots, N_U\}$. The set of users scheduled for transmission at each time slot corresponds to the one that maximizes the estimated sum rate over all possible user sets

$$\hat{\mathcal{S}}^* = \arg\max_{\mathcal{S}\in\mathcal{Q}} \sum_{k\in\mathcal{S}} \log_2(1 + \hat{\mathrm{SINR}}_k). \tag{5.3}$$

Since the base station has no access to perfect channel state information, the following SINR estimate is computed for the user set $\mathcal{S}$ and k-th user

$$\hat{\mathrm{SINR}}_k = \frac{E_k|\hat{\mathbf{h}}_k\mathbf{w}_k|^2}{\sum_{i\in\mathcal{S},i\neq k} E_i|\hat{\mathbf{h}}_k\mathbf{w}_i|^2 + N_0} \tag{5.4}$$

where $\mathbf{w}_k$ denotes the beamforming vector for user k.

5.3 Channel Model

In this section we present the model considered both for the user vector channels and the cell statistics. A non-geometrical stochastic channel is assumed, in which the channel physical parameters are described by probability density functions assuming an underlying geometry. The channel model we propose to use is mainly based on the work in [82], extended to multiuser scenarios. We consider an outdoor environment with NLOS between transmitter and receivers, in which local scatterers, that are randomly distributed around each mobile user, produce a clustering effect. The multipath components (MPC) arrive in clusters in both

space and time. For the sake of simplicity, we consider flat fading and hence all paths are assumed to arrive at zero delay. Furthermore, we assume that each user sees MPCs incoming from surrounding scatterers that are grouped into one cluster.

Each user is reached with a different mean angle of departure (AoD) $\overline{\theta}_k$. The AoDs associated to the multipath components are distributed around the mean according to a certain power angular spectrum (PAS), which depends on the spatial distribution of scatterers. In practice, we only consider the azimuth directions (angle of propagation with respect to the antenna array broadside) since the elevation angle spread is generally small compared to the azimuthal angle. Different probability density functions (PDF) are considered in the literature, such as Gaussian, uniform or Laplacian [83].

5.3.1 User Vector Channels

The signals from the base station arrive at each user terminal through a finite number of L paths, which have different AoDs with respect to the antenna array broadside but arrive at the receiver with the same delay. The AoD for the k-th user and l-th path can be expressed as $\theta_{kl} = \overline{\theta}_k + \Delta\theta_{kl}$, where $\overline{\theta}_k$ is the mean AoD for user k and $\Delta\theta_{kl}$ is the angle offset for the l-th multipath component. The multipath components have complex Gaussian distributed gains γ_{kl} with zero mean and unit variance. The channel of user k is given by

$$\mathbf{h}_k = \frac{1}{\sqrt{L}} \sum_{l=1}^{L} \gamma_{kl} \mathbf{a}(\theta_{kl}) \tag{5.5}$$

where $\mathbf{a}(\theta_{kl})$ are the steering vectors. An omnidirectional uniform linear array (ULA) is considered although the proposed technique can benefit from any array configuration. The steering vectors $\mathbf{a}(\theta_{kl})$ of a ULA are given by

$$\mathbf{a}(\theta_{kl}) = \left[1, e^{-j2\pi \frac{d \sin\theta_{kl}}{\lambda}}, \ldots, e^{-j2\pi \frac{(M-1)d \sin\theta_{kl}}{\lambda}}\right] \tag{5.6}$$

where λ is the wavelength, and d is the antenna spacing at the base station. As shown by the measurements presented in [84] the distribution of the angles

around the mean AoD can be assumed to have a double-sided Laplacian PDF, given by

$$f(\Delta\theta_{kl}) = \frac{1}{\sqrt{2}\sigma_\theta} \exp(-|\sqrt{2}\Delta\theta_{kl}/\sigma_\theta|) \tag{5.7}$$

where σ_θ is the angular standard deviation, $\sigma_\theta = \sqrt{E[|\Delta\theta_{kl}|^2]}$.

5.3.2 Spatial Cell Statistics

Most papers based on the above mentioned stochastic models assume that mean AoDs are uniformly distributed over all directions. In indoor scenarios, the relative cluster AoD is indeed uniformly distributed over $[0, 2\pi]$, as it has been seen from channel measurements [85], since the location of cluster centers is uniformly distributed over the cell. However, as noted in [85], this is not realistic in outdoor scenarios where the base station is elevated and the mobile stations are often surrounded by local scatterers. In these cases, the mean AoD is very dependent on the macroscopic characteristics of each particular scenario: topology, user distribution, mobility pattern, distribution of scatterers, etc. Hence, the mean AoDs for all users, $\overline{\theta}_k$, do not need to be uniformly distributed over the interval $[0, 2\pi]$. In our model, they are considered to be uniformly distributed over an arbitrary range of angles $\bigcup_i [\overline{\theta}_{\min_i}, \overline{\theta}_{\max_i}]$. A graphical representation of the broadcast channel model is depicted in Fig. 5.1.

5.4 Codebook Design

We present in this section the design of the user channel codebook. Compared to existing design approaches [42] we rely on a pure Monte Carlo based approach. This approach allows a wider range of distortion functions than the commonly used generalized Lloyd algorithm, and it also allows to exploit the cell statistics.

As discussed in [86], most techniques relying on limited channel state information consider separate feedback bits (and thus separate quantization) for channel direction information (CDI) and channel quality information (CQI). Since the amount of feedback is limited, a tradeoff arises between the amount of bits used

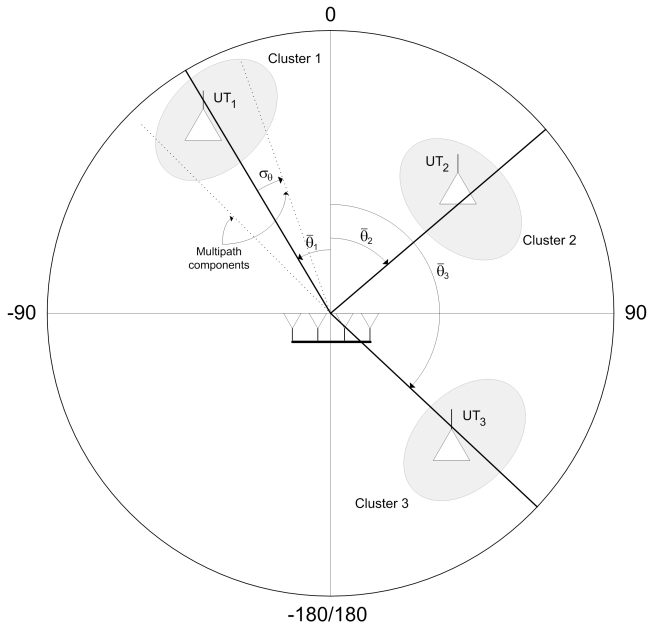

Figure 5.1: Broadcast channel model with user terminals (UT) surrounded by local scatterers grouped in clusters, located in different mean angles of departure (AoDs) with respect to uniform linear array (ULA) broadside.

for CDI quantization, which has an impact on the multiplexing gain, and the amount of bits used for CQI quantization, which has an impact on the multiuser diversity gain achieved from user selection. In this work, we consider joint quantization of CDI and CQI information. Channel quantization is done directly over the user vector channels rather than quantizing the norm and channel direction separately, thus providing better granularity. Hence, since the proposed channel quantization is adapted to the cell statistics, including the average SNR conditions and number of active users, the tradeoff between multiplexing gain and multiuser diversity is implicitly optimized.

The proposed approach consists of designing a channel quantization codebook valid for all users in the cell by minimizing the average sum-rate distortion of the scheduled users. Since scheduling and beamforming are performed jointly at each time slot, the distortion measure needs to account for both jointly. Hence, different linear beamforming techniques will result in different optimized codebooks. This criterion yields quantization codebooks that are statistically matched to the users that maximize the estimated sum rate, which are selected as described in (5.3). The quantization codebook is optimized during an initial training period, after which the codebook is fixed and broadcast to the users.

5.4.1 Design Criterion

The codebook of N codewords, is found by solving the optimization problem

$$\mathcal{C}^* = \arg\min_{\mathcal{C}} E[d(\mathcal{H}, \hat{\mathcal{H}})] \tag{5.8}$$

where $d(\mathcal{H}, \hat{\mathcal{H}})$ is the distortion measure between the set containing the unquantized user channels $\mathcal{H} = \{\mathbf{h}_1, \ldots, \mathbf{h}_{N_U}\}$ and the set containing the quantized user channels $\hat{\mathcal{H}} = \{\hat{\mathbf{h}}_1, \ldots, \hat{\mathbf{h}}_{N_U}\}$.

The distortion measure used throughout the chapter is the sum-rate loss due to the channel quantization. The resulting codebook depends on the number of scheduled users N_T for transmission, the number of active users N_U in the cell, the used beamforming technique, and the channel statistics. The distortion

measure can be described as

$$d(\mathcal{H}, \hat{\mathcal{H}}) = \mathrm{SR}(\mathcal{H}) - \mathrm{SR}(\hat{\mathcal{H}}). \tag{5.9}$$

The first term in the equation above corresponds to the maximum sum rate that can be achieved with the chosen linear beamforming technique and perfect channel state information, given by

$$\mathrm{SR}(\mathcal{H}) = \max_{\mathcal{S} \in \mathcal{Q}} \sum_{k \in \mathcal{S}} \log_2(1 + \mathrm{SINR}_k). \tag{5.10}$$

The beamforming vectors and the user set obtained in the case of perfect channel state information are in general different from the ones obtained on the basis of quantized channel information for a given time slot. The second term in (5.9) corresponds to the actual sum rate achieved by the system. The beamforming vectors are computed on the basis of the quantized channels and the users scheduled for transmission are selected as described in (5.3). Hence, the achieved sum rate is given by

$$\mathrm{SR}(\hat{\mathcal{H}}) = \sum_{k \in \hat{\mathcal{S}}^*} \log_2(1 + \mathrm{SINR}_k). \tag{5.11}$$

Note that, as opposed to the estimated SINR values employed for user selection, the above equation computes the effective SINR experienced by each of the users in the scheduled set $\hat{\mathcal{S}}^*$.

5.4.2 Codebook Design

We are using a Monte Carlo based codebook design algorithm to generate the channel quantization codebooks. The ability of this algorithm to work with arbitrary distortion functions makes it a prime candidate to solve (5.8).

The Monte Carlo codebook design algorithm generates random codebooks having the same distribution as the channel. For every one of these random codebooks the average distortion is estimated by averaging over a large number of channel realizations. Finally, the codebook with the lowest average distortion is kept. This codebook minimizes the long term sample average distortion, and

thus, provides a good solution to (5.8).

An alternative procedure consists of using the generalized Lloyd algorithm [35] to iteratively find the optimizing codebook and partition cells. However, the Monte Carlo codebook design avoids convergence to local minima exhibited by Lloyd's algorithm, and thus provides a better performance if the number of tried codebooks is sufficiently high. A codebook design that is more similar to the Monte Carlo based codebook design is random coding [17]. However, random coding just uses N random channel realizations as codebook, and does not allow to optimize an arbitrary distortion function.

5.4.3 Practical Considerations

The proposed technique for codebook design is expected to perform better in scenarios with strong spatial correlations. Different linear beamforming techniques will yield different performances, since quantization errors affect them differently. For instance, while TxMF and ZF beamforming exhibit similar behavior for a given error variance, optimized unitary beamforming proves to be very robust [87].

Since the statistics of the best N_T users govern the design, the quantization codebooks may favor certain spatial locations or directions that provide good sum rates, favoring the users in those particular locations. In a system with low mobility and slow variations, this situation may lead to a fairness issue. This behavior may be accentuated when incorporating shadowing and pathloss to the channel model. This effect can be attenuated by performing proportional fair scheduling (PFS), which would yield an average distortion function based on a weighted sum rate, penalizing the users that have already been scheduled.

Instead of simply generating the quantization codebooks during a training period, the base station may slowly adapt the codebook to changes in the environment: changes in traffic and mobility patterns, changes of scatterers, etc. Each time a user enters the system or in case there is a codebook update, the base station would send the updated codebook to the users, which in general changes from cell to cell. In addition, similarly to the work presented in Chapter 3 for single-user MIMO communications, the amount of feedback can be reduced by exploiting temporal correlations in the system.

5.5 Low-Complexity Beamforming and Scheduling

The limited channel knowledge at the transmitter side deteriorates the achievable performance of the system, but can also be exploited to reduce the computational load for beamforming and scheduling. The quantization of the user channels creates equivalence classes between the users. The users whose channels are quantized to the same entry in the codebook are members of the same equivalence class. Thus, the base station only knows which class a user belongs to, but it cannot distinguish between the users in the same class. It is thus sufficient to do the beamforming and the scheduling only based on the representative of the class, i.e., the codeword, instead of based on all the users in the class. We denote a set that consists of N_T representatives of different classes as a class set. The number of class sets to be considered for beamforming and scheduling $N_{\mathrm{CS}} = N^{N_T}$ is smaller than the number of user sets $N_{\mathrm{US}} = \binom{N_U}{N_T}$ for practical system parameters with $N \ll N_U$. Once the optimal class set is determined, a corresponding user set can be selected by choosing for every class in the class set a corresponding user. The user inside a specific class can be selected randomly or using a fairness constraint.

The complexity of determining the beamforming vectors and the class sets can be further reduced using a lookup table that stores for all the class sets the corresponding sum rate estimates and the beamforming vectors. We assume that this lookup table is sorted based on the estimated sum rate of the class sets, where the first entry contains the class set with the highest estimated sum rate. After the base station received the feedback from all the users, it checks if it has a matching user for every entry in the first class set. If not, then the base station does the same check for the following class sets in the lookup table until it finds a class set that has for every class in the class set an active user. The advantage of using precalculated beamforming vectors stored in a look-up table is that computational more complex beamforming schemes can be used, e.g., Dirty Paper Coding. Note that TxMF is a special case since there the different beamforming vectors are independent of the other users that are scheduled for transmission. Hence, the storage of only N beamforming vectors is sufficient.

The storage requirements for the lookup table can be reduced by storing only the most probable class sets. The probability that the first class set is selected increases with the number of users in the cell. For the event that no class set in the lookup table is selected, a user set can still be calculated using a low-complexity scheme, e.g., TxMF beamforming.

5.6 Simulation Results

We compare the performance of linear beamforming with quantized CSI feedback to OSDMA-LF. The used linear beamforming strategies are ZF and TxMF. We assume a 2-GHz system with an antenna spacing at the base station of $d = 0.4\lambda \approx 15$ cm. Each user channel is modelled with $L = 10$ multipath components. The mean AoD of the different users is uniformly distributed over the interval $[60°, 120°]$, and the angular spread is fixed to $\sigma_\theta = 30°$. We assume single-antenna users and a base station with $N_T = 2$ antennas. The data rate on the feedback link is limited to 3 bits/transmission. In order to make a fair comparison between the schemes, the SINR feedback of the OSDMA-LF algorithm is also quantized. Thus, the OSDMA-LF algorithm has to share the available 3 bits between the CDI, i.e., the index of the preferred beamforming vector, and the CQI, i.e., the SINR of the preferred beamforming vector. We simulate the performance of all possible CDI/CQI bit allocations, and finally select the allocation that results in the highest sum rate. The codebook to quantize the scalar CQI is designed with the generalized Lloyd algorithm [17], using the mean square error as distortion function. The performance of the different random codebooks, i.e., their resulting average sum rate, is estimated through averaging over the instantaneous sum rate of 10 000 channel realizations.

Fig. 5.2 depicts the performance for different numbers of users with a fixed SNR of 10 dB. We see that ZF and TxMF with quantized CSI outperform OSDMA-LF with quantized SINR feedback. The same result can be seen in Fig. 5.3 for different SNR values and $N_U = 10$ users. We see how the sum rate of the different schemes saturates at high SNR, where the performance is limited by the quantization error.

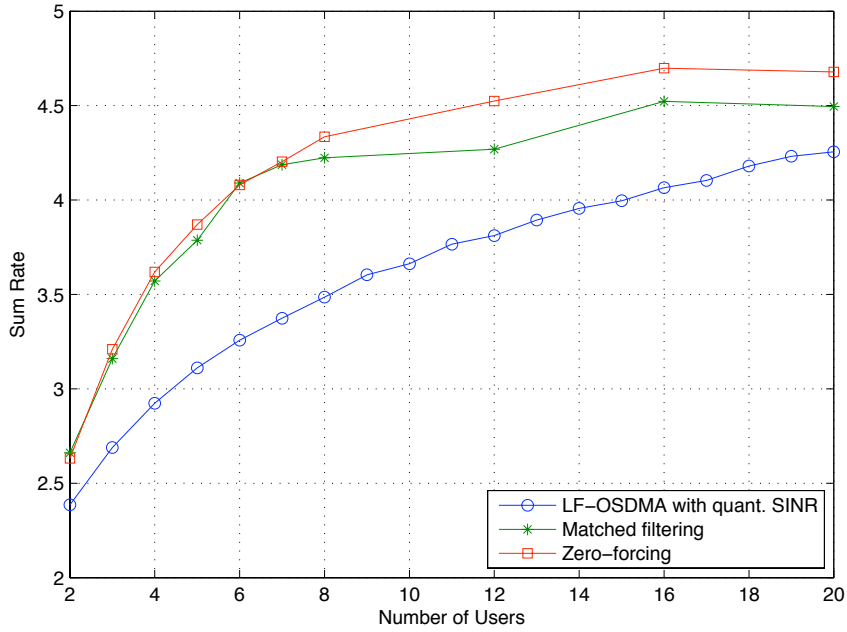

Figure 5.2: Sum rate for the correlated channel model for different numbers of users. ($N_T = 2$, SNR=10 dB)

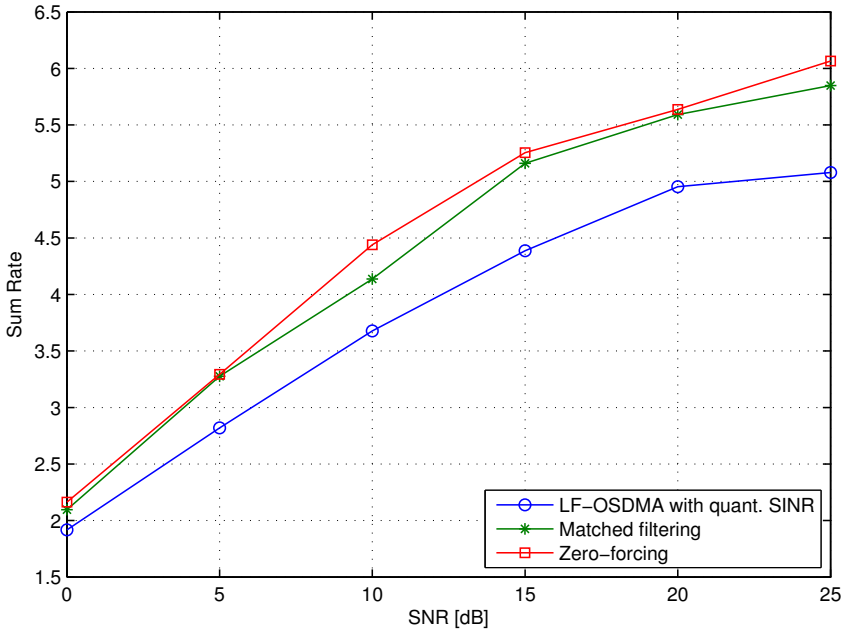

Figure 5.3: Sum rate for the correlated channel model for different SNR's. ($N_T = 2$, $N_U = 10$)

5.7 Conclusions

The problem of designing channel quantization codebooks for correlated broadcast channels with limited feedback has been addressed for systems where joint linear beamforming and multiuser scheduling is performed. The numerical results provided have shown the benefits of using quantization codebooks optimized according to the cell statistics. The generated codebooks perform well in scenarios with reduced angular spread and effective range of mean angles of departure. This makes the proposed approach particularly interesting in outdoor systems with spatial correlation and nonuniform user distribution.

Chapter 6

Predictive Vector Quantization*

In this chapter we apply Predictive Vector Quantization (PVQ) to quantize the channel state information of time-correlated broadcast channels. PVQ exploits the time-correlation of the channel to reduce the quantization error, and thus to improve the sum rate of the system. PVQ predicts the actual channel based on a number of previous channels, and then quantizes the difference between the prediction and the true channel. We further show how the corresponding codebooks can be designed, and we present a prediction strategy. The performance of PVQ for a broadcast system is depicted through numerical simulations.

6.1 Introduction

Space division multiple access (SDMA) has emerged in the last years as an attractive transmission scheme for multiple-input multiple-output (MIMO) broadcast channels [3, 7]. It has been shown to outperform time division multiple access (TDMA) [88]. The optimal SDMA scheme for the Gaussian MIMO broadcast channel is dirty-paper coding (DPC) [25, 26], i.e., the rate region of DPC cor-

*The results in this chapter have been published in [29].

responds to the capacity region of the channel. Unfortunately, DPC has a high computational complexity, and is thus difficult to implement. However, zero-forcing (ZF) beamforming has been lately shown [74] to reach asymptotically the same performance as DPC for a high number of users. Most existing SDMA schemes assume channel knowledge at the transmitter side. However, in general, channel state information (CSI) knowledge is only available at the receiver side, and must be fed back to the transmitter. The feedback link is generally assumed to be bandwidth limited, meaning that only a limited number of bits can be fed back to the transmitter. The CSI must thus be quantized before it can be fed back to the transmitter.

A low-complexity SDMA scheme that works with limited feedback is opportunistic SDMA (OSDMA) [76]. OSDMA is an extension of opportunistic beamforming [31] to multiple users. It uses a random set of orthonormal beamforming vectors at the base station with M antennas to simultaneously transmit independent data streams to the M users with the highest signal-to-noise ratio (SINR). Several extensions of OSDMA have been proposed lately [77, 89] to incorporate larger sets of beamforming vectors, and thus, to improve the performance for scenarios with a lower number of users. Even though the OSDMA algorithms have a good performance for i.i.d. channels, there exists, to the best of the authors' knowledge, no extension of these algorithms to exploit time-correlated channels.

In this chapter we present a scheme that uses Predictive Vector Quantization (PVQ) [90] to exploit the correlation between successive channel realizations in order to improve the quantization, and thus to improve the sum rate of the system. Further, our scheme does not make any assumptions on the scheduling function and on the transmission strategy, which allows for a high flexibility.

Notation: We use capital boldface letters to denote matrices, and small boldface letters to denote vectors. $E(\cdot)$ denotes expectation, $|\mathcal{A}|$ the cardinality of a set $\mathcal{A}$, and $\|\mathbf{a}\|$ the l^2-norm of a vector $\mathbf{a}$. $\mathbf{I}_m$ denotes the $m \times m$ identity matrix, and $\otimes$ represents the Kronecker product.

6.2 System Model

We assume the MISO broadcast channel as specified in Section 1.1.2, i.e., the downlink of a flat-fading multiuser system where the base station is equipped with N_T antennas, serving N_U single-antenna users. Given a set $\mathcal{S}$ of N_T users scheduled for transmission, the corresponding data model using linear beamforming at time instant t is

$$y_k[t] = \sum_{i \in \mathcal{S}} \mathbf{h}_k[t] \sqrt{E_i} \mathbf{w}_i[t] s_i[t] + n_k[t] \tag{6.1}$$

where $y_k \in \mathbb{C}$ is the received symbol of user k, $\mathbf{h}_k \in \mathbb{C}^{1 \times M}$ the channel vector of user k, E_i is the transmit energy assigned to user i, $\mathbf{w}_i \in \mathbb{C}^{M \times 1}$ the beamforming vector for user i, and s_i the data symbol transmitted to user i. The noise $n_k \in \mathbb{C}$ is i.i.d., and zero mean circularly symmetric complex Gaussian distributed with variance N_0.

Although the proposed methods work for more general channel models, we assume for simplicity that the different channel vectors are i.i.d., and that the channel correlation is separable in space and time:

$$\mathbf{R}_m = E(\mathbf{h}_k^H[t] \mathbf{h}_k[t-m]) = \mathbf{R} \rho_m \tag{6.2}$$

where $\mathbf{R}$ is the space-correlation matrix, and ρ_m is the time-correlation function. In this chapter, we will mainly concentrate on the time-correlation. Exploitation of the space-correlation for limited feedback in broadcast channels was studied in Chapter 5.

The data is transmitted in a block-wise fashion. We assume a data-rate limited feedback link that can feed back B bits at the beginning of each block. Further, the feedback is assumed to be instantaneous and error-free.

We assume that the receivers have achieved perfect CSI through the use of training, i.e., symbols both known to the transmitter and the receiver are transmitted over the channel and based on the received symbols the channel is estimated. Note that acquiring perfect CSI at the receiver is not possible for practical system, but we assume perfect CSI in order to keep the problem managable. The users then quantize the CSI to an element of a codebook $\mathcal{C}$, and feed back the

corresponding index to the base station. The base station then decides, based on the received feedback, which set of users to serve, and their corresponding beamforming vector.

The performance of the vector quantization (VQ) step can be improved by taking the time correlation of the channel into account. Vector quantizers with memory allow to quantize the actual channel more efficiently, i.e., the quantization error of VQ with memory is smaller than the quantization error of VQ without memory for the same amount of feedback. Even though there exists a large number of VQs with memory [17], we focus in this chapter solely on predictive VQ (PVQ) since its simplicity makes it a good candidate for practical systems. It allows to exploit the correlation of the channel by considering a variable number of previous channels, without an exponential increase of the storage requirements for the codebooks as is the case for finite-state vector quantizers.

6.2.1 Linear Beamforming

The most common linear beamforming schemes are transmit matched filtering and zero-forcing (ZF) beamforming [7]. Transmit matched filtering uses the normalized channel vector as beamforming vector. A scheme with a better performance is ZF beamforming. It provides a good tradeoff between the high-complexity schemes with good performance, e.g., DPC, and schemes like matched filtering.

The different ZF beamforming vectors are calculated based on the concatenated matrix $\hat{\mathbf{H}}$. The rows of $\hat{\mathbf{H}}$ consist of all the quantized channels $\hat{\mathbf{h}}_i$ of the users from the set $\mathcal{S}$. The ZF beamforming vectors are then the normalized columns of the pseudo-inverse of $\hat{\mathbf{H}}$.

6.2.2 User Selection

The optimal set of active users scheduled for transmission, denoted as $\mathcal{S}^*$, is selected to maximize the sum rate of the active users by an extensive search over

all possible combinations of users

$$\mathcal{S}^* = \arg\max_{\mathcal{S}} \sum_{k\in\mathcal{S}} \log_2(1+\mathrm{SINR}_k) \tag{6.3}$$

where the signal-to-interference-and-noise ratio (SINR) is calculated as

$$\mathrm{SINR}_k = \frac{E_k|\hat{\mathbf{h}}_k\mathbf{w}_k|^2}{\sum_{i\in\mathcal{S},i\neq k} E_i|\hat{\mathbf{h}}_k\mathbf{w}_i|^2 + N_0} \tag{6.4}$$

and $\hat{\mathbf{h}}_k$ is the quantized CSI known to the transmitter. Note that this exhaustive search is computational very expensive if a large number of users is in the cell. However, the focus of this chapter is CSI quantization, and thus, we use optimal scheduling.

6.3 Predictive Vector Quantization

This section gives an overview of PVQ and its application to channel quantization of broadcast channels. For simplicity reasons, we omit the user index here.

PVQ starts by estimating the actual channel $\mathbf{h}[t]$ based on the m previously quantized channels $\hat{\mathbf{h}}[t-i], i = 1\ldots m$, at both the base station and the users, resulting in

$$\tilde{\mathbf{h}}[t] = P(\hat{\mathbf{h}}[t-1], \hat{\mathbf{h}}[t-2], \ldots, \hat{\mathbf{h}}[t-m]) \tag{6.5}$$

where $P(\cdot)$ denotes the prediction function. Note that the channel estimate is used in the next steps both by the base station and the users. Is is thus essential that the prediction can be done by the base station and the users. The users, who have full CSI knowledge, then calculate the true error $\mathbf{e}[t]$ between the estimated channel $\tilde{\mathbf{h}}[t]$ and the true channel $\mathbf{h}[t]$:

$$\mathbf{e}[t] = \mathbf{h}[t] - \tilde{\mathbf{h}}[t] \tag{6.6}$$

The error is quantized by finding the entry in the quantization codebook $\mathcal{C}$ with

the smallest Euclidean distance to the true error

$$\mathbf{e}_Q[t] = \arg\min_{\mathbf{c}\in\mathcal{C}} \|\mathbf{e}[t] - \mathbf{c}\|^2. \tag{6.7}$$

The quantized error $\mathbf{e}_Q[t]$ is fed back to the base station, and the quantized channel at time instant t is then computed as

$$\hat{\mathbf{h}}[t] = \tilde{\mathbf{h}}[t] + \mathbf{e}_Q[t]. \tag{6.8}$$

The challenge of PVQ is to design the codebook and the prediction function.

6.3.1 Codebook Design

A popular approach to design a codebook for PVQ is the open-loop approach [17]. It does not have an iterative nature, and it relies on the assumption that the quantized channels are a good approximation of the real channels. The codebook design assumes that the prediction function is known, and it uses regular VQ without memory on a training set $\mathcal{T}$, where the different elements of the training set $\mathcal{T}$ are the ideal prediction errors calculated as

$$\mathbf{e}_{\text{ideal}}[t] = \mathbf{h}[t] - P(\mathbf{h}[t-1], \mathbf{h}[t-2], \ldots, \mathbf{h}[t-m]). \tag{6.9}$$

The application of a memoryless VQ is possible since the prediction step in (6.9) removes, in the ideal case, the time correlation between the channels at different time instants.

Note that the ideal prediction error $\mathbf{e}_{\text{ideal}}[t]$ differs from the true error $\mathbf{e}[t]$ in (6.6). The true error is calculated as a function of the previously quantized channels, and thus depends on the quantization codebook. Using the ideal prediction error to design the codebooks removes this dependence, hence the name open-loop approach. Iterative designs, i.e., closed-loop approaches [90], only provide a minor gain.

The most common algorithm to design codebooks is the generalized Lloyd algorithm (GLA) [35]. It is a descent algorithm [17], i.e., it reduces the average distortion of the codebook with every iteration. However, the GLA is not guaran-

teed to find the global optimal codebook for non-convex distortion functions [40], since it may get trapped in a local minimum.

A more robust approach to find good codebooks is a Monte-Carlo based codebook design. This approach generates random codebooks, estimates their performance through Monte-Carlo simulations, and finally keeps the codebook with the best performance. Even though this approach works well for small codebooks, it becomes computationally expensive for larger codebooks.

The optimal design aims at finding a codebook that maximizes the overal sum rate of the system. However, this design objective is computationally complex, and it depends on all the components of the system, e.g., the number of users, the selected beamforming strategy, the selection function.

To reduce the computational complexity, we focus instead on codebooks which minimize the average Euclidean distance between the ideal prediction error, and the quantized prediction error

$$\mathcal{C}^* = \arg\min_{\mathcal{C}} E(\|\mathbf{e}_{\text{ideal}}[t] - \mathbf{e}_{\text{ideal},Q}[t]\|^2) \tag{6.10}$$

with

$$\mathbf{e}_{\text{ideal},Q}[t] = \arg\min_{\mathbf{c}\in\mathcal{C}} \|\mathbf{e}_{\text{ideal}}[t] - \mathbf{c}\|^2. \tag{6.11}$$

6.3.2 Prediction Function

The other crucial part in designing the PVQ is the prediction function. A common technique for PVQ [17] is vector linear prediction [91].

Based on the previous m known channel vectors we want to predict the actual vector $\mathbf{h}[t]$ using coefficient matrices $\mathbf{A}_j$:

$$\widetilde{\mathbf{h}}[t]^H = -\sum_{j=1}^{m} \mathbf{A}_j \mathbf{h}[t-j]^H \tag{6.12}$$

The goal is to minimize the average mean square prediction error. Using the

orthogonality principle, the coefficient matrices can be derived from

$$\mathbf{R}_{0,j} = -\sum_{\mu=1}^{m} \mathbf{A}_\mu \mathbf{R}_{\mu j} \quad j = 1, \ldots, m \tag{6.13}$$

where $\mathbf{R}_{i,j}$ is the channel correlation matrix

$$\mathbf{R}_{i,j} = E(\mathbf{h}[t-i]^H \mathbf{h}[t-j]). \tag{6.14}$$

Stacking (6.13) in matrix form as

$$\begin{bmatrix} \mathbf{R}_{1,1} & \mathbf{R}_{1,2} & \ldots & \mathbf{R}_{1,m} \\ \mathbf{R}_{2,1} & \mathbf{R}_{2,2} & \ldots & \mathbf{R}_{2,m} \\ \vdots & \vdots & \ddots & \vdots \\ \mathbf{R}_{m,1} & \mathbf{R}_{m,2} & \ldots & \mathbf{R}_{m,m} \end{bmatrix} \begin{bmatrix} \mathbf{A}_1^H \\ \mathbf{A}_2^H \\ \vdots \\ \mathbf{A}_m^H \end{bmatrix} = - \begin{bmatrix} \mathbf{R}_{1,0} \\ \mathbf{R}_{2,0} \\ \vdots \\ \mathbf{R}_{m,0} \end{bmatrix} \tag{6.15}$$

the coefficient matrices $\mathbf{A}_j$ can now be found through simple matrix inversion. For the channel model presented in Section 6.2, we have that $\mathbf{R}_{i,j} = \mathbf{R}_{j,-i} = \mathbf{R}\rho_{j-i}$. In that case, (6.15) becomes

$$\left(\begin{bmatrix} \rho_0 & \rho_{-1} & \ldots & \rho_{-m} \\ \rho_1 & \rho_0 & \ldots & \rho_{-m+1} \\ \vdots & \vdots & \ddots & \vdots \\ \rho_m & \rho_{m-1} & \ldots & \rho_0 \end{bmatrix} \otimes \mathbf{R} \right) \begin{bmatrix} \mathbf{A}_1^H \\ \mathbf{A}_2^H \\ \vdots \\ \mathbf{A}_m^H \end{bmatrix} = - \begin{bmatrix} \rho_{-1} \\ \rho_{-2} \\ \vdots \\ \rho_{-m} \end{bmatrix} \otimes \mathbf{R}. \tag{6.16}$$

If $\mathbf{R}$ is assumed diagonal, it is clear that this equation can be solved for every channel entry separately.

6.4 Simulations

We start by comparing the sum rate, which we want to maximize, for PVQ with ZF beamforming, and of OSDMA-LF [77]. We assume a base station with $N_T = 2$ antennas, N_U users with SNR = 10 dB, and a data rate limited feedback link ($B = 3$ bits). The channel is modeled through (6.2) with $\mathbf{R} = \mathbf{I}_M$ and

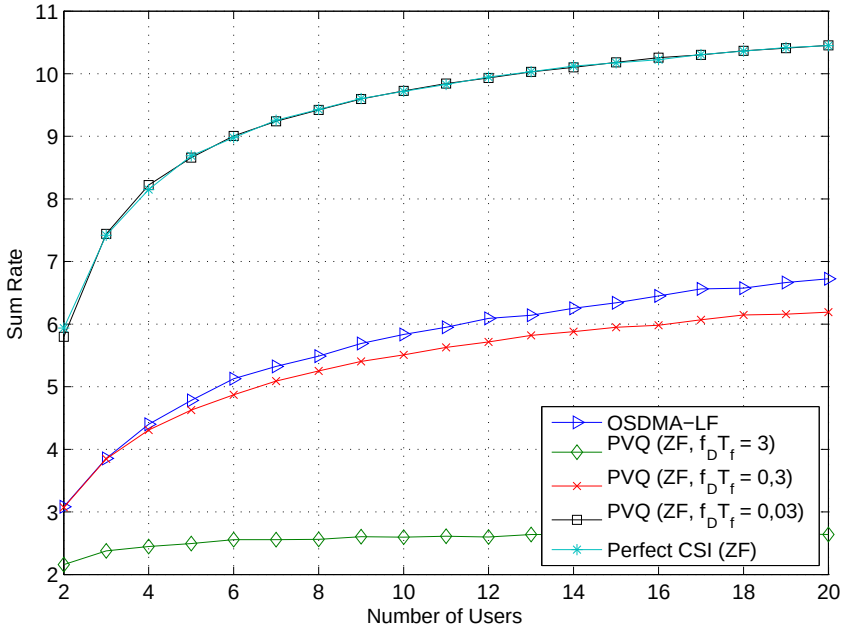

Figure 6.1: The sum rate for different number of users. ($N_T = 2$, and SNR = 10 dB)

$\rho_m = J_0(2\pi f_D T_f m)$ where J_0 is the Bessel function of zeroth-order, f_D the Doppler spread, and T_f the frame length (Jakes' model [66]). Thus, we simply have to simulate different products $f_D T_f$. The algorithm predicts the actual channel based on the last $m = 3$ channels using polynomial extrapolation of order $p = m - 1$. The initial channels are assumed to be known perfectly, which can be approximated by starting the algorithm with a high-resolution memoryless VQ. In order to make a fair comparison to OSDMA-LF possible, we enforce the feedback limitation, i.e., no scalar SINR feedback is allowed. Thus, we also have to quantize the SINR feedback of the OSDMA-LF scheme. The SINR codebook is generated with the GLA using the mean squared error as distortion function. We simulate all the possible bit-distributions between SINR quantization and beamforming indexing, and finally choose the distribution which results in the highest SINR [86]. We see in Fig. 6.1 how the performance of PVQ with ZF improves for higher $f_D T_f$ values, i.e., for scenarios with a higher time correlation between the channels. For $f_D T_f = 0,03$ the resulting SINR curve for PVQ with ZF and quantized feedback is similar to the performance of ZF with perfect CSI. Simulations depicting the performance of CSI quantization for spatially correlated channels can be found in Chapter 5.

Fig. 6.2 shows the influence of the initial quantization of the first m channels on the average sum rate. The plot compares the scenario where perfect CSI of the first m channels is available to scenarios where the first m channels have been quantized. We see how the sum rate increases after the first frame for larger codebooks. However, the importance of the quantization of the first m channels degrades over time, and all the schemes would converge to the same sum rate after a while.

6.5 Conclusions

We depicted through numerical simulations the benefits of using PVQ for time-correlated channels. PVQ uses a simple prediction step to remove the correlation between the channel to be quantized and the previous channels. This allows us to improve the performance of the quantization step.

We have seen in Chapter 5 and now in Chapter 6 that it is beneficial to

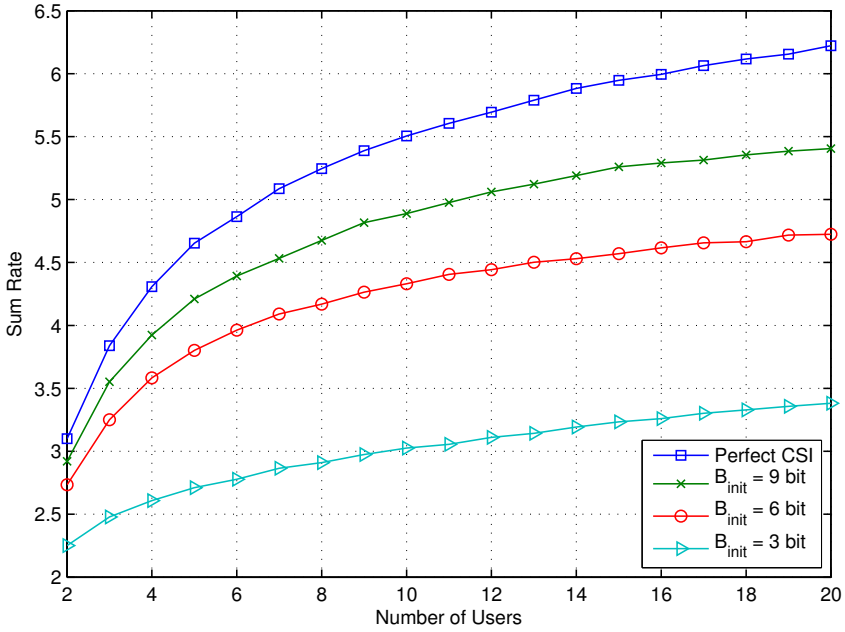

Figure 6.2: Influence of the size of the initialization codebook on the sum rate. ($N_T = 2$, $T_f = 10^{-2}$ s, $f_D = 30$ Hz, $B = 3$ bits, and SNR $= 10$ dB)

adapt the feedback mechanism to an existing temporal or spatial correlation of the broadcast channel. However, this requires that the nature of the correlation is known and that it is possible to train the feedback mechanism accordingly. A possible extension would be to investigate schemes that adapt at runtime to the channel statistics, i.e., similar to the ideas investigated in Section 3.4.

Part III

Scheduling in Multi-User MISO Channels

Chapter 7

Low-Delay Scheduling with Grassmannian Beamforming*

In the following part we are mainly concerned about scheduling the users. We propose in this chapter an algorithm to schedule the users of a broadcast channel in a near round-robin fashion, i.e., in every block every user is scheduled once. In the next chapter we then present an algorithm to realize true round robin scheduling, i.e., every user is scheduled at the same position in the block as long as possible.

We are presenting an algorithm for scheduling users in a single-cell broadcast scenario. The presented algorithm aims to minimize the number of transmissions that are necessary to serve all the users in the cell a single time, while the different users still fulfill a strict SINR constraint. Depending on the individual channel characteristics, the presented algorithm adapts the number of users scheduled for transmission on the fly, and dynamically allocates the transmit power to the scheduled users. A high-performance and a low-complexity variant of the algorithm are presented and their performance is evaluated through simulations.

*The results in this chapter have been published in [32].

7.1 Introduction

An important scenario in modern communications is the wireless broadcast channel. It covers the transmission from a single base station to multiple users. Transmission schemes for broadcast channels are generally designed to maximize the data rate from the base station to the users. The multiuser diversity in a broadcast channel allows high data-rates by simultaneously transmitting to a set of users, i.e., spatial division multiple access (SDMA) [3].

A popular low-complexity joint-beamforming-and-scheduling algorithm is opportunistic SDMA (OSDMA) [76]. OSDMA uses a random set of orthogonal beamforming vectors. The users calculate the individual signal-to-interference-plus-noise ratios (SINR) for the beamforming vectors and feed back the SINR and the index of the beamforming vector with the highest SINR. OSDMA is optimal for scenarios with a large number of users in the cell, i.e., the sum rate of OSDMA scales like the sum rate of dirty-paper-coding as a function of the number of users and the number of transmit antennas [76]. The OSDMA algorithm was extended to the use of multiple sets of orthogonal beamforming vectors in [77]. The transmission to a number of users that is higher than the number of antennas at the base station was presented in [92]. There, Grassmannian codebooks [93] were used as beamforming vectors. An algorithm that switches from time-division multiple access (TDMA) to SDMA based on statistical assumptions has been proposed in [94] .

These systems focus mainly on opportunistic or proportional-fair scheduling. This allows a high data-rate and achieves long-term fairness. However, improving the data-rate is not the only problem in practical systems. More important is that modern applications, e.g., audio and video communications systems, have strict delay requirements. Further, communication systems have strict SINR constraints, and improving the SINR over the minimum requirement does not yield any benefits. Even though opportunistic scheduling of the users has received much attention lately, scheduling schemes that minimize the maximal delay time, i.e., the time until all the users in the cell have been scheduled for transmission once, are not so well investigated, despite being of high practical relevance [95].

An exception is [96], where the problem of minimizing the frame duration by

dynamically switching between SDMA and TDMA is adressed. The presented algorithm, i.e., the Best Fit algorithm [96], explicitly aims to minimize the number of transmissions needed by the users to address the base station once. Further, all the scheduled users fulfill a strict SINR constraint.

We adapt the Best Fit scheduling algorithm for the broadcast channel with Grassmannian beamforming and imperfect channel state information (CSI) at the base station. The adapted algorithm further fulfills a strict transmit power constraint imposed by the base station. We present two variants of the algorithm, i.e., a high-performance variant and a low-complexity variant. The performance of the two variants is demonstrated through simulations, and it is shown that the adapted algorithm reduces the necessary transmission time while still guaranteeing the SINR constraint.

Notation: We use capital boldface letters to denote matrices, e.g., $\mathbf{A}$, and small boldface letters to denote vectors, e.g., $\mathbf{a}$. The $L2$-norm of a vector $\mathbf{a}$ is denoted as $|\mathbf{a}|$. $E(\cdot)$ denotes expectation, and the set $\mathcal{X}$ contains $|\mathcal{X}|$ elements.

7.2 System Model

We assume a narrowband single-cell system. The base station has M antennas, and there are K single-antenna users in the cell. The K users are indexed by integers and the set that contains all the indices is denoted $\mathcal{U}_{\text{all}} = \{1, \ldots, K\}$. The system equation for the transmission from the base station to the user i is [76]

$$y_i = \mathbf{h}_i \mathbf{x} + n_i \qquad \forall i \in \mathcal{U}_{\text{all}} \tag{7.1}$$

where $y_i \in \mathbb{C}$ is the data received by user i, $\mathbf{h}_i \in \mathbb{C}^{1\times M}$ is the channel between the base station and the user i, $\mathbf{x} \in \mathbb{C}^{M\times 1}$ is the data transmitted over the M antennas by the base station, and $n_i \in \mathbb{C}$ is the noise experienced by user i. The elements of the user channel are independent and identically distributed complex Gaussian with zero mean and unit variance. The noise is also independent and identically distributed complex Gaussian with zero mean, but with variance N_0. The channel is block-fading, i.e., it remains constant throughout a block of length

L. The maximal transmit energy of the data vector $\mathbf{x}$ is limited to E_T, i.e., $E\left\{\mathbf{x}^H\mathbf{x}\right\} \leq E_T$. All the users in the cell experience the same transmitted signal-to-noise ratio (SNR) of $\frac{E_T}{N_0}$.

We assume linear beamforming throughout the chapter. The base station simultaneously transmits data to the users in a set $\mathcal{T} \subseteq \mathcal{U}_{\text{all}}$ that contains $|\mathcal{T}|$ different users. The data symbol s_i, that is transmitted to user i, is picked from a PSK constellation with average unit-energy, e.g., QPSK. The different data symbols for the users in $\mathcal{T}$ are multiplied by a unit-norm beamforming vector $\mathbf{w}_i \in \mathbb{C}^{M\times 1}$ before transmission. The beamforming vectors are restricted to the elements of a codebook $\mathcal{W}$ with P elements which is known to the base station and all the users. We denote the mapping between each user and the index of its associated beamformer as $g : \mathcal{U}_{\text{all}} \rightarrow \{1, \ldots, P\}$. Thus the transmitted symbol vector is

$$\mathbf{x} = \sum_{i\in\mathcal{T}} \sqrt{E_i}\mathbf{w}_{g(i)}s_i \tag{7.2}$$

where E_i is a power normalization factor. Due to the overall transmit power restriction the individual powers have to fulfill the constraint

$$\sum_{i\in\mathcal{T}} E_i \leq E_T. \tag{7.3}$$

We assume perfect channel knowledge at the user side. Assuming a closed-loop scenario, there exists a feedback link between the users and the base station. The feedback link is only used for improving the downstream transmission, i.e., the transmission from the base station to the users. The link itself is assumed to be error-free and instantaneous.

7.3 Modified Grassmannian Beamforming

One of the differences between our approach and opportunistic schemes such as Grassmannian beamforming is that a user i does not feed back the resulting SINR of the strongest beam and the corresponding index, but the composite channel energy $\rho_{i,p} = |\mathbf{h}_i\mathbf{w}_p|^2$ for all the beamforming vectors $p = 1, \ldots, P$. The values

of the composite channel energy for all the beamforming vectors are necessary in the scheduling step to evaluate the interference produced by the other scheduled users, as explained in Section 7.5.

7.3.1 Beamformer Codebooks

The beamforming vectors are selected from a Grassmannian codebook $\mathcal{W} = \{\mathbf{w}_1, \ldots, \mathbf{w}_P\}$. [93].

The unit-norm entries in the codebook are representing 1-dimensional subspaces in $\mathbb{C}^M$, i.e., points in the complex Grassmannian space $\mathcal{G}(M, 1)$ [97]. The codebook is designed to maximize the smallest chordal distance between two unit-norm entries in the codebook

$$\mathcal{W} = \underset{\substack{\{\mathbf{w}_1,\ldots,\mathbf{w}_P\} \\ |\mathbf{w}_p|=1,\ p=1\ldots P}}{\arg\max} \min_{1\leq k<l\leq P} \sqrt{1 - |\mathbf{w}_k^H \mathbf{w}_l|^2}. \tag{7.4}$$

We design the codebook through a Monte-Carlo codebook design [17].

7.3.2 Training

The algorithm starts by estimating the individual user channels through training. Once every user has perfect CSI, he can calculate the matching ρ's for all the beamforming vectors, i.e., user i calculates

$$\rho_{i,p} = |\mathbf{h}_i \mathbf{w}_p|^2 \tag{7.5}$$

for $p = 1, \ldots, P$. These P ρ's are then transmitted to the base station. Note that we assume that $P < 2M$, and thus it is more efficient to feed back the P ρ's than feeding back the M complex channel coefficients.

If the ρ's are assumed to be noisy, due to erroneous CSI or due to quantization errors, then the base station allocates the available energy based on erroneous information. As a result, the users in $\mathcal{U}_{\text{sched}}$ are no longer guaranteed to fulfill the SINR constraint.

7.3.3 Beamformer Selection

For each user i the base station selects the beamforming vector that results in the highest composite channel energy ratio

$$g(i) = \underset{j=1,\ldots,P}{\arg\max}\, \rho_{i,j} \qquad \forall i \in \mathcal{U}_{\text{all}}. \tag{7.6}$$

The beamforming has to rely on the fed back ρ's, and thus, beamforming techniques that select the beamforming vector based on the CSI of the other scheduled users, e.g., ZF or MMSE beamforming, cannot be used.

7.4 Problem Formulation

We consider the problem of minimizing the time necessary to successively schedule the users in a single cell once. The different scheduled users must sustain a minimum SINR, denoted $\text{SINR}_{\min}$. This constraint allows to choose a fixed modulation and coding for all the users. Adapting these parameters would result in additional overhead, i.e., the base station would have to inform the users about the selected coding and modulation. However, due to the fading nature of the wireless channel, some user channels might be in a deep fade, and reliable communication is not possible to these users. Thus, we exclude the users that are not able to fulfill the SINR constraint even when there are no interfering users present and all available power is allocated to them, i.e., TDMA. The set of users in the cell that can fulfill the SINR constraint under TDMA is defined as

$$\mathcal{U}_{\text{sched}} = \left\{ u \in \mathcal{U}_{\text{all}} \mid \frac{E_T}{N_0} |\mathbf{h}_u \mathbf{w}_{g(u)}|^2 \geq \text{SINR}_{\min} \right\}. \tag{7.7}$$

Note that if $\mathcal{U}_{\text{sched}} = \emptyset$ then the algorithm stops without scheduling a single user.

We want to find an algorithm that is able to address all the users in $\mathcal{U}_{\text{sched}}$ once and in a minimum of time, as presented in (7.8). If $\mathcal{U}_{\text{sched}} \neq \emptyset$ then (7.8) provides a solution. The worst-case solution is that the elements of $\mathcal{U}_{\text{sched}}$ are scheduled in a TDMA fashion. The set of users scheduled for transmission at a time step k is denoted $\mathcal{T}[k]$. Every user has to have a SINR higher or equal $\text{SINR}_{\min}$. We further require that the sum of the energy assigned to a set is smaller than or

$$
\begin{aligned}
\text{minimize} \quad & N \\
\text{subject to :} \quad & \frac{E_i |\mathbf{h}_i \mathbf{w}_{g(i)}|^2}{\sum_{j \in \mathcal{T}[k], j \neq i} E_j |\mathbf{h}_i \mathbf{w}_{g(j)}|^2 + N_0} \geq \text{SINR}_{\min} \\
& \qquad \forall i \in \mathcal{T}[k],\ k = 1 \ldots N \\
& \bigcup_{k=1}^{N} \mathcal{T}[k] = \mathcal{U}_{\text{sched}} \quad \text{and} \quad \sum_{i \in \mathcal{T}[k]} E_i \leq E_T,\ k = 1 \ldots N \quad \text{and} \\
& g(i) \neq g(j),\ \forall i, j \in \mathcal{T}[k], i \neq j, k = 1 \ldots N
\end{aligned}
\tag{7.8}
$$

equal to E_T and that the users in a set are all assigned different beamforming vectors. The number of transmissions necessary to serve all the users in $\mathcal{U}_{\text{sched}}$ once is denoted N. We assume throughout the chapter that $L = N$. If $L > N$ then the algorithm would restart scheduling all the users again in the same way until the end of the block, and if $L < N$ then the algorithm would simply address the remaining users in the next block.

In solving (7.8), the base station decides based on the KP ρ's that are fed back from the users, which users to schedule for transmission.

7.5 Scheduling

The base station decides based on the feedback which users are scheduled for transmission. We assume that the composite channel energies are perfectly known to the base station, i.e., no quantization on the feedback link and perfect channel knowledge at the user side. Thus, we can rewrite the SINR constraint, that all the users in the set $\mathcal{T}$ must fulfill, from (7.8) as

$$
(\text{SINR}_{\min})^{-1} E_i \rho_{i,g(i)} \geq \sum_{j \in \mathcal{T}[k], j \neq i} E_j \rho_{i,g(j)} + N_0 \tag{7.9}
$$

where the terms on the right side yield the interference penalty for choosing additional users and the noise. Note, that we will omit the time index in the rest of the section.

We start by adapting the Best Fit algorithm [96] to work with the composite channel energies, and then we present two variants to find a solution to (7.8). The two variants have different complexities and different performances. However, both variants can serve the same set of scheduled users $\mathcal{U}_{\text{sched}}$, i.e., both algorithms are using TDMA $\mathcal{T} = \{i\}$ with $E_i = E_T$ for a user i with adverse channel conditions. The main difference between the two variants is how they allocate the power to the beamforming vectors.

7.5.1 Adapted Best Fit Algorithm

The algorithm starts by eliminating all the users from the original user set $\mathcal{U}_{\text{all}}$ that can not even fulfill the desired SINR constraint $\text{SINR}_{\min}$ when they are scheduled alone, i.e., in the TDMA mode. The set of users that can be scheduled for transmission is calculated as

$$\mathcal{U}_{\text{sched}} = \left\{ u \in \mathcal{U}_{\text{all}} \mid \frac{E_T}{N_0} \rho_{u,g(u)} \geq \text{SINR}_{\min} \right\}. \tag{7.10}$$

From the resulting set $\mathcal{U}_{\text{sched}}$ the user with the lowest composite channel energy is selected

$$u = \underset{i \in \mathcal{U}_{\text{sched}}}{\arg\min}\, \rho_{i,g(i)} \tag{7.11}$$

and the scheduled user set is initialized with $\mathcal{T} := \{u\}$. The scheduled user is removed from the set of users that can be scheduled $\mathcal{U}_{\text{sched}} := \mathcal{U}_{\text{sched}} \setminus \{u\}$. The algorithm now iteratively tries to add users to the set $\mathcal{T}$. How such an additional user u_{best} is selected varies on the possible power allocation for the beamforming vectors and is explained in the following two subsections. Once the best matching user u_{best} is found the set is updated $\mathcal{T} := \mathcal{T} \cup \{u_{\text{best}}\}$ and the user is removed from the set of scheduled users $\mathcal{U}_{\text{sched}} := \mathcal{U}_{\text{sched}} \setminus \{u_{\text{best}}\}$. This continues until the algorithm does not find an additional user anymore and the base station starts transmitting to the users in $\mathcal{T}$. Finally, the algorithm restarts with the updated set $\mathcal{U}_{\text{sched}}$ until $\mathcal{U}_{\text{sched}} = \emptyset$.

7.5.2 Low-Complexity Variant

The low-complexity variant equally distributes the available transmit energy E_T to the scheduled users

$$E_i = \frac{E_T}{|\mathcal{T}|}, \qquad i \in \mathcal{T}. \tag{7.12}$$

The user selection is done by

$$u_{\text{best}} = \underset{u \in \{l \in \mathcal{U}_{\text{sched}} \mid g(l) \neq g(i), i \in \mathcal{T}\}}{\arg\max} \min_{v \in \mathcal{T} \bigcup \{u\}} \left(\text{SINR}_{\min}\right)^{-1} \rho_{v,g(v)} - \sum_{j \in \mathcal{T}} \rho_{v,g(j)} - N_0 \frac{|\mathcal{T}| + 1}{E_T}. \tag{7.13}$$

The penalty for adding an additional user, i.e., the negative terms in (7.13), consists of the interference produced by the other scheduled users and the reduction of the power allocated to the individual users since the transmission power is now distributed over more users. Note that the selection function guarantees that the different elements in the set have unique beamforming vectors.

After a candidate u_{best} has been determined, the algorithm then checks if the SINR constraint (7.9) is still fulfilled. If (7.9) is not fulfilled, then u_{best} is not added to $\mathcal{T}$, and the base station starts transmitting to $\mathcal{T}$. Then $\mathcal{T}$ is removed from $\mathcal{U}_{\text{sched}}$ and the algorithm restarts. The SINR constraint can also be checked simultaneously with the user selection by checking if the SINR term inside the user selection remains positive for all the members in the set $\mathcal{T} \bigcup \{u\}$.

7.5.3 High-Performance Variant

The following variant can assign different transmit powers to the beamforming vectors in order to balance the SINRs of the different users. An algorithm to maximize the smallest SINR in a set of users with fixed beamforming vectors by adapting the power allocation assigned to the different users was presented in [98].

The high-performance variant selects the additional users by solving

$$u_{\text{best}} = \underset{\{u \in \mathcal{U}_{\text{sched}} \mid g(u) \neq g(i), i \in \mathcal{T}\}}{\arg\max} \min_{v \in \mathcal{T} \bigcup \{u\}} \left(\text{SINR}_{\min}\right)^{-1} E_v \rho_{v,g(v)} - \sum_{j \in \mathcal{T}} E_j \rho_{v,g(j)} - N_0(|\mathcal{T}| + 1) \quad (7.14)$$

under the constraint $\sum_{i \in \mathcal{T} \cup \{u\}} E_i = E_T$. Thus, for every considered set $\mathcal{T} \cup \{u\}$ the individual transmit powers E_i, $i \in \mathcal{T} \cup \{u\}$, have to be recalculated by using the algorithm in [98]. The computational most expensive step of this SINR-balancing algorithm is the calculation of the largest eigenvalue and the corresponding eigenvector of a complex matrix with the dimensions $|\mathcal{T}| + 1 \times |\mathcal{T}| + 1$. Thus, the high-performance variant of Section 7.5.3 has a much higher complexity than the low-complexity version presented in Section 7.5.2.

7.6 Simulation Results

In this section the performance of the high-performance (HP) variant and the low-complexity (LC) variant are compared. We assume that the base station has $M = 3$ antennas and that there are $K = 100$ single-antenna users present in the cell. We consider a beamforming codebook with $P = 4$ entries, and all the users experience the same SNR = 18 dB.

Fig. 7.1 depicts the number of transmissions needed to serve all the users in $\mathcal{U}_{\text{sched}}$. We see how for a growing $\text{SINR}_{\min}$ the two variants of the algorithm gradually require more transmissions to serve the $K = 100$ users. The two variants slowly switch from SDMA to a TDMA mode in order to fulfill the given SINR constraint (7.9). We see that the HP variant outperforms the LC variant over all possible SINR constraints. The HP variant performs better because it can allocate more energy to the weak users in the scheduled set, and thus, improve the smallest SINR in the scheduled set. We also see that N slightly decreases for a high $\text{SINR}_{\min}$. This is because even in TDMA mode, where the base station allocates all the power to the single scheduled user, it is not possible to fulfill the

high SINR constraint of all the users. Thus, for an increasing SINR constraint, the number of non-scheduled users also increases.

In Fig. 7.2 we compare our algorithm to the traditional Grassmannian beamforming algorithm [92]. We depict the ratio of the number of users that are scheduled for transmission $|\mathcal{U}_{\text{sched}}|$ to the number of users in the cell $|\mathcal{U}_{\text{all}}|$ for different SINR constraints. The Grassmannian beamforming algorithm feeds back one scalar, i.e., the SINR for the strongest beamformer, and one integer, i.e., the index of this beamformer. We see that feeding back the composite channel energies, and thus being able to adapt the number of scheduled users, allows a larger amount of users to be served for a given SINR constraint. Please note that it is not necessary to distinguish between the low-performance and the high-performance variant, since both variants resort to TDMA in the worst case.

The next simulation depicts how the different variants group their users into sets. We see in Fig. 7.3 that the HP variant collects in general more users in a set than the low-complexity variant. For increased values of SINR_{min} both variants are no longer able to schedule sets with the maximum number of users P. The amount of incomplete sets increases until for very high values of SINR_{min} most scheduled sets consist of a single users.

7.7 Conclusions

We have proposed two variants of the BestFit algorithm to schedule all the users in a broadcast channel once. The algorithm minimizes the amount of transmissions needed to schedule the different users under strict SINR constraints. The variants differ in their computational complexity. Both variants can switch between TDMA and SDMA depending on the channel conditions. The LC variant distributes the available transmit energy equally amongst the scheduled users, and the HP variant uses the available transmit energy to balance the SINR of users scheduled in the same time instant. The performance of both variants is compared through simulations. They show the benefit of carefully distributing the available transmit energy, i.e., the gain of the HP variant over the LC variant. A possible extension of the presented work would be the consideration of noisy feedback.

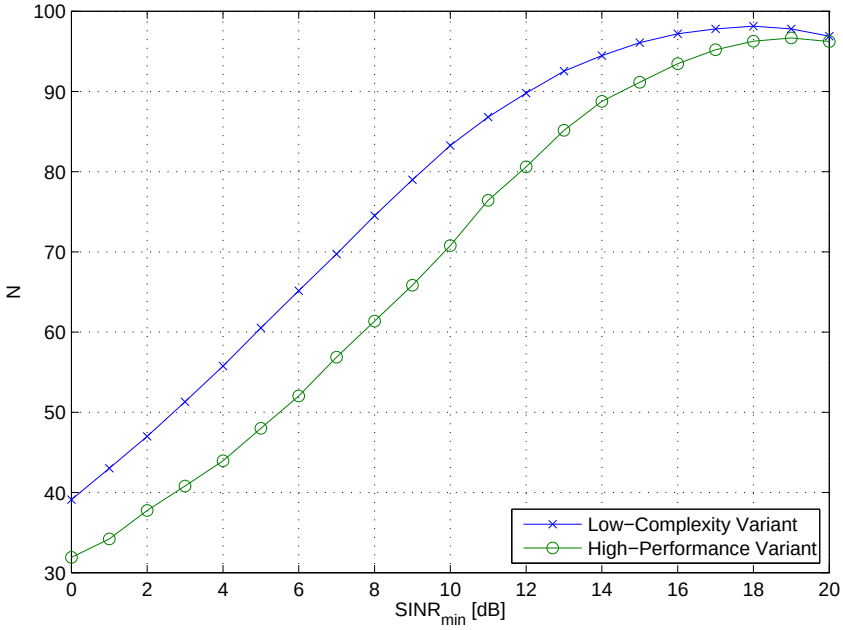

Figure 7.1: Number of transmissions N as a function of $\mathrm{SINR}_{\min}$. ($M = 3$, $P = 4$, $K = 100$, and $\mathrm{SNR} = 18$ dB)

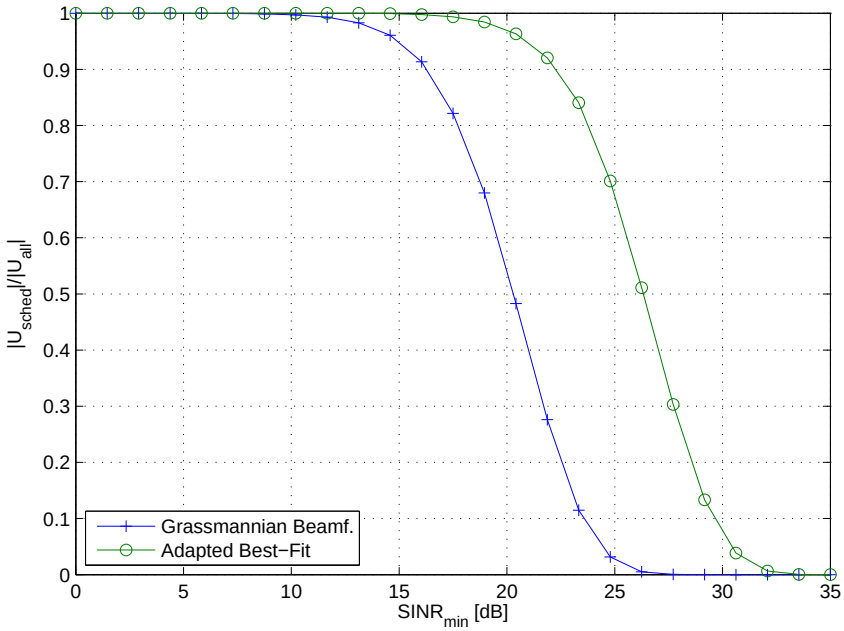

Figure 7.2: Ratio between $|\mathcal{U}_{\text{sched}}|$ and $|\mathcal{U}_{\text{all}}|$ as a function of $\text{SINR}_{\min}$. ($M = 3$, $P = 4$, $K = 100$, and $\text{SNR} = 18$ dB)

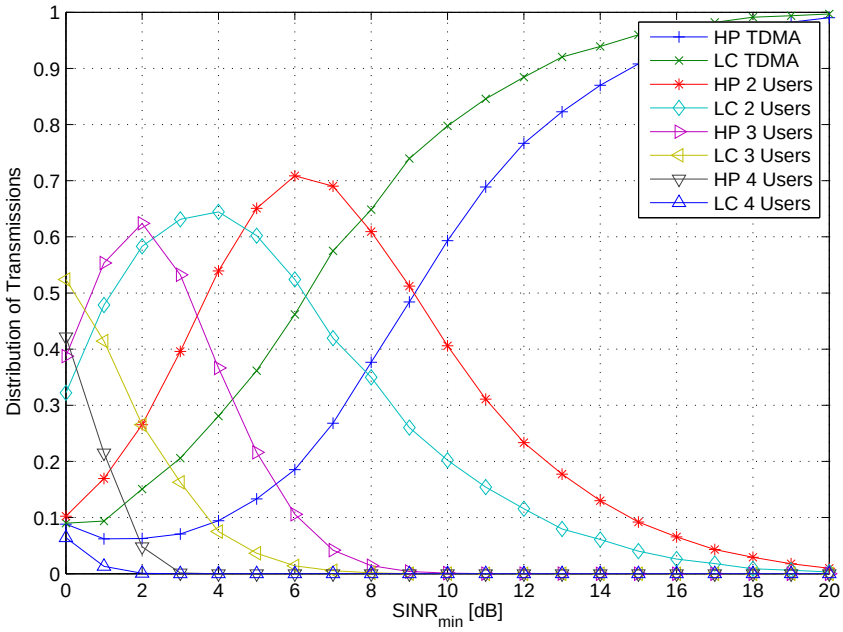

Figure 7.3: Distribution of the transmissions with different number of users for the high-performance variant (HP) and the low-complexity variant (LC). ($M = 3$, $P = 4$, $K = 100$, and SNR $= 18$ dB)

Chapter 8

Round-Robin Scheduling for Orthogonal Beamforming*

After the previous chapter proposed two variants of the BestFit algorithm for near-round-robin scheduling, we present in this chapter an algorithm for true round-robin scheduling. The proposed algorithm uses orthogonal beamforming to schedule users with a strict signal to interference-plus-noise ratio (SINR) constraint and it assumes a limited feedback link from the users to the base station. The presented algorithm aims at scheduling the users at identical slots over different blocks, in order to reduce the necessary scheduling overhead, and to minimize the maximum delay between serving the same user. The algorithm allocates the users using orthogonal beamforming based on the quantized feedback provided by the users. The quantized feedback consists of the estimated energy that is necessary to fulfill a predefined SINR constraint. Further, we propose an algorithm to design codebooks to quantize the estimated energy. Using the feedback, the base station redistributes energy from users with spare energy to users that lack energy so that they fulfill their SINR constraints. The performance of the algorithm is demonstrated through simulations.

*The results in this chapter have been published in [99].

8.1 Introduction

Some of the key drivers of wireless communication are delay-critical services like audio and video communication. Of special interest for these services is the vector Gaussian broadcast channel where the base station incorporates multiple antennas but the individual users just have a single antenna. The vector Gaussian broadcast channel promises large sum rates [100] if perfect channel state information (CSI) is available at the base station. CSI is easily acquired at the user side through training, but feeding back the CSI to the base station is problematic due to the inevitable data-rate limitation on the feedback link. This motivates the research into limited feedback systems where only partial CSI is fed back to the base station [101, 102].

Another challenging problem of multi-user schemes in general is scheduling. The scheduling algorithm should have a low complexity, but the transmissions to the users must still fulfill strict Quality-of-Service (QoS) constraints. An important QoS constraint is the minimum signal to interference-plus-noise ratio (SINR). The minimum SINR constraint requires that every scheduled user in the cell has an SINR larger than a predefined threshold. Further, especially for modern real-time multimedia communication systems, it is important that the delay between two transmissions to the same user remains constant, i.e., that the users are scheduled in a round-robin fashion. Another advantage of round-robin scheduling is the reduced overhead since the base station does not need to sacrifice transmission time to inform the users in every block about their allocated slot positions. However, due to the stochastic nature of the wireless channel, it is not possible to provide hard QoS guarantees, i.e., if the channel is in a deep fade it is not possible to fulfill the SINR constraint.

The large sum rate on the vector Gaussian broadcast channel is achievable with dirty paper coding (DPC) [25, 26, 100]. DPC has a high computational complexity, but the same performance gains are also possible with zero-forcing beamforming in the high user regions [74]. In [103], a scheduling algorithm for zero-forcing beamforming was proposed that takes the individual queue lengths at the base station into account. However, zero-forcing beamforming requires perfect CSI at the base station. One of the first schemes to exploit the multiuser

diversity assuming a data-rate limited feedback link is orthogonal beamforming (OB). OB was presented in [76] using opportunistic scheduling to maximize the instantaneous sum rate. The price of using opportunistic scheduling is the lack of short-term fairness, i.e., fairness is only achieved in the long run. The effect of partial CSI at the base station on zero-forcing beamforming was investigated in [104]. Another important aspect of beamforming is the distribution of the available energy over the different beamforming vectors. The solution to the power allocation for maximizing the minimum SINR of the scheduled user was presented in [98], and a solution to fulfill individual SINR constraints on the users was presented in [105].

An algorithm that takes the time-varying nature of the channel into account, but still provides strong bounds on the maximum delay, is the Channel Aware Round-Robin (CARR) scheduling algorithm [106]. It schedules every user once inside each block, but it does not implement true round-robin scheduling, since the positions of the users inside the block are dynamically allocated. The CARR algorithm chooses the positions depending on the channel state of the different users in the different slots. Thus, the maximum delay between two transmissions using the CARR algorithm is two block lengths. The main disadvantage of CARR scheduling compared to round-robin scheduling is the additional overhead. For CARR scheduling the base station has to inform the users for every block in what slot they are scheduled. A similar scheduling algorithm for space division multiple access (SDMA) is the Best Fit algorithm [107]. The Best Fit algorithm also tries to assign all the users in every block, but it uses SDMA to dynamically assign multiple users to the same slot depending on the resulting SINR. It further considers an SINR constraint. A low-complexity variant is the Partial Best Fit (PBF) algorithm [108]. It just adds new users according to the Best Fit strategy and removes the expired users, i.e., the users that have no more packets to transmit. An overview of other algorithms that consider scheduling under the exploitation of the spatial diversity can be found in [5].

Our proposed algorithm tries to schedule all the users in the cell in a round-robin fashion as long as possible. The application of orthogonal beamforming allows to reduce the interference between users scheduled at the same time instant. Further, it also reduces the feedback requirements from the users to the

base station since full CSI feedback is not necessary. We propose a corresponding feedback metric, and we consider the necessary quantization due to the data-rate limited feedback link. The feedback is used by the base station to dynamically divide the available transmit power among the users. This allows the weakest users, i.e., the users with the worst channel conditions, to fulfill the SINR constraint longer than with an equal power distribution. A user is rescheduled if he is no longer able to fulfill the SINR constraint despite receiving additional power, i.e., the user is scheduled at a different slot and with a different beamformer in the next block. The performance of the algorithm is depicted through simulations for a time-varying channel.

Notation: We use capital boldface letters to denote matrices, e.g., $\mathbf{A}$, and small boldface letters to denote vectors, e.g., $\mathbf{a}$. $E(\cdot)$ denotes expectation, and $P(\cdot)$ probability. We will denote the probability density function (pdf) of the random variable X as $f_X(x)$, and the cumulative distribution function (cdf) as $F_X(x)$. We write the logical conjunction between two values x and y as $x \wedge y$, and the logical disjunction as $x \vee y$.

8.2 System Model

We assume a narrowband single-cell scenario where a base station with M antennas transmits data to N single-antenna users. At a given time user i receives the symbol

$$y_i = \sum_{j \in \mathcal{S}} \mathbf{h}_i \mathbf{w}_{g(j)} \sqrt{E_j} s_j + n_i \tag{8.1}$$

where $\mathcal{S}$ contains the indices of the users scheduled at that time instant, $\mathbf{h}_i \in \mathbb{C}^{1\times M}$ is the channel of user i, and $\mathbf{w}_{g(j)} \in \mathbb{C}^{M\times 1}$ is the beamforming vector assigned to user j. The mapping $g(j)$ maps a beamforming vector from the beamformer codebook $\mathcal{W}$ to every user.

The energy assigned to user j is denoted E_j, and the data symbol s_j, that is transmitted to user j, is selected from a constellation with average unit energy. The noise n_i is complex Gaussian distributed with zero mean and variance N_0, i.e., $n_i \sim \mathcal{CN}(0, N_0)$. The total allocated transmit energy is limited to $E_T =$

$\sum_{i \in \mathcal{S}} E_i$, and the signal-to-noise ratio (SNR) of the system is $\text{SNR} = \frac{E_T}{N_0}$.

The users have the possibility to feed back information to the base station at the start of every block. The feedback link itself is instantaneous, error-free, and data-rate limited to B bits. All the users have to fulfill a strict SINR constraint denoted $\text{SINR}_{\min}$. We assume that the individual users acquire perfect channel state information (CSI) at the start of each block through training. The time-correlated channel is modeled according to Jakes' model [66].

Every block consists of K slots. We further assume that the channel is block-fading, i.e., the channel is constant throughout the K slots of a block. The block index k starts at $k = 0$, and the slot index l restarts at the beginning of each new block at $l = 0$. Thus, the relation between the current time step t and the current block/slot index is $t = kK + l$.

We are using a set of orthogonal beamforming vectors from a codebook $\mathcal{W}$ to simultaneously transmit to maximally M users [76]. The codebook $\mathcal{W}$ contains M orthogonal beamforming vectors $\mathbf{w}_m$. The M beamformers in the codebook all have unit norm, i.e., $\|\mathbf{w}_m\|_2 = 1, m \in \mathcal{M} = \{1, \ldots, M\}$. The codebook $\mathcal{W}$ is known to the users and to the base station. Note that a possible extension would be to consider multiple orthogonal beamforming codebooks.

8.3 Problem Description

The main objective is to schedule the users in a round-robin fashion. If a user i has been scheduled at time instant $t = (k-1)K + l$ using the beamformer $\mathbf{w}_m$, then we want to schedule him also at time instant $t = kK + l$ using the beamformer $\mathbf{w}_m$. Further, all the scheduled users have to fulfill a strict SINR constraint, i.e., they need to have an SINR higher than $\text{SINR}_{\min}$.

Serving the users in a round-robin fashion should result in a packet delay variation of zero. However, due to the time-varying nature of the wireless channel, there is a non-zero probability that the channel is in a deep fade, i.e., reliable communication is not possible. Thus, it is not possible to guarantee the QoS constraints, i.e., to have hard QoS guarantees. The problem is now to exploit the available feedback link to schedule the users as long as possible in a round-robin fashion while still fulfilling the SINR constraint.

8.4 Algorithm Overview

We assume that the different users are able to acquire perfect CSI at the beginning of each block, i.e., user i knows h_i at time $t = kK, \forall k$. Due to the block-fading nature of the channel, an individual user thus has perfect channel knowledge for every slot in the block. Using this channel knowledge the user then calculates how much energy the base station has to assign to him in order to reach the SINR constraint.

Next, this minimum energy is quantized and fed back to the base station. Once the base station receives all the feedback from the users, it checks for every time slot if the sum of the fed back quantized minimum energies exceeds the maximally allocatable transmit energy E_T at the base station. If the sum is lower, then all the users in that slot can be scheduled using the available transmit energy. However, if the sum is higher then it is not possible to schedule all the users. The users with the highest energy demands are dropped until the sum of the required energy for the remaining users is lower than the available transmit energy.

In the next step, the dropped users from the previous block and the users who just entered the cell are scheduled. Once all the users have been assigned to a slot, their required energy is assigned to them and the remaining energy is equally distributed to all the users in that slot.

8.4.1 Feeding Back the Required Energy

The SINR for user i is calculated as

$$\mathrm{SINR}_i = \frac{|\mathbf{h}_i \mathbf{w}_{g(i)}|^2 E_i}{\sum_{j \in \mathcal{S} \setminus \{i\}} |\mathbf{h}_i \mathbf{w}_{g(j)}|^2 E_j + N_0}. \tag{8.2}$$

We see that the SINR of user i depends on the individual transmit energies of the users in the set $\mathcal{S}$. In order to determine the minimum amount of energy that is required by user i to reach $\mathrm{SINR}_{\min}$, it is necessary to know the amount of energy that is assigned to the other users scheduled in the same slot. However, the individual energy levels assigned to the other users in the set are not known to the individual users. A solution is to feed back the full CSI to the base station

and to balance the SINR between the different users using the algorithm in [98]. The drawback is that it requires full channel knowledge or at least knowledge of the composite channel energies $|\mathbf{h}_i\mathbf{w}_{g(j)}|^2, j \in \mathcal{S}$ at the base station and thus incorporates a lot of feedback.

In this chapter, we try to find an estimate of the energy assigned to user i that fulfills the SINR constraint, and that does not depend on the energy levels assigned to the other users in the set $\mathcal{S}$. This required energy will be denoted $\hat{E}_i$. We start by defining an estimate of the true SINR, denoted $\hat{\text{SINR}}_i$, that does not depend on how the total transmit energy is distributed over the users in $\mathcal{S}$, but that is guaranteed to be smaller than the true SINR

$$\hat{\text{SINR}}_i \leq \text{SINR}_i. \tag{8.3}$$

Due to (8.3), it is certain that if the estimated SINR fulfills the SINR constraint, so does the true SINR, i.e., if $\text{SINR}_{\min} \leq \hat{\text{SINR}}_i$ then $\text{SINR}_{\min} \leq \text{SINR}_i$. We propose to use

$$\hat{\text{SINR}}_i = \frac{|\mathbf{h}_i\mathbf{w}_{g(i)}|^2 E_i}{\max_{j\in\mathcal{M}\setminus\{g(i)\}} |\mathbf{h}_i\mathbf{w}_j|^2(E_T - E_i) + N_0} \tag{8.4}$$

which is lower than or equal to the real SINR since inserting (8.4) and (8.2) into (8.3) results in

$$\sum_{j\in\mathcal{S}\setminus\{i\}} |\mathbf{h}_i\mathbf{w}_{g(j)}|^2 E_j \leq \max_{j\in\mathcal{M}\setminus\{g(i)\}} |\mathbf{h}_i\mathbf{w}_j|^2(E_T - E_i) \tag{8.5}$$

which is always true. The minimum energy assigned to a user i that fulfills the SINR constraint and that only depends on the total energy can thus be calculated as

$$\hat{E}_i = \frac{\max_{j\in\mathcal{M}\setminus\{g(i)\}} |\mathbf{h}_i\mathbf{w}_j|^2 E_T + N_0}{\frac{1}{\text{SINR}_{\min}}|\mathbf{h}_i\mathbf{w}_{g(i)}|^2 + \max_{j\in\mathcal{M}\setminus\{g(i)\}} |\mathbf{h}_i\mathbf{w}_j|^2}. \tag{8.6}$$

Next, the energy $\hat{E}_i$ is quantized and fed back to the base station.

The probability distribution of the required energy depends on whether the user is scheduled for the first time or not. If a user is scheduled for the first time,

then it chooses the beamforming vector that maximizes its SINR, i.e., the user chooses the beamforming vector

$$g(i) := \arg\max_{j \in \mathcal{M}} |\mathbf{h}_i \mathbf{w}_j|^2. \tag{8.7}$$

For the successive blocks, the beamforming vector $g(i)$ might no longer be the beamforming vector that results in the highest SINR for user i. However, even with this suboptimal beamforming vector, the user i might fulfill the SINR constraint.

As mentioned, if a user is scheduled for the first time, then its beamforming vector is determined using (8.7). For that case we call the required energy the initial required energy. The cdf and the pdf of the initial required energy are derived in Appendix 8.B. For every successive scheduling instant, however, the true channel changes according to the assumed channel model, but the selected beamforming vector remains the same. Note that then the index of the beamforming vector has to be fed back just once. In order to simplify the derivation of the cdf and the pdf of the required energy we assume, just for the derivation, that the channel is i.i.d. between the scheduling instances. This corresponds to a scenario where the channel has a high Doppler spread or where the user has been scheduled for a long time in the same slot. We call the resulting required energy, the regular required energy. The cdf and the pdf of the regular required energy are derived in Appendix 8.A.

8.4.2 Quantizing the Feedback

The data rate limitation on the feedback link makes a quantization of the minimum energy necessary before it can be fed back to the base station. The quantization Q maps the minimum energy $\hat{E}_i$ to an element of a predefined codebook $\mathcal{C} = \{c_1, \ldots, c_b\}$, i.e., $Q : \mathbb{R}^+ \to \mathcal{C}$. We assume that the codebook size is limited to $b = 2^B$ entries in order to fulfill the data-rate limitation of the feedback link. The required energy $\hat{E}_i$ of user i is quantized using

$$Q(\hat{E}_i) = \arg\min_{c_q \in \mathcal{C}} \; c_q - \hat{E}_i \quad \text{s.t.} \quad \hat{E}_i \leq c_q \tag{8.8}$$

and the index q of the element $c_q = Q(\hat{E}_i)$ of the codebook $\mathcal{C}$ is fed back to the base station. The quantized minimum energy of user i is denoted $\hat{E}_{Q,i} = Q(\hat{E}_i)$.

In order to prevent that a user gets too little energy assigned due to the quantization error, the condition $\hat{E}_i \leq Q(\hat{E}_i)$ has to be fulfilled, and therefore we must define $c_b = +\infty$. We further define $c_{b-1} = E_T$. However, this might not be optimal in the sense of maximizing the number of scheduled users. This is best visualized by imagining the case of having only 1 bit available to quantize the required energy. Then, using the previous reasoning, we would use the codebook $\mathcal{C}_1 = \{E_T, +\infty\}$. The disadvantage of $\mathcal{C}_1$ is that the users can only be scheduled in a TDMA fashion, since every user requests either all the available transmit energy E_T, or he declares that he cannot be scheduled. If we would use the codebook $\mathcal{C}_2 = \{\frac{E_T}{M}, +\infty\}$, then only users would be scheduled that reach the SINR constraint assuming an equal power allocation and $M-1$ interfering users. The disadvantage of codebook $\mathcal{C}_2$ is that if user i has a required energy between $\frac{E_T}{M} < \hat{E}_i \leq E_T$ he cannot be scheduled, whereas that user could have been scheduled with codebook $\mathcal{C}_1$. On the other hand, the use of $\mathcal{C}_2$ allows the scheduling of up to M users simultaneously. We see that the number of users in the cell and also the number of available slots inside a block must be taken into account when a codebook is designed that maximizes the average number of scheduled users. However, in order to keep the problem tractable, we assume that the number of users in the cell remains small enough so that the TDMA mode is beneficial, i.e., we always take $c_{b-1} = E_T$.

8.4.3 Codebook Design

In order to simplify the notation we will substitute $\hat{E}_i$ with x throughout this section. Designing the codebook requires the definition of a distortion metric $d(x, Q(x))$ which serves as a measure for the quality of the quantization. The most popular metric used in the quantization literature is the mean squared error [37]. However, for quantizing the required energy, the absolute error is a better metric, since it corresponds to minimizing the overall energy loss due to the quantization. Using this metric, the average distortion D of a codebook $\mathcal{C}$ is

calculated as

$$D(\mathcal{C}) = \int_{-\infty}^{+\infty} |x - Q(x)| f_E(x) dx \tag{8.9}$$

where $f_E(x)$ is the pdf of the required energy. Inserting the selection function (8.8), we can rewrite (8.9) as

$$D(\mathcal{C}) = \sum_{q=1}^{b} \int_{c_{q-1}}^{c_q} (c_q - x) f_E(x) dx \tag{8.10}$$

with $c_0 = 0$ since the required energy of a user is always positive. We see that, compared to classic quantizer design, the codebook elements and the regions are directly linked. However, fixing $c_b = +\infty$ makes (8.10) ill-defined since the occurence of an element in the region $(E_T, +\infty)$ leads to an infinite average distortion. However, since c_{b-1} and c_b are already fixed, we can also restrict ourselves to minimizing the simplified distortion function

$$D_s(\mathcal{C}) = \sum_{i=1}^{b-1} \int_{c_{i-1}}^{c_i} (c_i - x) f_E(x) dx \tag{8.11}$$

with $c_0 = 0$ and $c_{b-1} = E_T$. We start by rewriting (8.11) as

$$D_s(\mathcal{C}) = \left(\sum_{i=1}^{b-1} \int_{c_{i-1}}^{c_i} c_i f_E(x) dx \right) - k \qquad \text{with} \qquad k = \int_0^{E_T} x f_E(x) dx. \tag{8.12}$$

It is possible to show through simulations that $D_s(\mathcal{C})$ is not convex and not quasiconvex. Thus, we cannot solve the problem directly using standard tools. We start by looking for the codebooks that are critical points of the simplified distortion function D_s. The gradient of the distortion function is zero for the critical points of the distortion function

$$\nabla D_s(\mathcal{C}) = \mathbf{0}_{b-2} \tag{8.13}$$

where $\mathbf{0}_{b-2}$ is a $(b-2)$-dimensional column vector with all entries being 0. Since c_{b-1} is determined beforehand we just have $b-2$ variables in our problem. The

critical points are found by solving

$$\frac{\partial}{\partial c_i} \sum_{j=1}^{b-1} \int_{c_{j-1}}^{c_j} c_j f_E(x) dx = 0 \qquad \text{for } i = 1, \ldots, b-2 \tag{8.14}$$

which can be simplified to

$$\frac{\partial}{\partial c_i} \int_{c_{i-1}}^{c_i} c_i f_E(x) dx + \frac{\partial}{\partial c_i} \int_{c_i}^{c_{i+1}} c_{i+1} f_E(x) dx = 0 \qquad \text{for } i = 1, \ldots, b-2. \tag{8.15}$$

We use the Leibniz Integral Rule to solve (8.15) and receive

$$\int_{c_{i-1}}^{c_i} f_E(x) dx - (c_{i+1} - c_i) f_E(c_i) = 0 \qquad \text{for } i = 1, \ldots, b-2. \tag{8.16}$$

A codebook $\mathcal{C}$ that fulfills (8.16) is a critical point. It is not possible to design the codebook based on the Lloyd's Method 1 [34] since there are no iterative optimality conditions to solve, i.e., nearest neighbor condition and centroid condition. However, it is possible to design the codebook using variational techniques, e.g., Lloyd's Method 2 [34]. The core idea is to solve (8.16) by fixing c_1 and then to calculate the remaining elements c_i for $i = 2, \ldots, b-2$ as

$$c_{i+1} = \frac{1}{f_E(c_i)} \int_{c_{i-1}}^{c_i} f_E(x) dx + c_i \tag{8.17}$$

until finally we have c_{b-1}. We assumed initially that c_{b-1} should be E_T. However, the resulting c_{b-1} provided by (8.17) might not result in $c_{b-1} = E_T$. Thus, if $h(c_1) = c_{b-1} - E_T$ is negative (positive), then it means that c_1 was chosen too small (large). Then we choose a larger (smaller) c_1 until we finally find $h(c_1) = 0$ and thus $c_{b-1} = E_T$. Using the results from Appendices 8.A and 8.B, the problem can be easily solved numerically.

Note that we implicitly assume that the codeword c_{b-1} is a strictly monotonically increasing function of c_1. Numerical simulations show that this holds for the investigated cases. The solution is then also assumed to be the unique solution of (8.11), although we cannot rigorously prove this.

8.5 Scheduling

After the base station receives the instantaneous feedback from all users, it schedules the users for the current block k using the following three steps.

Validation of the Scheduled Users

The base station starts by assigning for every slot $l = 0, \ldots, K-1$ in the current block k the same users that were scheduled in the same slot in the previous block, i.e., $\mathcal{S}[kK + l] := \mathcal{S}[(k-1)K + l]$, using the same beamforming vectors as in the previous block. Then, the base station calculates the sum of the required energies for every slot using the fed back required energies. If the sum is larger than the available transmit energy E_T then it is not possible to schedule the users so that they all fulfill the SINR constraint while still using the same slot and the same beamformer as in the last block. The straightforward solution is to remove the user from the set that has the highest energy demand, i.e., the user that feeds back the highest required energy. The dropped user is added to the set $\mathcal{U}_{\text{resched}}[kK]$ and will be treated in the next block. This is repeated until the sum of the minimum energies of the remaining users is smaller than the available transmit energy E_T. This first step of the scheduling algorithm is described in Algorithm 2.

Algorithm 2 Validation of the Scheduled Users

$\mathcal{U}_{\text{resched}}[kK] := \emptyset$
for $l = 0$ to $K - 1$ **do**
  $t := kK + l$
  $\mathcal{S}[t] := \mathcal{S}[t - K]$
  while $\sum_{i \in \mathcal{S}[t]} \hat{E}_{Q,i}[kK] > E_T$ **do**
    $i := \arg\max_{i \in \mathcal{S}[t]} \hat{E}_{Q,i}[kK]$
    $\mathcal{S}[t] := \mathcal{S}[t] \setminus \{i\}$
    $\mathcal{U}_{\text{resched}}[kK] := \mathcal{U}_{\text{resched}}[kK] \cup \{i\}$
  end while
end for

Scheduling the New Users and Rescheduling the Dropped Users

We collect the dropped users from the previous block $\mathcal{U}_{\text{resched}}[(k-1)K]$ and the new users entering the cell $\mathcal{U}_{\text{new}}[kK]$ in the set $\mathcal{U}[kK] := \mathcal{U}_{\text{resched}}[(k-1)K] \cup \mathcal{U}_{\text{new}}[kK]$. All these users feed back their required energy as well as the index of the corresponding beamforming vector. Thus, user $i \in \mathcal{U}[kK]$ feeds back $g(i)$ from (8.7) and $\hat{E}_{Q,i}[kK]$. If we assume that the data-rate limitation on the feedback link is strict, then we have to use a codebook with $2^{B-\lceil \log_2 M \rceil}$ entries to quantize $\hat{E}_i[kK]$. The base station then tries to successively schedule all the users in $\mathcal{U}[kK]$ according to their fed back minimum energy. The algorithm starts by scheduling the user with the largest energy requirement first. Once this user has been found, the base station looks for a slot that is not yet using the preferred beamformer of the considered user. For every one of these free slots the base station calculates the sum of the minimum energy levels of the users in the slot, assuming the considered user is added, and finally chooses the slot that results in the lowest sum. If the base station does not find a valid slot then the user is skipped for the current block and added to $\mathcal{U}_{\text{resched}}[kK]$. However, if the base station finds a slot then the user is scheduled for transmission. This second step of the scheduling algorithm is described in Algorithm 3.

Energy Assignment

Once all the users are scheduled, every scheduled user is assigned its required minimum energy. The remaining transmit energy is uniformly distributed over the remaining users in the same slot. Thus, the transmit energy for user i, that is allocated to $t = kK + l$, is calculated as

$$E_i[t] := \hat{E}_{Q,i}[kK] + \frac{E_T - \sum_{j \in \mathcal{S}[t]} \hat{E}_{Q,j}[kK]}{|\mathcal{S}[t]|}. \tag{8.18}$$

Note that this approach tries to balance the SINRs of the different users in the same slot. However, due to the quantization, and due to the unknown interference between the users in the set $\mathcal{S}[t]$, it is not possible to truly balance the SINRs as it is possible with full CSI at the base station [98]. It is also possible to save energy at the base station by solely assigning the required energy to the users

Algorithm 3 Scheduling the New Users and Rescheduling the Dropped Users

$\mathcal{U} := \mathcal{U}_{\text{resched}}[(k-1)K] \cup \mathcal{U}_{\text{new}}[kK]$
while $|\mathcal{U}| > 0$ **do**
  $i := \arg\max_{i \in \mathcal{U}} \hat{E}_{Q,i}[kK]$
  Temp_Index $:= -1$
  Temp_Energy $:= E_T$
  for $l = 0$ to $K-1$ **do**
    if $\sum_{j \in \mathcal{S}[kK+l]} \hat{E}_{Q,j}[kK] + \hat{E}_{Q,i}[kK] \leq$ Temp_Energy **and** $g(i) \neq g(j), \forall j \in \mathcal{S}[kK+l]$ **then**
      Temp_Index $:= l$
      Temp_Energy $:= \sum_{j \in \mathcal{S}[kK+l]} E_{Q,j}[kK] + \hat{E}_{Q,i}[kK]$
    end if
  end for
  if Temp_Index $\neq -1$ **then**
    $\mathcal{S}[kK + \text{Temp\_Index}] := \mathcal{S}[kK + \text{Temp\_Index}] \cup \{i\}$
  else
    $\mathcal{U}_{\text{resched}}[kK] := \mathcal{U}_{\text{resched}}[kK] \cup \{i\}$
  end if
  $\mathcal{U} := \mathcal{U} \setminus \{i\}$
end while

and not redistributing the spare energy. Then, (8.18) simply becomes

$$E_i[t] := \hat{E}_{Q,i}[kK]. \tag{8.19}$$

8.6 Extensions

8.6.1 Exploiting the Time-Correlation of the Channel

We can also use the time-correlation of the channel to better exploit the data-rate limited feedback link. A simple variant of predictive quantization [17] is difference quantization. There, the difference between the previously fed back quantized required energy and the current required energy is quantized and fed back. The required energy is calculated at the base station as

$$\hat{E}_{Q,i}[kK] = \hat{E}_{Q,i}[(k-1)K] + Q(\Delta \hat{E}_i[kK]) \tag{8.20}$$

and the fed back quantized energy difference is calculated as

$$Q(\Delta\hat{E}_i[kK]) = \arg\min_{c_q \in \mathcal{C}} \; c_q - (\hat{E}_i[kK] - \hat{E}_{Q,i}[(k-1)K]) \tag{8.21}$$

$$\text{s.t.} \quad c_q \geq \hat{E}_i[kK] - \hat{E}_{Q,i}[(k-1)K]. \tag{8.22}$$

Note that the additional constraint guarantees that the estimated required energy is greater than or equal to the true required energy. The predictive quantization requires the use of two quantization codebooks. The first codebook $\mathcal{C}_{\text{init}}$ is used to quantize the initial required energy when no prediction is possible, i.e., the user is scheduled for the first time or the user is rescheduled. The second codebook $\mathcal{C}$ is used afterwards to quantize the prediction difference (8.21). The performance of predictive quantization can be additionally improved by using a more sophisticated prediction. However, the prediction algorithm has to be matched to the underlying channel model.

8.6.2 Entropy Coding

Similar to the work in Section 3.4, the time-correlation of the channel can also be exploited in this chapter by the use of entropy coding [17]. Entropy coding uses short codewords to feed back highly probable indices, in order to reduce the required average feedback, e.g., a 1-bit codeword is used as feedback when the quantized required energy is identical to the quantized required energy from the previous feedback.

8.7 Simulations

We start by comparing the performance of the codebook design algorithm from Section 8.4.3 to different common codebook design strategies. We design two codebooks using the algorithm from Section 8.4.3. The first codebook, denoted the regular codebook, is designed using the statistics from Appendix 8.A, and the second codebook, denoted the initial codebook, is designed using the statistics from Appendix 8.B. Their performance is compared with a uniform codebook and with an equiprobable codebook. All the codebooks contain the values E_T

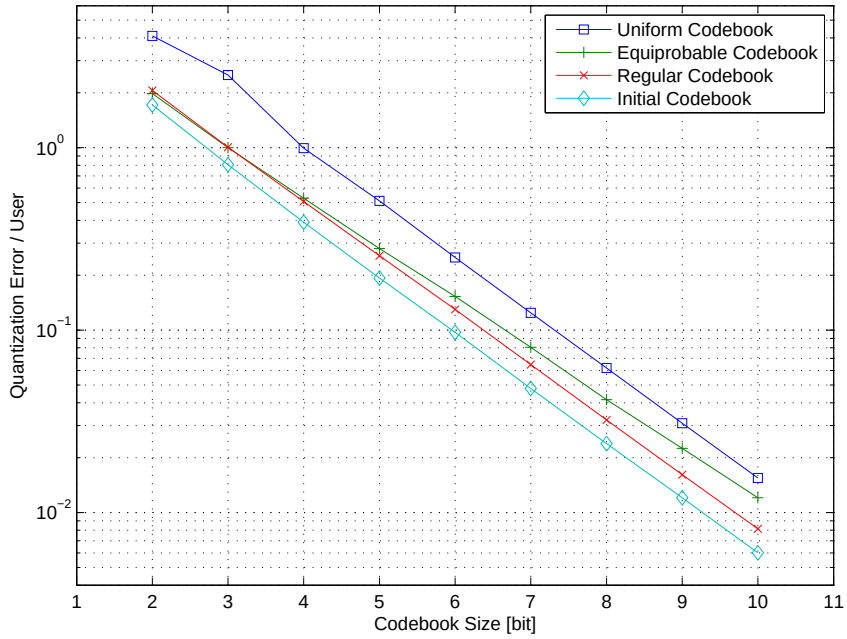

Figure 8.1: Comparison of different codebook design approaches for scheduling a user at the first slot. ($M = 4$, $|\mathcal{S}| = 4$, SNR = 10 dB, $\text{SINR}_{\min} = 7$ dB)

and $+\infty$ as their two largest elements. Thus, we can only freely choose the remaining $b-2$ elements from the codebooks. The ith element of the uniform codebook is calculated as $i\frac{E_T}{b-1}$ with $i = 1, \ldots, b-2$. The equiprobable codebook is designed such that all the elements of the codebook are selected with the same probability. First calculating $P_{\text{avg}} = \frac{P(0 \leq \hat{E}_i \leq E_T)}{b-1}$, the different elements are successively calculated by solving $F_X(c_i) - F_X(c_{i-1}) = P_{\text{avg}}$ where $c_0 = 0$ for $i = 1, \ldots, b-2$. For the simulations presented in Fig. 8.1 and Fig. 8.2, we consider the average quantization error per user as a function of the codebook size. The simulations consider an average SNR of 10 dB, $M = 4$, and a minimum required SINR of 7 dB. The Rayleigh channel model was used for both simulations. We also created some simple test cases to investigate the optimality of the proposed codebook design algorithm. In all these test cases, the critical point turned out to be the optimal point.

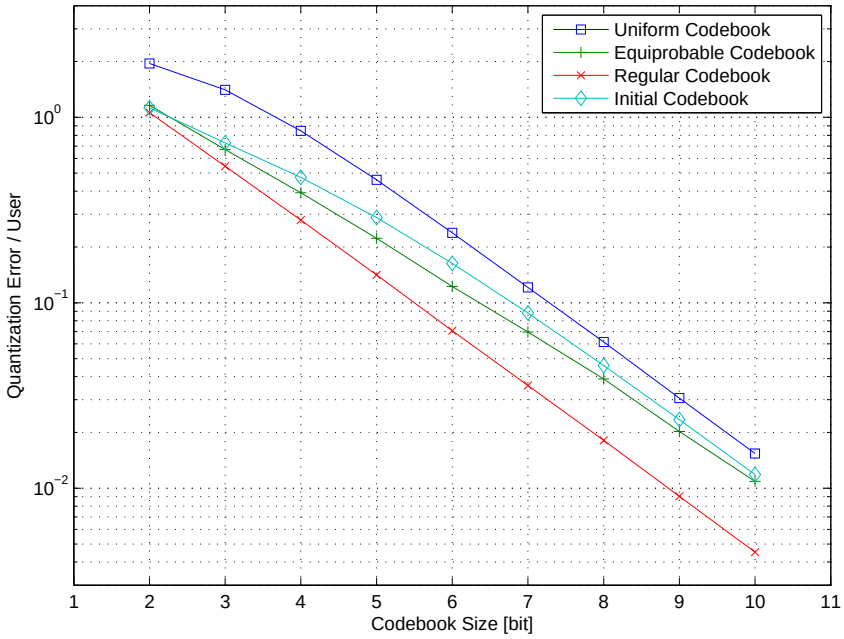

Figure 8.2: Comparison of different codebook design approaches for scheduling a user at a later slot. ($M = 4$, $S = 4$, SNR $= 10$ dB, $\text{SINR}_{\min} = 7$ dB)

We see in Fig. 8.1 that the intial codebook has a lower quantization error $E(\hat{E}_{Q,i} - \hat{E}_i)$ than the other codebooks for quantizing the energy immediately after scheduling. This is expected since the initial codebook is designed using the proper statistics for the first scheduling instance from Appendix 8.A. Further, we see in Fig. 8.1 that the regular codebook, which is designed using the mismatched statistics, performs as good as the equiprobable codebook that is designed using the correct statistics, at least for small codebook sizes. However, with every successive block the assumption that the user uses its optimal beamformer, i.e., the beamforming vector that maximizes the SINR, becomes weaker.

The extreme case is depicted in Fig. 8.2. There we assume that the beamforming vector is selected randomly amongst all the available beamforming vectors. This corresponds to the case where the user is able to fulfill its SINR constraint successively over a prolonged time using the same beamformer. We see that the

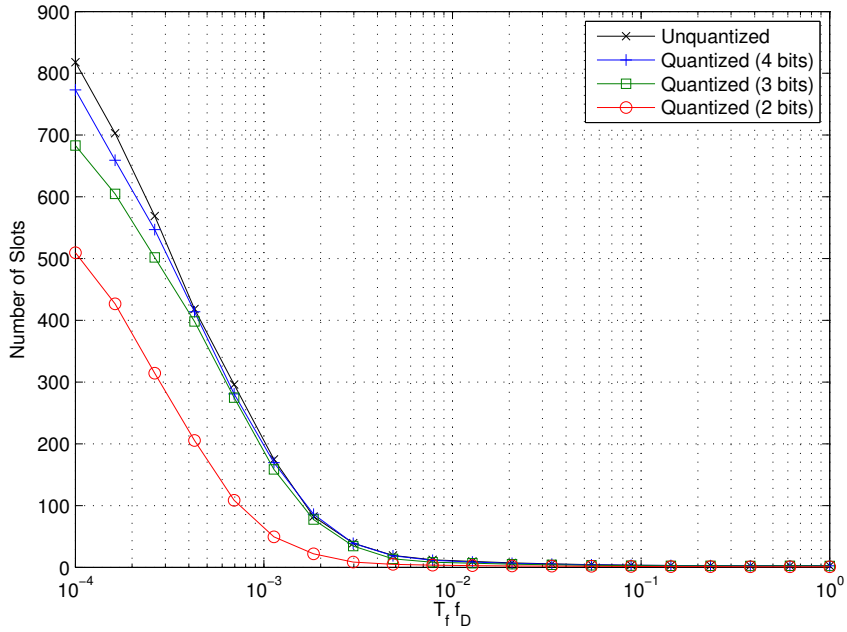

Figure 8.3: Average number of slots that a user is successively scheduled for a varying product of block length T_f and Doppler frequency f_D. ($M = 2$, $K = 100$, 150 users, 1000 blocks, SNR = 15 dB, $\text{SINR}_{\min} = 5$ dB)

regular codebook performs well for both cases, and thus, for the sake of simplicity, we use the regular codebook for the following simulations. Note that a codebook switching strategy, where we use the initial codebook for the first slot, and then switch to the regular codebook should provide a minor performance gain, but requires more storage capacity from the users and from the base station.

The simulation depicted in Fig. 8.3 shows how long the different users are successively scheduled on the average as a function of the product of the Doppler frequency f_{D} and the block length T_{f}. We assume a homogeneous cell where all the users experience SNR = 15 dB. The SINR constraint is fixed to $\text{SINR}_{\min} =$ 5 dB. The time-correlation between the blocks is modeled according to Jakes'

model. At time instant t the pth element from the channel $\mathbf{h}_i[t]$ is modelled as

$$[\mathbf{h}_i[t]]_p = \frac{1}{\sqrt{Q}} \sum_{q=1}^{Q} a_{p,q} \exp(j\, 2\pi T_\mathrm{f} f_\mathrm{D} \lceil t/K \rceil \cos \alpha_{p,q}) \tag{8.23}$$

where Q is the number of scatterers, $a_{p,q}$ is i.i.d. complex Gaussian distributed with zero mean and variance 1, and $\alpha_{p,q}$ is uniformly distributed over $[0, 2\pi]$. We assume $Q = 30$ scatterers. The influence of quantizing the fed back minimum energy is depicted for multiple codebooks and for no quantization. We see that for slowly changing channels, i.e., channels with a low product of Doppler frequency f_D and block length duration T_f, the average number of consecutive blocks increases. We simulate 1000 blocks for every channel realization, and thus the maximum number of blocks a user can be successively scheduled is limited to 1000. However, if $f_\mathrm{D} T_\mathrm{f}$ increases, then the channel becomes more volatile. This increases $P(\sum_{i \in \mathcal{S}[t-K]} \hat{E}_{Q,i}[t] > E_T \mid \sum_{i \in \mathcal{S}[t-K]} \hat{E}_{Q,i}[t-K] \leq E_T)$, i.e., the probability that the users from the set $\mathcal{S}[t-K]$ in the slot $t-K$ cannot fulfill the SINR constraint in the slot t and thus have to be rescheduled.

The next simulation, depicted in Fig. 8.4, shows the average number of users that have to rescheduled per block as a function of $T_\mathrm{f} f_\mathrm{D}$. The users have to be rescheduled if they cannot fulfill the SINR constraint for the current slot using the same beamforming as in the previous slot, or if they could not be scheduled for the current block at all. We see that the number of rescheduling operations is low if the channel exhibits a strong time correlation, and that the number of rescheduling operations increases as the channel becomes more volatile. We see that more users have to be rescheduled if the energy loss due to the quantization is higher. For the codebook with 4 entries (2 bit), the system works in TDMA mode, i.e., every user is assigned to one

Fig. 8.5 depicts the average number of users that are scheduled per block as a function of $T_\mathrm{f} f_\mathrm{D}$. We see that the average number of scheduled users decreases as the channel becomes more volatile. This is because the probability that a user has to be rescheduled increases with the volatility of the channel, and every rescheduled user is not scheduled for at least one block. We also see the effects of quantizing the required energy. A smaller codebook size leads to a larger

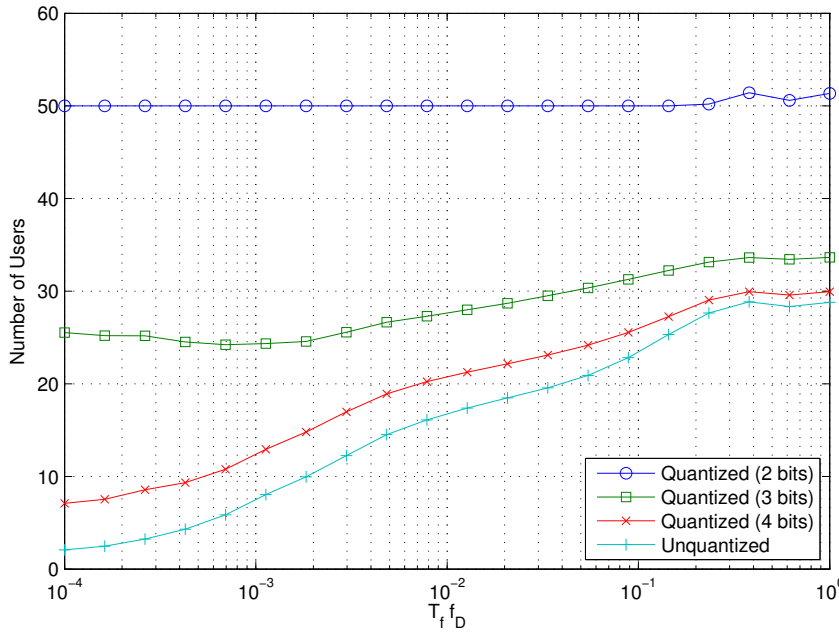

Figure 8.4: Average number of users that have to be rescheduled every slot for a varying product of block length T_f and Doppler frequency f_D. ($M = 2$, $K = 100$, 150 users, 1000 blocks, SNR = 15 dB, $\text{SINR}_{\text{min}} = 5$ dB)

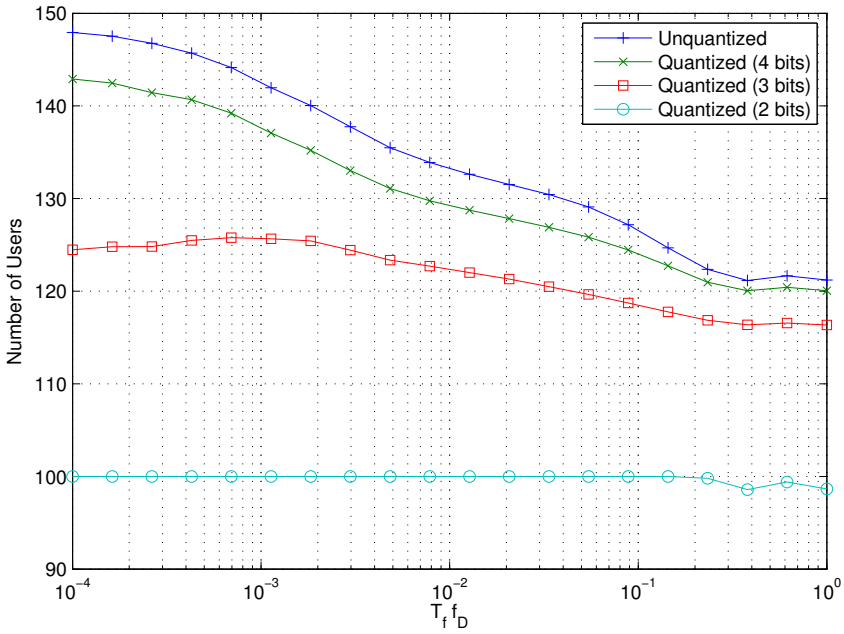

Figure 8.5: Average number of users that are scheduled per block for a varying product of block length T_f and Doppler frequency f_D. ($M = 2$, $K = 100$, 150 users, 1000 blocks, $Q = 30$, SNR $= 15$ dB, $\text{SINR}_{\text{min}} = 5$ dB)

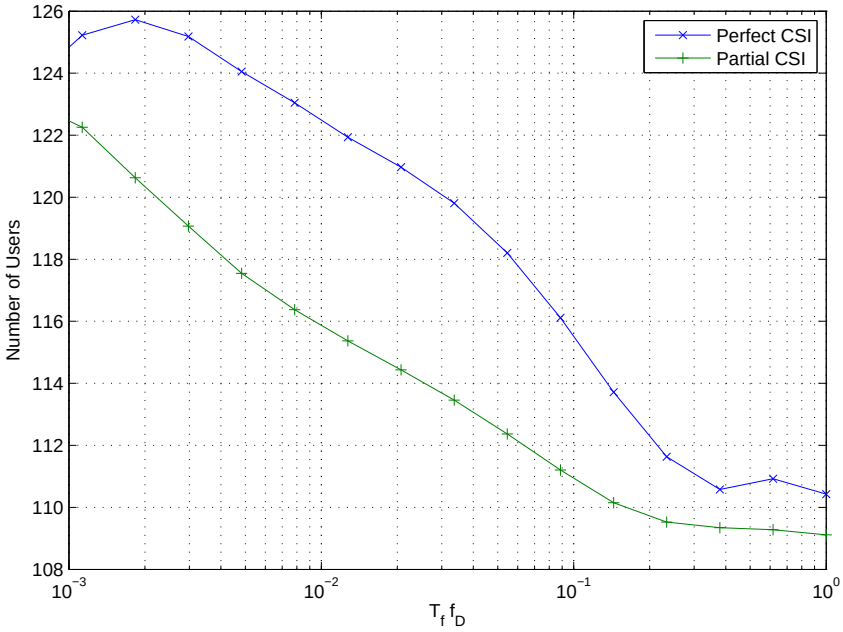

Figure 8.6: Average number of users that are scheduled in the same slot as in the previous slot for a varying product of block length T_f and Doppler frequency f_D. ($M = 3$, $K = 100$, 150 users, 1000 blocks, $Q = 30$, SNR = 15 dB, $\text{SINR}_{\min}$ = 5 dB)

energy loss since the user requests more energy than he actually needs, due to the quantization error. For small codebooks, the system nearly operates exclusively in TDMA mode, i.e., every slot has just a single user assigned to.

The next simulation, Fig. 8.6, compares the feedback of the required energy to having full CSI at the base station. We assume that in both cases Algorithm 3 is used to schedule the new and the dropped users. However, the base station with full CSI uses the results from [98] to calculate the optimal energy assigned to every beamforming vector to balance the resulting SINRs. We see that having full CSI allows to schedule more users successively in the same slot.

Fig. 8.7 shows the effect of erroneous CSI on the scheduling. We create the noisy channel estimate $\mathbf{h}_{i,\text{noisy}}$ by adding noise to the true channel, i.e., $\mathbf{h}_{i,\text{noisy}} = \mathbf{h}_{i,\text{true}} + \mathbf{e}_i$ with $\mathbf{e}_i \in \mathbb{C}^{1\times M}$. The different components of the noise

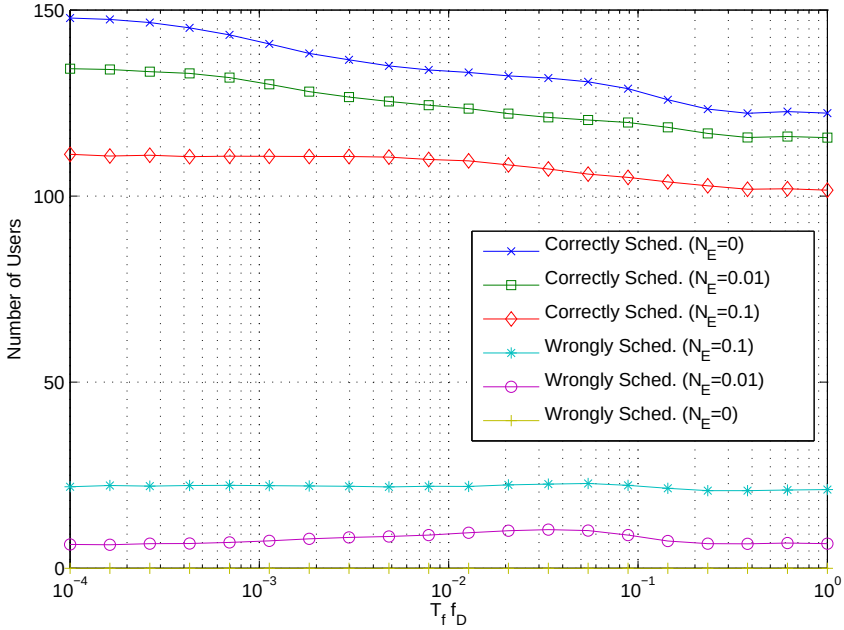

Figure 8.7: The effect of erroneous CSI on the number of correctly and wrongly scheduled users in the slot for a varying product of block length T_f and Doppler frequency f_D. ($M = 2$, $K = 100$, 150 users, 1000 blocks, $Q = 30$, SNR = 15 dB, $\text{SINR}_{\text{min}} = 5$ dB)

vector are complex Gaussian distributed with zero mean and variance N_E. The users calculate their required energy based on the noisy channel, and feed it back to the base station. Then, the base station uses the feedback to schedule the users. Next, we check, using the true channel, how many of the scheduled users really fulfill the SINR constraint. We see that, as the noise on the feedback channel increases, the number of wrongly scheduled users increases.

8.8 Conclusions

We presented a scheme to implement round-robin scheduling using orthogonal beamforming and data-rate limited feedback. The scheme uses scalar feedback from the users to divide the transmit energy amongst the users so that they all fulfill a given SINR constraint. The simulations show that the presented algorithm is attractive to implement round-robin scheduling for time-varying channels. We further propose an algorithm to design the codebooks used to quantize the feedback, and the codebooks outperform other popular codebooks.

8.A CDF and PDF of the Regular Required Energy

We assume that the channel $\mathbf{h}_i$ of user i is a random variable. Thus, the resulting required energy $\hat{E}_i$ is also a random variable, and we want to derive the corresponding cdf

$$F_E(z) = P(\hat{E}_i \leq z) \tag{8.24}$$

$$= P\left(\frac{\max_{j \in \mathcal{M} \setminus g(i)} |\mathbf{h}_i \mathbf{w}_j|^2 E_T + N_0}{\frac{1}{\mathrm{SINR}_{\min}} |\mathbf{h}_i \mathbf{w}_{g(i)}|^2 + \max_{j \in \mathcal{M} \setminus g(i)} |\mathbf{h}_i \mathbf{w}_j|^2} \leq z \right) \tag{8.25}$$

and pdf $f_E(z) = \frac{d}{dz} F_E(z)$. We assume in this section that the function $g : \{1, \ldots, K\} \to \mathcal{M}$ randomly assigns a beamforming vector to a user. The set of orthogonal beamforming vectors are unit-norm $\|\mathbf{w}_m\|_2 = 1$, $\forall m$ and known. The different elements of the channel $\mathbf{h}_i$ are assumed i.i.d. and circular Gaussian

distributed according to $\mathcal{CN}(0,1)$. In order to simplify the notation we will write (8.25) as

$$F_E(z) = P\left(\frac{X_A E_T + N_0}{X_B + X_A} \leq z\right) \tag{8.26}$$

where $X_A = \max_{j \in \mathcal{M} \setminus g(i)} |\mathbf{h}_i \mathbf{w}_j|^2$, and $X_B = \frac{1}{\text{SINR}_{\min}} |\mathbf{h}_i \mathbf{w}_{g(i)}|^2$. The real part and the imaginary part of $\mathbf{h}_i \mathbf{w}_j$ are independently Gaussian distributed $\mathcal{N}(0, \frac{1}{2})$. We define the continuous random variable $X_1 = |\mathbf{h}_i \mathbf{w}_j|^2$, and model this variable as $X_1 = \frac{1}{2}(X_{11}^2 + X_{12}^2)$, with $X_{11} \sim \mathcal{N}(0,1)$ and $X_{12} \sim \mathcal{N}(0,1)$. The term $X_{11}^2 + X_{12}^2$ is $\chi^2(2)$ distributed. The pdf $f_{X_1}(x)$ of X_1 then is

$$f_{X_1}(x) = \begin{cases} e^{-x} & \text{if } x \geq 0 \\ 0 & \text{otherwise} \end{cases} \tag{8.27}$$

and the corresponding cdf $F_{X_1}(x)$ is

$$F_{X_1}(x) = \begin{cases} 1 - e^{-x} & \text{if } x \geq 0 \\ 0 & \text{otherwise} \end{cases}. \tag{8.28}$$

The different realizations of $|\mathbf{h}_i \mathbf{w}_j|^2$ are identical and independently distributed for all $j \in \mathcal{M}$. The cdf of $X_A = \max_{j \in \mathcal{M} \setminus g(i)} |\mathbf{h}_i \mathbf{w}_j|^2$ then is

$$F_{X_A}(x) = (F_{X_1}(x))^{M-1} = \begin{cases} (1 - e^{-x})^{M-1} & \text{if } x \geq 0 \\ 0 & \text{otherwise} \end{cases}. \tag{8.29}$$

The resulting pdf of $X_A = \max_{j \in \mathcal{M} \setminus i} |\mathbf{h}_i \mathbf{w}_j|^2$ is

$$f_{X_A}(x) = \begin{cases} e^{-x}(1 - e^{-x})^{M-2}(M-1) & \text{if } x \geq 0 \\ 0 & \text{otherwise} \end{cases}. \tag{8.30}$$

The pdf of $X_B = \frac{1}{\mathrm{SINR}_{\min}} |\mathbf{h}_i \mathbf{w}_{g(i)}|^2$ corresponds to $X_B = \frac{1}{\mathrm{SINR}_{\min}} X_1$, and is

$$f_{X_B}(x) = \begin{cases} \hat{\mathrm{SINR}}_{\min} \, e^{-x \, \hat{\mathrm{SINR}}_{\min}} & \text{if } x \geq 0 \\ 0 & \text{otherwise} \end{cases}. \tag{8.31}$$

Since the random variables X_A and X_B are always positive, we can rewrite (8.26) as

$$F_E(z) = P\left((E_T - z)X_A - zX_B \leq -N_0\right). \tag{8.32}$$

The random variable $(E_T - z)X_A - zX_B$ will be abbreviated as X_C in order to keep the notation compact. We use (8.30) to find the pdf of the random variable $(E_T - z)X_A$ which is

$$f_{(E_T - z)X_A}(x) = \frac{M-1}{|E_T - z|} e^{-\frac{x}{E_T - z}} (1 - e^{-\frac{x}{E_T - z}})^{M-2} \tag{8.33}$$

if $(x \geq 0 \wedge E_T \geq z) \vee (x \leq 0 \wedge E_T \leq z)$ and $f_{(E_T - z)X_A}(x) = 0$ otherwise. The pdf of $-zX_B$ is found by using (8.31), and is

$$f_{-zX_B}(x) = \begin{cases} \frac{\mathrm{SINR}_{\min}}{|z|} \, e^{\frac{x}{z} \mathrm{SINR}_{\min}} & \text{if } (x \geq 0 \wedge z \leq 0) \vee (x \leq 0 \wedge z \geq 0) \\ 0 & \text{otherwise} \end{cases}. \tag{8.34}$$

Since $(E_T - z)X_A$ and $-zX_B$ are statistically independent, the pdf f_{X_C} can be calculated as

$$f_{X_C}(x) = \int_{-\infty}^{+\infty} f_{(E_T - z)X_A}(x - y) f_{-zX_B}(y) dy. \tag{8.35}$$

The product $f_{(E_T - z)X_A}(x - y) f_{-zX_B}(y)$ is not zero when

$$[(x \geq y \wedge E_T \geq z) \vee (x \leq y \wedge E_T \leq z)] \wedge [(y \geq 0 \wedge z \leq 0) \vee (y \leq 0 \wedge z \geq 0)]. \tag{8.36}$$

Using Boolean algebra this can be rewritten as

$$(E_T \leq z \wedge x \leq y \wedge y \leq 0 \wedge z \geq 0) \vee (E_T \leq z \wedge x \leq y \wedge y \geq 0 \wedge z \leq 0)$$
$$\vee (E_T \geq z \wedge x \geq y \wedge y \leq 0 \wedge z \geq 0) \vee (E_T \geq z \wedge x \geq y \wedge y \geq 0 \wedge z \leq 0). \quad (8.37)$$

We can thus distinguish between the following four cases:

- Case 1: $E_T \leq z \wedge x \leq y \wedge y \leq 0 \wedge z \geq 0$
- Case 2: $E_T \leq z \wedge x \leq y \wedge y \geq 0 \wedge z \leq 0$
- Case 3: $E_T \geq z \wedge x \geq y \wedge y \leq 0 \wedge z \geq 0$
- Case 4: $E_T \geq z \wedge x \geq y \wedge y \geq 0 \wedge z \leq 0$

We see in (8.26) that $F_E(z) = 0$, $\forall z < 0$. Thus, we can ignore Case 2 and Case 4. Next, we rewrite (8.35) as

$$f_{X_C}(x) = \begin{cases} f_{X_C,1}(x) & 0 \leq z \leq E_T \\ f_{X_C,2}(x) & E_T \leq z \\ 0 & \text{otherwise} \end{cases} \quad (8.38)$$

with

$$f_{X_C,1}(x) = \int_{-\infty}^{\min(0,x)} \frac{M-1}{|E_T - z|} e^{-\frac{x-y}{E_T - z}} (1 - e^{-\frac{x-y}{E_T - z}})^{M-2} \frac{\text{SINR}_{\min}}{z} e^{\frac{y}{z}\text{SINR}_{\min}} dy \quad (8.39)$$

$$f_{X_C,1}(x) = \frac{(M-1)\text{SINR}_{\min}}{|E_T - z|z} e^{-\frac{x}{E_T - z}} \int_{-\infty}^{\min(0,x)} e^{y\left(\frac{1}{E_T - z} + \frac{\text{SINR}_{\min}}{z}\right)} (1 - e^{-\frac{x-y}{E_T - z}})^{M-2} dy. \quad (8.40)$$

Since we assume that $M \leq 2$ we can rewrite the previous equation as

$$f_{X_C,1}(x) = \frac{(M-1)\mathrm{SINR}_{\min}}{|E_T - z|z} e^{-\frac{x}{E_T - z}} \int_{-\infty}^{\min(0,x)} e^{y\left(\frac{1}{E_T - z} + \frac{\mathrm{SINR}_{\min}}{z}\right)} \sum_{k=0}^{M-2} \binom{M-2}{k} \left(-e^{-\frac{x-y}{E_T - z}}\right)^k dy \quad (8.41)$$

$$f_{X_C,1}(x) = \frac{(M-1)\mathrm{SINR}_{\min}}{|E_T - z|z} e^{-\frac{x}{E_T - z}} \sum_{k=0}^{M-2} \binom{M-2}{k} (-1)^k e^{-\frac{kx}{E_T - z}} \int_{-\infty}^{\min(0,x)} e^{y\left(\frac{k+1}{E_T - z} + \frac{\mathrm{SINR}_{\min}}{z}\right)} dy. \quad (8.42)$$

Similarly, the second case in (8.38) becomes

$$f_{X_C,2}(x) = \frac{(M-1)\mathrm{SINR}_{\min}}{|E_T - z|z} e^{-\frac{x}{E_T - z}} \sum_{k=0}^{M-2} \binom{M-2}{k} (-1)^k e^{-\frac{kx}{E_T - z}} \int_{x}^{0} e^{y\left(\frac{k+1}{E_T - z} + \frac{\mathrm{SINR}_{\min}}{z}\right)} dy. \quad (8.43)$$

Using f_{X_C} we can now calculate the cdf

$$F_E(z) = \begin{cases} F_{E,1}(z) = \int_{-\infty}^{-N_0} f_{X_C,1}(x)dx & 0 \leq z \leq E_T \\ F_{E,2}(z) = \int_{-\infty}^{-N_0} f_{X_C,2}(x)dx & E_T \leq z \\ 0 & \text{otherwise} \end{cases}. \quad (8.44)$$

On the region $0 \leq z \leq E_T$ the cdf is given by

$$F_{E,1}(z) = \sum_{k=0}^{M-2} \binom{M-2}{k} (-1)^k \frac{(M-1)z}{zk + z + \mathrm{SINR}_{\min}(E_T - z)} e^{-N_0 \frac{\mathrm{SINR}_{\min}}{z}}. \quad (8.45)$$

The cdf $F_{E,1}(z)$ can be written in a more compact form. We start by rewriting (8.45) as

$$F_{E,1}(z) = (M-1)! \sum_{k=0}^{M-2} \frac{(-1)^k}{(M-2-k)!k!(k+1+\mathrm{SINR}_{\min}(\frac{E_T}{z}-1))} e^{-N_0 \frac{\mathrm{SINR}_{\min}}{z}} \quad (8.46)$$

Using Lemma 1 we can rewrite it as

$$F_{E,1}(z) = \Gamma(M) \frac{\Gamma(1+\mathrm{SINR}_{\min}(\frac{E_T}{z}-1)}{\Gamma(M+\mathrm{SINR}_{\min}(\frac{E_T}{z}-1)} e^{-N_0 \frac{\mathrm{SINR}_{\min}}{z}}. \quad (8.47)$$

On the region $E_T < z$ the cdf is given by

$$F_{E,2}(z) = -\sum_{k=0}^{M-2} \binom{M-2}{k} (-1)^k \frac{(M-1)\mathrm{SINR}_{\min}}{zk+z+\mathrm{SINR}_{\min}(E_T-z)} \left(\frac{E_T-z}{-1-k} e^{-N_0 \frac{-1-k}{E_T-z}} - \frac{z}{\mathrm{SINR}_{\min}} e^{-N_0 \frac{\mathrm{SINR}_{\min}}{z}} \right). \quad (8.48)$$

Using (8.44) the pdf of the required energy can now be derived as

$$f_E(z) = \begin{cases} f_{E,1}(z) = \frac{d}{dz} F_{E,1}(z) & 0 < z < E_T \\ f_{E,2}(z) = \frac{d}{dz} F_{E,2}(z) & E_T < z \\ 0 & \text{otherwise} \end{cases} \quad (8.49)$$

with (8.56) and (8.57).

Using Lemma 1, we can write (8.56) in a more compact form as

$$f_{E,1}(z) = \frac{\mathrm{SINR}_{\min}}{z^2} \left(N_0 + E_T \left(\psi \left(M + \mathrm{SINR}_{\min} \left(\frac{E_T}{z} - 1 \right) \right) - \psi \left(1 + \mathrm{SINR}_{\min} \left(\frac{E_T}{z} - 1 \right) \right) \right) \right) F_{E,1}(z) \quad (8.50)$$

where $\psi(\cdot)$ denotes the digamma function.

Lemma 1. *Let $a \in \mathbb{R}$ with $x > 0$, and $b \in \mathbb{N}$. Then, the identity*

$$\sum_{k=0}^{b} \frac{(-1)^k}{k!(b-k)!(k+1+a)} = \prod_{j=1}^{b+1} \frac{1}{a+j} \tag{8.51}$$

is true.

Proof. We prove the lemma by induction. It is easy to see that the equation is valid for the induction basis, i.e., $b = 0$. Next, we have to show that (8.51) is true for b if it is true for $b-1$. We start by rewriting (8.51) as

$$\sum_{k=0}^{b} \frac{(-1)^k}{k!(b-k)!(k+1+a)} = \frac{1}{a+b+1} \prod_{j=1}^{b} \frac{1}{a+j}. \tag{8.52}$$

Now, we insert the induction hypothesis and receive

$$\sum_{k=0}^{b} \frac{(-1)^k}{k!(b-k)!(k+1+a)} = \frac{1}{a+b+1} \sum_{k=0}^{b-1} \frac{(-1)^k}{k!(b-1-k)!(k+1+a)} \tag{8.53}$$

$$\Rightarrow \sum_{k=0}^{b} \frac{(-1)^k}{k!(b-k)!} = 0. \tag{8.54}$$

Using the identity

$$\sum_{k=0}^{b} (-1)^k \binom{b}{k} = 0 \tag{8.55}$$

from [109], we see that (8.54) is true. Thus, the induction step is proved as well. □

$$f_{E,1}(z) = -\sum_{k=0}^{M-2} \binom{M-2}{k} (-1)^k (|\mathcal{M}|-1) \left(\left(\frac{\frac{N_0+N_0 k}{(E_T-z)} - 1}{(zk+z+\mathrm{SINR}_{\min}(E_T-z))} - \frac{(E_T-z)\,(k+1-\mathrm{SINR}_{\min})}{(zk+z+\mathrm{SINR}_{\min}(E_T-z))^2} \right) \right.$$
$$\left. \frac{\mathrm{SINR}_{\min}}{-1-k} e^{\frac{N_0+N_0 k}{E_T-z}} - e^{-N_0 \frac{\mathrm{SINR}_{\min}}{z}} \left(\frac{z+N_0 \mathrm{SINR}_{\min}}{z\,(zk+z+\mathrm{SINR}_{\min}(E_T-z))} - \frac{z\,(k+1-\mathrm{SINR}_{\min})}{(zk+z+\mathrm{SINR}_{\min}(E_T-z))^2} \right) \right) \quad (8.56)$$

$$f_{E,2}(z) = \sum_{k=0}^{M-2} \binom{M-2}{k} (-1)^k (M-1) \left(e^{-N_0 \frac{\mathrm{SINR}_{\min}}{z}} \right) \left(\frac{z+N_0\,\mathrm{SINR}_{\min}}{z\,(zk+z+\mathrm{SINR}_{\min}(E_T-z))} - \frac{z\,(k+1-\mathrm{SINR}_{\min})}{(zk+z+\mathrm{SINR}_{\min}(E_T-z))^2} \right) \quad (8.57)$$

8.B CDF and PDF of the Initial Required Energy

As in Appendix 8.A we want to calculate the cdf of the initial required energy

$$F_E(z) = P(\hat{E}_{\min} \leq z) \tag{8.58}$$

$$= P\left(\frac{\max_{j \in \mathcal{M} \setminus g(i)} |\mathbf{h}_i \mathbf{w}_j|^2 E_T + N_0}{\frac{1}{\mathrm{SINR}_{\min}} |\mathbf{h}_i \mathbf{w}_{g(i)}|^2 + \max_{j \in \mathcal{M} \setminus g(i)} |\mathbf{h}_i \mathbf{w}_j|^2} \leq z \right) \tag{8.59}$$

and its corresponding pdf $f_E(z) = \frac{d}{dz} F_E(z)$. However, in contrast to Appendix 8.A we assume that $g(i) = \arg\max_{j \in \mathcal{M}} |\mathbf{h}_i \mathbf{w}_j|^2$. Thus, we cannot assume that $\max_{j \in \mathcal{M} \setminus g(i)} |\mathbf{h}_i \mathbf{w}_j|^2$ and $|\mathbf{h}_i \mathbf{w}_{g(i)}|^2$ are statistically independent anymore. We define again the continuous random variable $X_1 = |\mathbf{h}_i \mathbf{w}_j|^2$, with the pdf (8.27), and the cdf (8.28). Using ordering statistics notation, we write $X_{(M-1)} = \max_{j \in \mathcal{M} \setminus g(i)} |\mathbf{h}_i \mathbf{w}_j|^2$ and $X_{(M)} = |\mathbf{h}_i \mathbf{w}_{g(i)}|^2$ with $X_{(1)} \leq X_{(2)} \leq \ldots \leq X_{(M)}$, and thus

$$F_E(z) = P\left(\frac{X_{(M-1)} E_T + N_0}{\frac{1}{\mathrm{SINR}_{\min}} X_{(M)} + X_{(M-1)}} \leq z \right). \tag{8.60}$$

The problem can be reformulated as

$$F_E(z) = P((X_{(M-1)}, X_{(M)}) \in D_z) = \iint_{D_z} f_j(x, y)\, dx\, dy \tag{8.61}$$

where the region D_z is

$$D_z = \{(x, y) \in \mathbb{R}^2 \mid \frac{x E_T + N_0}{\frac{1}{\mathrm{SINR}_{\min}} y + x} \leq z\} \tag{8.62}$$

and the joint density f of $X_{(M-1)}$ and $X_{(M)}$ is calculating using [110, Eq. (2.1.6)] as

$$f(x, y) = \begin{cases} \frac{M!}{(M-2)!} F_{X_1}[x]^{M-2} f_{X_1}(y) f_{X_1}(x) & \text{if } x < y \\ 0 & \text{otherwise} \end{cases}. \tag{8.63}$$

However, since (8.27), (8.28), and (8.63) are piecewise functions, the evaluation of (8.61) is cumbersome. Thus, we define the region $D_1 \subset D_z$

$$D_1 := \{(x, y) \in D_z \mid 0 \leq x \wedge 0 \leq y \wedge x \leq y\} \tag{8.64}$$

where f is non-zero. Next, we define the function $f_1 : D_1 \to \mathbb{R}$ as

$$f_1(x, y) = \frac{M!}{(M-2)!}(1 - e^{-y})^{M-2} e^{-y} e^{-x}. \tag{8.65}$$

Then, using (8.64) and (8.65), we can rewrite (8.61) as

$$F_E(z) = \iint_{D_z} f(x, y)\, dx\, dy = \iint_{D_1} f_1(x, y)\, dx\, dy \tag{8.66}$$

The domain D_1 can now be calculated as

$$D_1 = \begin{cases} D_2 = \{(x, y) \in \mathbb{R} \mid 0 < x < ay - b \wedge 0 < x \leq y\} & \text{if } E_T - z > 0 \\ D_3 = \{(x, y) \in \mathbb{R} \mid ay - b < x \wedge 0 < x \leq y \wedge 0 \leq y\} & \text{if } E_T - z < 0 \end{cases} \tag{8.67}$$

with $a = \frac{z}{(E_T - z)\mathrm{SINR}_{\min}}$ and $b = \frac{N_0}{E_T - z}$. We start by calculating D_2, i.e., we assume that $E_T - z > 0$. We see that D_2 is bounded by the line $L_1 = \{(x, y) \in \mathbb{R}^2 \mid x = ay - b\}$ and $L_2 = \{(x, y) \in \mathbb{R}^2 \mid x = y\}$. We differentiate between the following three cases:

- $a > 1 \Leftrightarrow z > \frac{E_T \mathrm{SINR}_{\min}}{1 + \mathrm{SINR}_{\min}}$
- $a = 1 \Leftrightarrow z = \frac{E_T \mathrm{SINR}_{\min}}{1 + \mathrm{SINR}_{\min}}$
- $a < 1 \Leftrightarrow z < \frac{E_T \mathrm{SINR}_{\min}}{1 + \mathrm{SINR}_{\min}}$

Line L_1 and L_2 intersect at a point with the exception of the second case, i.e., $a = 1$, where L_1 and L_2 are parallel. The intersection point (x_c, y_c) is calculated as

$$x_c = y_c = -\frac{N_0 \mathrm{SINR}_{\min}}{\mathrm{SINR}_{\min}(E_T - z) - z}. \tag{8.68}$$

Another point of interest is the intersection of L_1 with the y-axis. This point, denoted $(0, y_0)$, is calculated as

$$y_0 = \frac{N_0 \text{SINR}_{\min}}{z}. \tag{8.69}$$

We start by investigating $a > 1$. We assume that L_1 and L_2 intersect on the line segment $\{(x, x) \in \mathbb{R}^2 \mid x < 0\}$, i.e., we assume that

$$-\frac{N_0 \text{SINR}_{\min}}{\text{SINR}_{\min}(E_T - z) - z} < 0 \tag{8.70}$$

$$\Rightarrow \quad \frac{E_T \text{SINR}_{\min}}{\text{SINR}_{\min} + 1} > z \tag{8.71}$$

which contradicts that $a > 1$, and thus L_1 and L_2 must intersect on $\{(x, x) \in \mathbb{R}^2 \mid x \geq 0\}$. We can now define the domain D_2 for $\frac{E_T \text{SINR}_{\min}}{1+\text{SINR}_{\min}} < z < E_T$ as

$$D_2 = \{(x, y) \in \mathbb{R} \mid (0 < x < ay - b \wedge y_0 < y < y_c) \vee (0 < x < y \wedge y_c < y))\}. \tag{8.72}$$

Next, we investigate $a = 1$, i.e., L_1 and L_2 are parallel. Since $b > 0$, the border of D_2 is defined by L_1, and L_1 intersects with the y-axis at y_0. We can then define the domain D_2 for $z = \frac{E_T \text{SINR}_{\min}}{1+\text{SINR}_{\min}}$ as

$$D_2 = \{(x, y) \in \mathbb{R} \mid 0 < x < ay - b \wedge y_0 < y)\}. \tag{8.73}$$

Finally, we assume that $a < 1$. We approach this case as the $a > 1$ case: We can prove that the intersection of L_1 and L_2 has negative coordinates, and next, we determine the intersection of L_1 and the y-axis. We can then define the domain D_2 for $0 < z < \frac{E_T \text{SINR}_{\min}}{1+\text{SINR}_{\min}}$ as

$$D_2 = \{(x, y) \in \mathbb{R} \mid 0 < x < ay - b \wedge y_0 < y\}. \tag{8.74}$$

We see that we can omit to treat the $a = 1$ case separately by including it with $a > 1$ or $a < 1$. We choose $a > 1$, and thus $a \geq 1$ covers the region $\frac{E_T \text{SINR}_{\min}}{1+\text{SINR}_{\min}} \leq z < E_T$.

Finally, we can express the region D_2 as

$$D_2 = \{(x, y) \in \mathbb{R} \mid (0 < x < ay - b \wedge y_0 < y)\} \tag{8.75}$$

if $0 < z < \frac{E_T \mathrm{SINR}_{\min}}{1+\mathrm{SINR}_{\min}}$ and as

$$D_2 = \{(x, y) \in \mathbb{R} \mid (0 < x < ay - b \wedge y_0 < y < y_c) \vee (0 < x < y \wedge y_c < y))\} \tag{8.76}$$

if $\frac{E_T \mathrm{SINR}_{\min}}{1+\mathrm{SINR}_{\min}} \leq z < E_T$.

We can now proceed to determine the region D_3. Using the fact that $z > E_T$ and using (8.71) we see that the intersection point of L_1 and L_2 has positive coordinates. Since $a < 0$, the region D_3 is

$$D_3 = \{(x, y) \in \mathbb{R} \mid (ay - b < x < y \wedge y_c < y < y_0) \vee (0 < x < y \wedge y_0 < y)\} \tag{8.77}$$

and thus all the domaines are determined. The resulting cdf is

$$F_E(z) = \begin{cases} 0 & z < 0 \\ F_{E1}(z) & 0 < z < \frac{E_T \mathrm{SINR}_{\min}}{1+\mathrm{SINR}_{\min}} \\ F_{E2}(z) & \frac{E_T \mathrm{SINR}_{\min}}{1+\mathrm{SINR}_{\min}} < z < E_T \\ F_{E3}(z) & E_T < z \end{cases}. \tag{8.78}$$

The different pieces of the cdf can now be determined using straightforward integration. On the domain $(0, \frac{E_T \mathrm{SINR}_{\min}}{1+\mathrm{SINR}_{\min}})$ the cdf $F_E(z)$ is

$$F_{E1}(z) = \int_{y_0}^{+\infty} \int_{0}^{ay-b} f_1(x, y)\, dx\, dy \tag{8.79}$$

$$= \sum_{k=0}^{M-2} (-1)^k \frac{M!}{k!(M-2-k)!} \frac{z}{(E_T - z)\mathrm{SINR}_{\min} + z(k+1)} e^{-\frac{N_0 \mathrm{SINR}_{\min}}{z}}. \tag{8.80}$$

On the domain $[\frac{E_T \mathrm{SINR}_{\min}}{1+\mathrm{SINR}_{\min}}, E_T)$, $F_E(z)$ is

$$F_{E2}(z) = \int_{y_0}^{y_c} \int_{0}^{ay-b} f_1(x,y)\,dx\,dy + \int_{y_c}^{+\infty} \int_{0}^{y} f_1(x,y)\,dx\,dy \tag{8.81}$$

which results in (8.86). and finally, on the domain $[E_T, +\infty)$, the cdf F_E is calculated as

$$F_{E3}(z) = \int_{y_c}^{y_0} \int_{ay-b}^{y} f_1(x,y)\,dx\,dy + \int_{y_0}^{+\infty} \int_{0}^{y} f_1(x,y)\,dx\,dy \tag{8.82}$$

which results in (8.87). We see that $F_{E3} = F_{E2}$, and thus the cdf is now

$$F_E(z) = \begin{cases} 0 & z < 0 \\ F_{E1}(z) & 0 < z < \frac{E_T \mathrm{SINR}_{\min}}{1+\mathrm{SINR}_{\min}} \\ F_{E2}(z) & \frac{E_T \mathrm{SINR}_{\min}}{1+\mathrm{SINR}_{\min}} < z \end{cases}. \tag{8.83}$$

The pdf can now be found by derivation as

$$f_E(z) = \begin{cases} 0 & z < 0 \\ f_{E1}(z) = \frac{d}{dz} F_{E1}(z) & 0 < z < \frac{E_T \mathrm{SINR}_{\min}}{1+\mathrm{SINR}_{\min}} \\ f_{E2}(z) = \frac{d}{dz} F_{E2}(z) & \frac{E_T \mathrm{SINR}_{\min}}{1+\mathrm{SINR}_{\min}} < z \end{cases} \tag{8.84}$$

with

$$f_{E1}(z) = \sum_{k=0}^{S-2} (-1)^k \frac{S!}{k!(S-2-k)!} \\ \frac{\mathrm{SINR}_{\min}(N_0(1+k-\mathrm{SINR}_{\min})z + E_T(N_0\mathrm{SINR}_{\min}+z))}{z(E_T\mathrm{SINR}_{\min} + (1+k-\mathrm{SINR}_{\min})z)^2} e^{-\frac{N_0 \mathrm{SINR}_{\min}}{z}} \tag{8.85}$$

and (8.88).

$$F_{E2}(z) = \sum_{k=0}^{M-2} \frac{M!}{k!(M-2-k)!(-k-1)}(-1)^k \left(\left(\frac{(E_T - z)\mathrm{SINR}_{\min}}{(-k-1)z - (E_T - z)\mathrm{SINR}_{\min}} + \right. \right.$$
$$\left. \left. \frac{1}{k+2} \right) e^{\frac{N_0 \mathrm{SINR}_{\min}(k+2)}{\mathrm{SINR}_{\min}(E_T - z) - z}} - \left(\frac{(E_T - z)\mathrm{SINR}_{\min}}{(-k-1)z - (E_T - z)\mathrm{SINR}_{\min}} + 1 \right) e^{-\frac{N_0 \mathrm{SINR}_{\min}}{z}} \right) \quad (8.86)$$

$$F_{E3}(z) = \sum_{k=0}^{M-2} \frac{M!(-1)^k}{k!(M-2-k)!} \frac{1}{-k-1} \left(\left(\frac{1}{k+2} + \frac{(E_T - z)\mathrm{SINR}_{\min}}{(-k-1)z - (E_T - z)\mathrm{SINR}_{\min}} \right) \right.$$
$$\left. e^{\frac{(k+2)N_0 \mathrm{SINR}_{\min}}{\mathrm{SINR}_{\min}(E_T - z) - z}} - \left(\frac{(E_T - z)\mathrm{SINR}_{\min}}{(-k-1)z - (E_T - z)\mathrm{SINR}_{\min}} + 1 \right) e^{-\frac{N_0 \mathrm{SINR}_{\min}}{z}} \right). \quad (8.87)$$

$$f_{E2}(z) = \sum_{k=0}^{M-2} (-1)^k \frac{M!}{k!(M-2-k)!} \left[\left(e^{-\frac{N_0 \mathrm{SINR}_{\min}}{z} + N_0 \mathrm{SINR}_{\min}\left(\frac{1}{z} + \frac{2+k}{E_T \mathrm{SINR}_{\min} - (1+\mathrm{SINR}_{\min})z}\right)} \right) \right.$$
$$\frac{\mathrm{SINR}_{\min}(E_T \mathrm{SINR}_{\min}(-E_T + N_0 + N_0 \mathrm{SINR}_{\min}) + (E_T + N_0(1 + k - \mathrm{SINR}_{\min}))(1 + \mathrm{SINR}_{\min})z)}{(E_T \mathrm{SINR}_{\min} + (1 + k - \mathrm{SINR}_{\min})z)^2 (E_T \mathrm{SINR}_{\min} - (1 + \mathrm{SINR}_{\min})z)} -$$
$$\left. \frac{\mathrm{SINR}_{\min}(-E_T N_0 \mathrm{SINR}_{\min} - E_T z - N_0 z - k N_0 z + N_0 \mathrm{SINR}_{\min} z)}{z(-E_T \mathrm{SINR}_{\min} - z - kz + \mathrm{SINR}_{\min} z)^2} e^{-\frac{N_0 \mathrm{SINR}_{\min}}{z}} \right] \quad (8.88)$$

Part IV

Conclusions

Chapter 9

Review and Future Work

In the following chapter we will conclude the thesis by reviewing the results from the different topics and we will propose possible extensions as future work.

Linear Precoding for Single-User MIMO Channels

In Chapter 3 we address the problem whether it is possible to use vector quantization techniques to quantize unitary precoding matrices for MIMO transmission, i.e., Problem 1. We apply several vector quantization techniques to this problem and we show the benefits of the applied techniques through simulations. However, all the presented codebooks are found by Monte-Carlo designs. Even for the most simplest distortion functions there still exists no optimal design approaches. An interesting, but very hard topic, would be the investigation of improved codebook design algorithms, i.e., algorithm that do not converge to a local optimum but to the global optimum.

The next chapter, Chapter 4, considers Problem 2, i.e., the extrapolation of the current channel based on previously known channel realizations. The used technique, i.e., geodesic extrapolation, shows promise for the investigated channel model. As future work it would be interesting to do a comparative study of geodesic extrapolation with other extrapolation techniques.

Correlated Multi-User MISO Channels

In the next part of the thesis we visit similar problems in the context of multi-user MISO channels.

In Chapter 5 we design codebooks for a spatially correlated channel using a Monte-Carlo codebook design. As in the previously mentioned single-user case, the next step would be the investigation of improved codebook design algorithms. The same is true for the results of Chapter 6 where we design codebooks for temporally correlated channels.

Scheduling in Multi-User MISO Channels

The next two chapters are concerned with Problem 5. In Chapter 7 we present an extension of the BestFit algorithm for near-round-robin scheduling. The following chapter, Chapter 8, then considers true round-robin scheduling. The presented algorithm tries to allocate the users in the same position in a block as long as possible by distributing the available energy correspondingly. We further present an algorithm to generate the codebooks to quantize the feedback. The next step should be to prove the optimality of the presented codebook generation algorithm.

Adaptive Codebooks

Throughout the thesis we generate the codebooks offline based on known and fixed channel statistics. However, we have to assume that in real systems the channel statistics are not known and maybe even not time-invariant. The codebooks should adapt during runtime to the changing channel characteristics. A possible solution is the application of self-adapting codebooks. We already present some basic work in this particular direction in Chapter 3.

Imperfect CSI

A topic not considered in this thesis, but of great practical importance, is imperfect channel knowledge, i.e., acquiring perfect CSI is not possible due to the limited time available for training in practical systems. As a consequence, the applied algorithm should be robust against imperfect CSI.

Beyond Narrowband

Further, as we mentioned in the problem statements in Chapter 1.1, we just considered narrowband single-carrier transmission throughout the thesis. However, the proposed techniques can also be implemented for other systems, e.g., quantizing the subcarriers of an OFDM system.

Implementation

It is important to note that the performance of the presented algorithms in this thesis is evaluated by simulations. These simulations rely on various optimal assumptions on the underlying system, e.g., Rayleigh fading. However, in order to judge the practical relevance of the presented algorithms, they have to be implemented, and their performance in real systems has to be evaluated.

Acknowledgements

First of all I would like to thank my advisor Geert Leus for giving me the opportunity to do a Ph.D. as his research assistant. His door was always open for me, and his deep insights into DSP problems were invaluable. Further, I would like to thank Alle-Jan van der Veen for welcoming me in his group, and for providing dinner company on a regularly basis. I feel both privileged and grateful for the opportunity to have met them both.

I would also like to thank all the scientific and non-scientific members of the CAS group for making the stay in Delft so pleasant: Antoon Frehe for maintaining the Condor cluster which made the simulations in this thesis possible. Laura Bruns for taking care of all the administrative hurdles. My fellow students, Vijay and Kun, and especially, my lovely office mates Yiyin and Yu for providing such a pleasant work environment.

Abbreviations

AoD	angle of departure
BER	bit error rate
CARR	channel aware round-robin
CDI	channel direction information
CDMA	code division multiple access
CQI	channel quality information
CSI	channel state information
DPC	dirty paper coding
FDD	frequency-division duplexing
FSVQ	finite state vector quantization
GLA	generalized Lloyd algorithm
HP	high performance
i.i.d.	independent and identically distributed
LC	low complexity
LMMSE	linear minimum mean square error
MC	Monte-Carlo
MI	mutual information
MIMO	multiple-input multiple-output
MISO	multiple-input single-output
ML	maximum likelihood
MMSE	minimum mean square error
MPC	multipath components
MSE	mean square error

MSV	minimum singular value
NLOS	no line of sight
NPF	non-prefix-free
OB	orthogonal beamforming
OFDM	orthogonal frequency-division multiplexing
OSDMA	opportunistic SDMA
OSDMA-LF	OSDMA with limited feedback
OSTBC	orthogonal space-time block code
PAS	power angular spectrum
PBF	partial Best Fit
PDF	probability density function
PF	prefix-free
POTS	plain old telephone service
PSK	phase-shift keying
PVQ	predictive vector quantization
QAM	quadrature amplitude modulation
QoS	Quality-of-Service
QPSK	quadrature phase-shift keying
RVQ	random vector quantization
SDMA	space-division multiple access
SER	symbol error rate
SINR	signal-to-noise-plus-interference ratio
SISO	single-input single-ouput
SVD	singular value decomposition
TDD	time-division duplexing
TDMA	time-division multiple access
TxMF	transmit matched filtering
ULA	uniform linear array
UT	user terminal
VQ	vector quantizer
ZF	zero-forcing

About the Author

Claude Simon received the electrical engineering degree (Dipl.-Ing) from the Technical University of Kaiserslautern, Germany, in 2005. His semester thesis "Performance tradeoffs in the implementation of the sphere decoder algorithm for MIMO wireless communication," and his diploma thesis "An information-theoretic evaluation of soft-output MIMO detectors," were carried out at the Communication Theory Group headed by Prof. Helmut Bölcskei at the ETH Zurich. He works since August 2005 as a Ph.D. student under Dr. Geert Leus at the Circuits and Systems Group, headed by Prof. Alle-Jan van der Veen, at the Technical University Delft, The Netherlands.

Publication List

1. C. Simon and G. Leus, "Round-robin scheduling for orthogonal beamforming with limited feedback," in *IEEE Transactions on Wireless Communications*, vol.10, no. 8, pp. 2486-2496, Aug. 2011.

2. C. Simon and G. Leus, "Round-robin scheduling for time-varying channels with limited feedback," in *Proc. IEEE Workshop on Signal Processing Advances in Wireless Communications (SPAWC)*, Perugia, Italy, Jun. 2009.

3. C. Simon and G. Leus, "Low-delay scheduling for Grassmannian beamforming with a SINR constraint," in *Proc. IEEE International Conference on Acoustics, Speech, and Signal Processing (ICASSP)*, Taipei, Taiwan, Apr. 2009.

4. R. de Francisco, C. Simon, D. Slock and G. Leus, "Beamforming for Correlated Broadcast Channels with Quantized Channel State Information," in *Proc. IEEE Workshop on Signal Processing Advances in Wireless Communications (SPAWC)*, Recife, Brazil, Jul. 2008.

5. C. Simon and G. Leus, "Feedback quantization for linear precoded spatial multiplexing," in *EURASIP Journal on Advances in Signal Processing*, vol. 2008, Article ID 683030, 13 pages, 2008.

6. C. Simon and G. Leus, "Feedback compression for correlated broadcast channels," in *Proc. IEEE Symposium on Communications and Vehicular Technology in the Benelux (SCVT)*, Delft, The Netherlands, Nov. 2007.

7. C. Simon and G. Leus, "Feedback reduction for spatial multiplexing with linear precoding," in *Proc. International Conference on Acoustics, Speech, and Signal Processing (ICASSP)*, Honolulu, HI, USA, Apr. 2007.

8. C. Simon and G. Leus, "Adaptive feedback reduction for precoded spatial multiplexing MIMO systems," in *Proc. International ITG/IEEE Workshop on Smart Antennas (WSA)*, Vienna, Austria, Feb. 2007.

9. G. Leus and C. Simon, "Quantized feedback and feedback reduction for precoded spatial multiplexing MIMO systems," in *Proc. International Symposium on Signal Processing and its Applications (ISSPA)*, Sharjah, United Arabic Emirates, Feb. 2007.

10. G. Leus, C. Simon and N. Khaled, "Spatial multiplexing with linear precoding in time-varying channels with limited feedback," in *Proc. European Signal Processing Conference (EUSIPCO)*, Florence, Italy, Sep. 2006.

11. A. Burg, M. Borgmann, C. Simon, M. Wenk, M. Zellweger, and W. Fichtner, "Performance tradeoffs in the VLSI implementation of the sphere decoding algorithm," in *Proc. IEE 3G Mobile Communications Technologies Conference (3G)*, London, United Kingdom, Oct. 2004.

Abstract

The number of deployed wireless communication systems has grown rapidly in the last years. Their popularity is mainly due to the effortlessness with which the systems can be deployed. Further, the new generation of wireless systems, e.g., 802.11n, starts to close the performance gap to their wired counterparts. The performance of these systems can be improved if channel state information (CSI) is available at the transmitter. Unfortunately, having perfect CSI at the transmitter all the time is difficult to realize. CSI can be acquired through training, but becomes outdated very quickly afterwards due to the inevitable time-variability of the wireless channel. However, if the coherence time of the channel is sufficiently large, then the CSI becomes time correlated. One of the main topics of this thesis is to exploit this time correlation to improve the performance of the wireless system. Another problem is that the CSI can often just be acquired at the receiver and must be fed back to the transmitter over a data-rate limited feedback link. Thus, the CSI has to be quantized before it can be fed back. The application of tools from the large vector quantization framework to CSI quantization is the other main topic of the thesis. Throughout the thesis we investigate different scenarios where CSI knowledge at the transmitter plays a paramount role.

In the first part of the thesis we consider a single-link MIMO system. We start by investigating how the unitary precoder can be extrapolated based on the knowledge of previous precoders using geodesic interpolation. Next, we apply tools from vector quantization to quantize the precoders by exploiting the time correlation of the channel.

In the next part we consider the MISO broadcast channel. There, we propose

the use of predictive vector quantization to exploit the time correlation to improve the CSI quantization. Further, we introduce a novel channel model, and generate the corresponding CSI quantization codebooks.

We investigate in the last part the feedback of different metrics to enable round-robin scheduling, and near round-robin scheduling, assuming a limited feedback link. We present different metrics, and also propose an algorithm to design the corresponding codebooks.

Samenvatting

Het aantal geïnstalleerde draadloze communicatiesystemen is de laatste jaren snel gegroeid. Hun populariteit is voornamelijk te danken aan het gemak waarmee de systemen kunnen worden geinstalleerd. Ook heeft de nieuwe generatie draadloze systemen, zoals 802.11n, een prestatie die steeds dichter tegen die van bedrade systemen aanligt. De prestatie van deze systemen kan worden verbeterd als kanaalinformatie beschikbaar is bij de zender. Helaas is het zeer moeilijk om continu perfecte kanaalinformatie bij de zender te krijgen. Kanaalinformatie kan verkregen worden via training, maar de informatie veroudert snel vanwege de onvermijdelijke variaties in het draadloze kanaal. Echter, als de coherentietijd van het kanaal voldoende lang is, is de kanaalinformatie gecorreleerd in de tijd. Een van de hoofdonderwerpen in dit proefschrift is het benutten van deze tijdcorrelatie en hierdoor de prestatie van het systeem te verbeteren.

Een ander probleem is dat de kanaalinformatie meestal enkel bij de ontvanger gemeten kan worden, en teruggestuurd moet worden naar de zender over een retourkanaal met beperkte capaciteit. De informatie moet gecomprimeerd worden voordat het kan worden teruggestuurd. Het gebruik van technieken uit de vectorkwantisatie voor de compressie van kanaalinformatie is een ander hoofdthema in het proefschrift. We bestuderen diverse scenarios waarbij kanaalinformatie bij de zender een belangrijke rol speelt.

In het eerste deel van het proefschrift beschouwen we een enkele verbinding in een multi-kanaals (MIMO) systeem. We beginnen met het bestuderen hoe de unitaire precoder geextrapoleerd kan worden gebaseerd op de kennis van voorgaande coders met gebruikmaking van geodetische interpolatie. Vervolgens passen we gereedschappen uit de vectorkwantisatie toe om deze precoders te kwantiseren

met gebruikmaking van de tijdcorrelatie van het kanaal.

In het volgende deel beschouwen een MISO omroepkanaal. Hiervoor stellen we het gebruik van voorspellende vectorkwantisatie voor, waarin de tijdcorrelatie gebruikt wordt voor verbeterde kanaalkwantisatie. We introduceren een nieuw kanaalmodel, en genereren de bijbehorende kanaalkwantisatie codeboeken.

In het laatste deel onderzoeken we het terugsturen van diverse parameters om "round-robin" schema's mogelijk te maken over een beperkt retourkanaal. We bestuderen diverse parameters, en stellen een algoritme voor om de bijbehorende codeboeken te ontwerpen.

Bibliography

[1] Eurostat. Number of mobile phone subscriptions.

[2] International Telecommunications Union (ITU). (2010, Dec.) The world in 2010: ICT facts and figures. [Online]. Available: http://www.itu.int/ITU-D/ict/statistics/

[3] H. Bölcskei, D. Gesbert, C. B. Papadias, and A.-J. van der Veen, Eds., *Space-Time Wireless Systems: From Array Processing to MIMO Communications*. Cambridge University Press, 2006.

[4] I. E. Telatar, "Capacity of multi-antenna gaussian channels," *European Trans. Telecommun.*, vol. 10, no. 6, pp. 585–595, Nov. 1999.

[5] W. Ajib and D. Haccoun, "An overview of scheduling algorithms in MIMO-based fourth-generation wireless systems," *IEEE Network*, vol. 19, no. 5, pp. 43–48, Sep. 2005.

[6] H. Fattah and C. Leung, "An overview of scheduling algorithms in wireless multimedia networks," *IEEE Wireless Commun. Mag.*, vol. 9, no. 5, pp. 76–83, Oct. 2002.

[7] A. Paulraj, R. Nabar, and D. Gore, *Introduction to Space-Time Wireless Communications*. Cambridge University Press, 2003.

[8] G. G. Raleigh and J. M. Cioffi, "Spatio-temporal coding for wireless communication," *IEEE Trans. Commun.*, vol. 46, no. 3, pp. 357–366, Mar. 1998.

[9] T. M. Cover and J. A. Thomas, *Elements of Information Theory.* Wiley, 1991.

[10] J. Salz, "Digital transmission over cross-coupled linear channels," *AT&T Bell Labs Technical Journal*, vol. 64, pp. 1147–1159, Jul.-Aug. 1985.

[11] H. Sampath and A. Paulraj, "Joint transmit and receive optimization for high data rate wireless communication using multiple antennas," in *Proc. Asilomar Conference on Signals, Systems, and Computers*, vol. 1, Pacific Grove, CA, USA, Oct. 1999, pp. 215–219.

[12] A. Scaglione, P. Stoica, S. Barbarossa, G. B. Giannakis, and H. Sampath, "Optimal designs for space-time linear precoders and decoders," *IEEE Trans. Signal Processing*, vol. 50, no. 5, pp. 1051–1064, May 2002.

[13] D. J. Love and R. W. Heath Jr., "Limited feedback precoding for spatial multiplexing systems using linear receivers," in *Proc. Military Communications Conference (MILCOM)*, vol. 1, Oct. 2003, pp. 627 – 632.

[14] J. C. Roh and B. D. Rao, "An efficient feedback method for MIMO systems with slowly time-varying channels," in *Proc. IEEE Wireless Communications and Networking Conference (WCNC)*, vol. 2, Atlanta, USA, Mar. 2004, pp. 760–764.

[15] B. C. Banister and J. R. Zeidler, "A simple gradient sign algorithm for transmit antenna weight adaptation with feedback," *IEEE Trans. Signal Processing*, vol. 51, no. 5, pp. 1156–1171, May 2003.

[16] K. Huang, B. Mondal, R. W. Heath Jr., and J. G. Andrews, "Markov models for limited feedback MIMO systems," in *Proc. IEEE Int. Conf. Acoust., Speech, and Signal Process. (ICASSP)*, vol. 4, Toulouse, France, May 2006, pp. 9–12.

[17] A. Gersho and R. M. Gray, *Vector Quantization and Signal Compressing.* Kluwer Academic Publishers, 1995.

[18] C. Simon and G. Leus, "Feedback reduction for spatial multiplexing with linear precoding," in *Proc. IEEE Int. Conf. Acoust., Speech, and Signal Process. (ICASSP)*, vol. 3, Honolulu, HI, USA, Apr. 2007, pp. 33–36.

[19] G. Leus and C. Simon, "Quantized feedback and feedback reduction for precoded spatial multiplexing MIMO systems," in *Proc. Int. Symp. Signal Process. and Applicat. (ISSPA)*, Sharjah, United Arab Emirates, Feb. 2007.

[20] C. Simon and G. Leus, "Adaptive feedback reduction for precoded spatial multiplexing MIMO systems," in *Proc. Int. ITG/IEEE Workshop Smart Antennas (WSA)*, Vienna, Austria, Feb. 2007.

[21] ——, "Feedback quantization for linear precoded spatial multiplexing," *EURASIP Journal Advances Signal Process.*, vol. 2008, 2008.

[22] H. T. Nguyen, G. Leus, and N. Khaled, "Precoder and decoder prediction in time-varying MIMO channels," in *Proc. IEEE International Workshop on Computational Advances in Multi-Sensor Adaptive Processing (CAMSAP)*, Puerto Vallarta, Mexico, Dec. 2005, pp. 153–156.

[23] D. Asimov and A. Buja, "The grand tour via geodesic interpolation of 2-frames," in *I&ST/SPIE Symposium*, San Jose, CA, USA, 1994.

[24] G. Leus, C. Simon, and N. Khaled, "Spatial multiplexing with linear precoding in time-varying channels with limited feedback," in *Proc. European Signal Process. Conf. (EUSIPCO)*, Florence, Italy, Sep. 2006.

[25] H. Weingarten, Y. Steinberg, and S. Shamai (Shitz), "The capacity region of the Gaussian multiple-input multiple-output broadcast channel," *IEEE Trans. Inform. Theory*, Sep. 2006.

[26] M. H. Costa, "Writing on dirty paper," *IEEE Trans. Inform. Theory*, vol. 29, no. 3, pp. 439–441, May 1983.

[27] B. M. Hochwald, C. B. Peel, and A. L. Swindlehurst, "A vector-perturbation technique for near-capacity multiantenna multiuser communication - Part II: Perturbation," *IEEE Trans. Commun.*, vol. 53, no. 3, pp. 537–544, Mar. 2005.

[28] R. de Francisco, C. Simon, D. T. Slock, and G. Leus, "Beamforming for correlated broadcast channels with quantized channel state information," in *Proc. IEEE Workshop Signal Process. Advances Wireless Commun. (SPAWC)*, Recife, Brazil, Jul. 2008, pp. 161–165.

[29] C. Simon, R. de Francisco, D. T. Slock, and G. Leus, "Feedback compression for correlated broadcast channels," in *Proc. IEEE Symp. Commun. and Vehicular Technology Benelux (SCVT)*, Delft, The Netherlands, Nov. 2007.

[30] D. N. Tse and P. Viswanath, *Fundamentals of Wireless Communication*. Cambridge University Press, 2005.

[31] P. Viswanath, D. N. Tse, and R. Laroia, "Opportunistic beamforming using dumb antennas," *IEEE Trans. Inform. Theory*, vol. 48, no. 6, pp. 1277–1294, Jun. 2002.

[32] C. Simon and G. Leus, "Low-delay scheduling for Grassmannian beamforming with a SINR constraint," in *Proc. IEEE Int. Conf. Acoust., Speech, and Signal Process. (ICASSP)*, Taipei, Taiwan, Apr. 2009, pp. 2377–2380.

[33] ——, "Round-robin scheduling for time-varying channels with limited feedback," in *Proc. IEEE Workshop Signal Process. Advances Wireless Commun. (SPAWC)*, Perugia, Italy, Jun. 2009, pp. 231–234.

[34] S. P. Lloyd, "Least squares quantization in PCM," Bell Laboratories, Whippky, NJ, United States, Tech. Rep., Jul. 1957.

[35] Y. Linde, A. Buzo, and R. M. Gray, "An algorithm for vector quantizer design," *IEEE Trans. Commun.*, vol. 28, no. 1, pp. 84–95, Jan. 1980.

[36] P. F. Panter and W. Dite, "Quantization distortion in pulse-count modulation with nonuniform spacing of levels," *Proc. I.R.E.*, vol. 39, no. 1, pp. 44–48, Jan. 1951.

[37] Z. Wang and A. C. Bovik, "Mean squared error: Love it or leave it?" *IEEE Signal Processing Mag.*, vol. 26, no. 1, pp. 98–117, Jan. 2009.

[38] J. Max, "Quantizing for minimum distortion," *IEEE Trans. Inform. Theory*, vol. 6, no. 1, pp. 7–12, Mar. 1960.

[39] P. Fleischer, "Sufficient conditions for achieving minimum distortion in a quantizer," in *Proc. IEEE Int. Convention Records*, 1964, pp. 104–111.

[40] M. J. Sabin and R. M. Gray, "Global convergence and empirical consistency of the generalized Lloyd algorithm," *IEEE Trans. Inform. Theory*, vol. 32, no. 2, pp. 148–155, Mar. 1986.

[41] D. P. Palomar, M. Bengtsson, and B. Ottersten, "Minimum BER linear transceivers for MIMO channels via primal decomposition," *IEEE Trans. Signal Processing*, vol. 53, no. 8, pp. 2866–2882, Aug. 2005.

[42] A. Narula, M. J. Lopez, M. D. Trott, and G. W. Wornell, "Efficient use of side information in multiple-antenna data transmission over fading channels," *IEEE J. Select. Areas Commun.*, vol. 16, no. 8, pp. 1423–1436, Oct. 1998.

[43] E. Visotsky and U. Madhow, "Space-time transmit precoding with imperfect feedback," *IEEE Trans. Inform. Theory*, vol. 47, no. 6, pp. 2632–2639, Sep. 2001.

[44] S. A. Jafar, S. Vishwanath, and A. Goldsmith, "Channel capacity and beamforming for multiple transmit and receive antennas with covariance feedback," in *Proc. 2001 IEEE International Conference on Communications (ICC 2001)*, vol. 7, Jun. 2001, pp. 2266–2270.

[45] A. Goldsmith, S. A. Jafar, N. Jindal, and S. Vishwanath, "Capacity limits of MIMO channels," *IEEE J. Select. Areas Commun.*, vol. 21, no. 5, pp. 684–702, Jun. 2003.

[46] D. J. Love, R. W. Heath Jr., and T. Strohmer, "Quantized maximum ratio transmission for multiple-input multiple-output wireless systems," in *Conference Record of the Thirty-Sixth Asilomar Conference on Signals, Systems and Computers*, vol. 1, Nov. 2002, pp. 531–535.

[47] K. K. Mukkavilli, A. Sabharwal, E. Erkip, and B. Aazhang, "On beamforming with finite rate feedback in multiple-antenna systems," *IEEE Trans. Inform. Theory*, vol. 49, no. 10, pp. 2562–2579, Oct. 2003.

[48] D. J. Love and R. W. Heath Jr., "Limited feedback unitary precoding for spatial multiplexing systems," *IEEE Trans. Inform. Theory*, vol. 51, no. 8, pp. 2967–2976, Aug. 2005.

[49] J. C. Roh and B. D. Rao, "Transmit beamforming in multiple-antenna systems with finite rate feedback: A VQ-based approach," *IEEE Trans. Inform. Theory*, vol. 52, no. 3, pp. 1101–1112, Mar. 2006.

[50] S. Zhou and B. Li, "BER criterion and codebook construction for finite-rate precoded spatial multiplexing with linear receivers," *IEEE Trans. Signal Processing*, vol. 54, no. 5, pp. 1653–1665, May 2006.

[51] H. Sampath, P. Stoica, and A. Paulraj, "Generalized linear precoder and decoder design for MIMO channels using the weighted MMSE criterion," *IEEE Trans. Commun.*, vol. 49, no. 12, pp. 2198–2206, Dec. 2001.

[52] J. C. Roh and B. D. Rao, "Channel feedback quantization methods for MISO and MIMO systems," in *Proc. 15th IEEE International Symposium on Personal, Indoor and Mobile Radio Communications (PIMRC)*, vol. 2, Barcelona, Spain, Sep. 2004, pp. 805–809.

[53] D. J. Love and R. W. Heath Jr., "Limited feedback unitary precoding for orthogonal space-time block codes," *IEEE Trans. Signal Processing*, vol. 53, no. 1, pp. 64–73, Jan. 2005.

[54] ——, "Limited feedback precoding for spatial multiplexing systems," in *Proc. IEEE Global Telecommunications Conference (GLOBECOM)*, vol. 4, San Francisco, USA, Dec. 2003, pp. 1857 – 1861.

[55] K. Huang, B. Mondal, R. W. Heath Jr., and J. G. Andrews, "Multi-antenna limited feedback for temporally-correlated channels: Feedback compression," in *Proc. Global Telecommunications Conf. (GLOBECOM)*, Dec. 2006.

[56] J. S. Vitter, "Design and analysis of dynamic Huffman codes," *Journal of the ACM*, vol. 4, no. 34, pp. 825–845, Oct. 1987.

[57] D. E. Knuth, "Dynamic Huffman coding," *J. Algorithms*, vol. 6, no. 2, pp. 163–180, 1985.

[58] R. G. Gallager, "Variations on a theme by Huffman," *IEEE Trans. Inform. Theory*, vol. 24, no. 6, pp. 668–674, Nov. 1978.

[59] R. Samanta and R. W. Heath Jr., "Codebook adaptation for quantized MIMO beamforming systems," in *Proc. Asilomar Conference on Signals, Systems, and Computers*, Pacific Grove, CA, USA, Oct. 2005, pp. 376–380.

[60] S. Zhou, B. Li, and P. Willett, "Recursive and trellis-based feedback reduction for MIMO-OFDM with rate-limited feedback," *IEEE Trans. Wireless Commun.*, vol. 5, no. 12, pp. 3400–3405, Dec. 2006.

[61] A. K. Krishnamurthy, S. C. Ahalt, D. E. Melton, and P. Chen, "Neural networks for vector quantization of speech and images," *IEEE J. Select. Areas Commun.*, vol. 8, no. 8, pp. 1449–1457, Oct. 1990.

[62] B. M. Hochwald, T. L. Marzetta, T. J. Richardson, W. Sweldens, and R. Urbanke, "Systematic design of unitary space-time constellations," *IEEE Trans. Inform. Theory*, vol. 46, no. 6, pp. 1962–1973, Sep. 2000.

[63] A. van Zelst, "MIMO OFDM for wireless LANs," Ph.D. dissertation, TU Eindhoven, Apr. 2004.

[64] D. J. Love and R. W. Heath Jr., "Multimode precoding for MIMO wireless systems," *IEEE Trans. Signal Processing*, vol. 53, no. 10, pp. 3674–3687, Oct. 2005.

[65] N. Khaled, B. Mondal, R. W. Heath Jr., G. Leus, and F. Petré, "Quantized multi-mode precoding for spatial multiplexing MIMO-OFDM systems," in *Proc. IEEE 62nd Vehicular Technology Conference (VTC)*, vol. 2, Sep. 2005, pp. 867–871.

[66] W. C. Jakes, Jr., *Microwave Mobile Communications*. John Wiley & Sons, 1974.

[67] T. A. Thomas and F. W. Vook, "MIMO strategies for equal-rate data streams," in *Proc. IEEE Vehicular Technology Conference (VTC)*, vol. 2, Atlantic City, NJ, USA, Oct. 2001, pp. 548–552.

[68] D. P. Palomar, J. M. Cioffi, and M. A. Lagunas, "Joint TX-RX beamforming design for multicarrier MIMO channels: A unified framework for convex optimization," *IEEE Trans. Signal Processing*, vol. 51, no. 9, pp. 2381–2401, Sep. 2003.

[69] A. Edelman, T. A. Arias, and S. T. Smith, "The geometry of algorithms with orthogonality constraints," *Siam J. Matrix Anal. Appl.*, vol. 20, no. 2, pp. 203–353, 1998.

[70] A. Scaglione, "Statistical analysis of the capacity of MIMO frequency selective Rayleigh fading channels with arbitrary number of inputs and outputs," in *Proc. IEEE Int. Symp. Inform. Theory (ISIT)*, Jun. 2002, pp. 278–282.

[71] R. A. Horn and C. R. Johnson, *Matrix Analysis*. Cambridge University Press, 1999.

[72] N. Khaled, C. Desset, S. Theon, and H. D. Man, "On spatial-mode selection for the joint transmit and receive MMSE design," in *Proc. IEEE International Conference on Communications (ICC)*, vol. 5, Paris, France, Jun. 2004, pp. 2812–2816.

[73] H. Weingarten, Y. Steinberg, and S. Shamai (Shitz), "The capacity region of the Gaussian MIMO broadcast channel," in *Proc. 38th Conf. Inform. Sciences and Systems (CISS'04)*, Princeton, NJ, USA, Mar. 2004.

[74] T. Yoo and A. Goldsmith, "On the optimality of multiantenna broadcast scheduling using zero-forcing beamforming," *IEEE J. Select. Areas Commun.*, vol. 24, no. 3, pp. 528–541, Mar. 2006.

[75] N. Jindal, "MIMO broadcast channels with finite-rate feedback," *IEEE Trans. Inform. Theory*, vol. 52, no. 11, pp. 5045–5060, Nov. 2006.

[76] M. Sharif and B. Hassibi, "On the capacity of MIMO broadcast channels with partial side information," *IEEE Trans. Inform. Theory*, vol. 51, no. 2, pp. 506–522, Feb. 2005.

[77] K. Huang, J. G. Andrews, and R. W. Heath Jr., "Orthogonal beamforming for SDMA downlink with limited feedback," in *Proc. IEEE Int. Conf. Acoust., Speech, and Signal Process. (ICASSP)*, vol. 3, Honolulu, HI, USA, Apr. 2007, pp. 97–100.

[78] W. Santipach and M. Honig, "Asymptotic capacity of beamforming with limited feedback," in *Proc. IEEE Int. Symp. Inform. Theory (ISIT))*, Chicago, IL, USA, Jul. 2004.

[79] T. Yoo, N. Jindal, and A. Goldsmith, "Finite-rate feedback MIMO broadcast channels with a large number of users," in *Proc. IEEE Int. Symp. Inform. Theory (ISIT)*, Seattle, Washington, USA, Jul. 2006.

[80] C. Oh and A. Yener, "Adaptive CDMA cell sectorization with linear multiuser detection," in *Proc. IEEE Veh. Tech. Conf. (VTC'03 Fall)*, Orlando, FL, USA, Oct. 2003.

[81] M. T. Ivrlac, R. L.-U. Choi, R. D. Murch, and J. A. Nossek, "Effective use of long-term transmit channel state information in multi-user MIMO communication systems," in *Proc. IEEE Veh. Tech. Conf. (VTC'03 Fall)*, Orlando, FL, USA, Oct. 2003.

[82] J. W. Wallace and M. A. Jensen, "Statistical characteristics of measured MIMO wireless channel data and comparison to conventional models," in *Proc. 54th IEEE Vehicular Technology Conference Fall (VTC)*, vol. 2, Atlantic City, NJ, USA, Oct. 2001, pp. 1078–1082.

[83] J. Fuhl, A. Molisch, and E. Bonek, "Unified channel model for mobile radio systems with smart antennas," *IEE Proc. Radar, Sonar and Navigation*, vol. 145, no. 1, pp. 32–41, 1998.

[84] Q. Spencer, B. Jeffs, M. Jensen, and A. Swindlehurst, "Modeling the statistical time and angle of arrival characteristics of an indoor multipath

channel," *IEEE J. Select. Areas Commun.*, vol. 18, no. 3, pp. 347–360, Mar. 2000.

[85] V. Erceg et al., "TGn channel models," *IEEE 802.11-03/940r4*, May 2004.

[86] M. Kountouris, R. de Francisco, D. Gesbert, D. T. Slock, and T. Sälzer, "Multiuser diversity - multiplexing tradeoff in MIMO broadcast channels with limited feedback," in *Proc. Asilomar Conference on Signals, Systems, and Computers*, Oct. 2006, pp. 364–368.

[87] R. de Francisco and D. T. Slock, "An iterative optimization method for unitary beamforming in MIMO broadcast channels," in *Proc. 45th Annual Allerton Conf. on Communication, Control and Computing*, Monticello, IL, USA, Sep. 2007.

[88] N. Jindal and A. Goldsmith, "Dirty-paper coding versus TDMA for MIMO broadcast channels," *IEEE Trans. Inform. Theory*, vol. 51, no. 5, pp. 1783–1794, May 2005.

[89] W. Choi, A. Forenza, J. G. Andrews, and R. W. Heath Jr., "Opportunistic space-division multiple access with beam selection," *IEEE Trans. Commun.*, vol. 55, no. 12, pp. 2371–2380, Dec. 2007.

[90] A. Gersho and V. Cuperman, "Vector quantization: A pattern-matching technique for speech coding," *IEEE Commun. Mag.*, vol. 21, no. 9, pp. 15–21, Dec. 1983.

[91] J. Makhoul, "Linear prediction: A tutorial review," *Proc. IEEE*, vol. 63, no. 4, pp. 561–580, Apr. 1975.

[92] N. Zorba and A. I. Pérez-Neira, "Opportunistic Grassmannian beamforming for multiuser and multiantenna downlink communications," *IEEE Trans. Wireless Commun.*, vol. 7, no. 4, pp. 1174–1178, Apr. 2008.

[93] D. J. Love, R. W. Heath Jr., and T. Strohmer, "Grassmannian beamforming for multiple-input multiple-output wireless systems," *IEEE Trans. Inform. Theory*, vol. 49, no. 10, p. 2735, Oct. 2003.

[94] M. Kountouris, D. Gesbert, and T. Sälzer, "Distributed transmit mode selection for MISO broadcast channels with limited feedback: Switching from SDMA to TDMA," in *Proc. IEEE Workshop Signal Process. Advances Wireless Commun. (SPAWC)*, Recife, Brazil, Jul. 2008, pp. 371–375.

[95] M. Andrews, K. Kumaran, K. Ramanan, A. Stolyar, P. Whiting, and R. Vijayakumar, "Providing quality of service over a shared wireless link," *IEEE Commun. Mag.*, vol. 39, no. 2, pp. 150–154, Feb. 2001.

[96] F. Shad, T. D. Tod, V. Kezys, and J. Litva, "Indoor SDMA capacity using a smart antenna basestation," in *Proc. IEEE International Conference on Universal Personal Communications Record (ICUPC)*, vol. 2, San Diego, CA, USA, Oct. 1997, pp. 868–872.

[97] J. H. Conway, R. H. Hardin, and N. J. Sloane, "Packing lines, planes, etc.: Packings in Grassmannian spaces," *Experimental Mathematics*, vol. 5, pp. 139–159, 1996.

[98] W. Yang and G. Xu, "Optimal downlink power assignment for smart antenna systems," in *Proc. IEEE Int. Conf. Acoust., Speech, and Signal Process. (ICASSP)*, vol. 6, Seattle, Washington, USA, Apr. 1998, pp. 3337–3340.

[99] C. Simon and G. Leus, "Round-robin scheduling for orthogonal beamforming with limited feedback," *IEEE Trans. Wireless Commun.*, vol. 10, no. 8, pp. 2486–2496, Aug. 2011.

[100] P. Viswanath and D. N. Tse, "Sum capacity of the vector Gaussian broadcast channel and uplink-downlink duality," *IEEE Trans. Inform. Theory*, vol. 49, no. 8, pp. 1912–1921, Aug. 2003.

[101] D. J. Love, R. W. Heath Jr., V. Lau, D. Gesbert, B. D. Rao, and M. Andrews, "An overview of limited feedback in wireless communication systems," *IEEE J. Select. Areas Commun.*, vol. 26, no. 8, pp. 1341–1365, Oct. 2008.

[102] D. Gesbert, M. Kountouris, R. W. Heath Jr., C.-B. Chae, and T. Sälzer, "Shifting the MIMO paradigm," *IEEE Signal Processing Mag.*, vol. 24, no. 5, pp. 36–46, Sep. 2007.

[103] C. Swannack, E. Uysal-Biyikoglu, and G. W. Wornell, "Low complexity multiuser scheduling for maximizing throughput in the MIMO broadcast channel," in *Proc. Allerton Conf. on Comm. Control and Comp.*, Sep. 2004.

[104] ——, "MIMO broadcast scheduling with limited channel state information," in *Proc. Allerton Conference on Communication, Control, and Computing*, Sep. 2005.

[105] M. Schubert and H. Boche, "Solution of the multiuser downlink beamforming problem with individual SINR constraints," *IEEE Trans. Veh. Commun.*, vol. 53, no. 1, pp. 18–28, Jan. 2004.

[106] H.-Y. Wei and R. Izmailov, "Channel-aware soft bandwidth guarantee scheduling for wireless packet access," in *Proc. IEEE Wireless Communications and Networking Conference (WCNC)*, vol. 2, Atlanta, GA, USA, Mar. 2004, pp. 1276–1281.

[107] F. Shad, T. D. Tod, V. Kezys, and J. Litva, "Dynamic slot allocation (DSA) in indoor SDMA/TDMA using a smart antenna basestation," *IEEE/ACM Trans. Networking*, vol. 9, no. 1, pp. 69–81, Feb. 2001.

[108] H. Yin and H. Liu, "Performance of space-division multiple-access (SDMA) with scheduling," *IEEE Trans. Wireless Commun.*, vol. 1, no. 4, pp. 611–618, Oct. 2002.

[109] M. Abramowitz and I. A. Stegun, Eds., *Handbook of Mathematical Functions*. Dover, 1972.

[110] A. E. Sarhan and B. G. Greenberg, Eds., *Contributions to Order Statistics*. John Wiley & Sons, Inc., 1962.